Premigratory and Migratory Neural Crest Cells are Multipotent In Vivo

and

The Roles of Sall4 in Melanoma

Dissertation

zur

Erlangung der Doktorwürde

(Dr. sc. Nat)

vorgelegt der

Mathematisch-naturwissenschaftlichen Fakultät

der

Universität Zürich

von

Arianna Virginia Giulia Baggiolini

von Pregassona, TI

Promotionskomitee

Prof. Dr. Konrad Basler

Prof. Dr. Reinhard Dummer

Prof. Dr. Sebastian Jessberger (Vorsitz)

Prof. Dr. Lukas Sommer (Leitung der Dissertation)

Zürich, 2015

Table of contents

Table of figures and tables

1 Summary

The neural crest (NC) is a transient embryonic stem/progenitor cell population and a hallmark of vertebrate development. The NC is induced during neurulation at the border between the neuronal and non-neuronal ectoderm. Upon induction NC cells undergo an epithelial to mesenchymal transition (EMT), delaminate from the neural folds and migrate extensively through the developing embryo. NC cells give rise to a broad variety of cell types including the sensory and autonomic neurons of the peripheral nervous system, the myelinating Schwann cells and the melanocytes, among others. Despite the broad differentiation potential of NC cells it has been highly debated whether the NC consisted of multipotent cells or whether it was rather a heterogeneous population of restricted progenitors. In fact, although several earlier studies have described multipotency of NC cells, the existence of multipotent NC cells has been questioned both by cell culture experiments and in recent in vivo studies performed in chick embryos. In this study, we solved a longstanding controversy regarding a pivotal question in the field of stem cells. Using genetic lineage tracing in the mouse, we revealed for the first time the broad developmental potential of NC cells in a mammalian system and we demonstrated that the majority of premigratory and migratory NC cells are multipotent in vivo.

Embryogenesis and tumorigenesis share several mechanisms in common and it has become more and more evident that knowledge in developmental biology can provide further insights into tumor biology. For instance, melanoma, a malignancy of NC-derived melanocytes, can exploit various NC developmental programs for disease progression. Malignant melanoma cells can indeed aberrantly activate EMT master regulators, such as members of the Snail, Twist and Zeb families, which are normally activated by NC cells during migration in the embryo. In the course of melanoma progression malignant cells brake through the basament membrane, invade the underlying mesenchyme, reach blood and lymphatic vessels and metastasize to distant organs. Moreover, similar to NC cells, melanoma cells can possess multipotency features and be able to express different lineage markers.
We discovered that the zinc-finger transcription factor Sall4 is expressed in NC cells and it is downregulated upon differentiation. Sall4 is a crucial factor for the maintenance of self-renewal and pluripotency of embryonic stem cells. Moreover, SALL4 has been associated with tumorigenesis and to worse patient outcome in various cancer types. However, whether SALL4 may also play a role in melanoma

formation and progression has not been addressed so far. We observed that SALL4 was mostly expressed in human proliferative melanoma cell lines, while it was absent in more invasive melanoma cell lines or upon EMT induction. Interestingly, SALL4 downregulation induced, in turn, an EMT signature in a proliferative melanoma cell line, suggesting that there may be a regulatory feedback loop. In vivo we induced Sall4 loss in the *Tyr::NRas*^{Q61K} *Ink4a*$^{-/-}$ *Tyr::Cre*^{ERT2} *Sall4*$^{lox/lox}$ *R26R::GFP* melanoma mouse model and could observed that primary tumor formation was impaired. However, Sall4 loss was linked to a reduced survival of the knock out animals and recombined cells were detected in lymph nodes and in some lungs. Further investigations now urge to be performed to prove whether Sall4 loss is necessary and sufficient for EMT induction.

2 Zusammenfassung

Die Neuralleiste ist eine temporäre embryonale Stammzellenpopulation und ein Charakteristikum der Wirbeltierentwicklung. Die Neuralleiste wird während der Neurulation an der Grenze zwischen dem neuronalen und dem nicht neuronalen Ektoderm gebildet. Nach der Entstehung der Neuralleiste durchleben die Neuralleistenzellen einen epithelialen zu mesenchymalen Wandel (EMT). Nach Ablösung der Neuralleistenzellen vom neuronalen Epithelium wandern die Zellen ausgiebig durch den sich entwickelnden Embryo. Die Neuralleiste bringt viele verschiedene Zelltypen hervor, wie zum Beispiel Neuronen und Gliazellen des peripheren Nervensystems sowie Melanozyten. Trotzt dem hohen Differenzierungspotential der Neuralleistenzellen war es höchst umstritten, ob Neuralleistenzellen multipotent sind oder, ob die Neuralleiste eher aus einer heterogenen Population von spezialisierten Mutterzellen besteht. Auch wenn Pionierstudien die Neuralleiste zuvor als multipotent charakterisiert hatten, ließen andere in vitro Studien und in vivo Studien an Hühnerembryonen an deren Existenz zweifeln. Durch unsere Studie ist es uns nun gelungen, diese langandauernde Debatte der Stammzellenforschung zu beenden. Mit Hilfe von Mausgenetik haben wir zum ersten Mal gezeigt, dass die Neuralleiste der Säugetiere ein beeindruckendes Differenzierungspotential besitzt und, dass die Mehrheit der Neuralleistenzellen vor und während der Besiedelung des Embryos multipotent ist.

Die Embryogenese und die Karzinogenese haben viele Gemeinsamkeiten und es wird zunehmend ersichtlich, dass detaillierte Kenntnisse der mechanistischen Prozessen während der embryonalen Entwicklung die Grundlage für ein besseres Verständnis der Tumorbiologie ist. Das Melanom, ein bösartiger Tumor der Melanozyten, hat zum Beispiel seinen Ursprung in der Neuralleiste. Dieser schwarze Hautkrebs (Krebsart) nutzt viele Prozesse, die während der embryonalen Entwicklung essentiell sind, zu seiner Etablierung aus. Das maligne Melanom exprimiert unter anderen Transkritionsfaktoren der Snail, Zeb und Twist Familie, die für die EMT verantwortlich sind und die normalerweise in der Neuralleiste aktiviert werden, um deren Wanderung durch den Embryo während der Entwicklung gewährleisten zu können. Auf diese Weise können maligne Melanomzellen die Basalmembran der Haut durchbrechen, in das unterliegende Mesenchym eindringen und so die Blut- und Lymphgefässe erreichen, um zu metastasieren. Zudem können

Melanomzellen, vergleichbar mit der Neuralleiste, einige multipotente Eigenschaften besitzen und Merkmale verschiedener differenzierter Zellenlinien exprimieren.

Wir haben entdeckt, dass der Transkriptionsfaktor Sall4 spezifisch in Neuralleistenzellen exprimiert ist und, dass die Sall4 Expression nach der Differenzierung der Neuralleistenzellen herunterreguliert wird. Sall4 ist für die uneingeschränkte Teilung und die Pluripotenz von embryonalen Stammzellen notwendig. Außerdem ist SALL4 oft mit Karzinogenese und einer schlechteren Patientenprognose in verschiedenen Krebsarten assoziiert. Ob SALL4 auch eine Rolle in der Entwicklung maligner Melanome spielen könnte, ist es bis jetzt jedoch noch nicht untersucht geworden. In unserer Studie haben wir nun beobachtet, dass SALL4 am häufigsten in Zellen schnell wachsender Melanomen vorhanden ist, aber dass es in invasiven Melanomen oder nach der EMT Induktion nicht mehr detektierbar ist. Bemerkenswerterweise löst die Herunterregulierung von SALL4 in proliferativen, wenig invasiven Melanomzellen typische Kennzeichen der EMT aus. Insgesamt deuten diese Resultate darauf hin, dass eine negative Rückkopplungsregulierung existieren könnte. Mit Hilfe des transgenen Mausmodels *Tyr::NRas^{Q61K} Ink4a$^{-/-}$ Tyr::Cre^{ERT2} Sall4$^{lox/lox}$ R26R::GFP* konnten wir außerdem zeigen, dass der Verlust von Sall4 die Entstehung maligner Tumore verhindert. Der Verlust von Sall4 war jedoch mit einem schlechteren Überleben der Versuchstiere und mit der Präsenz rekombinierte Melanozyten in Lymphknoten und einigen Lungen verbunden. Weitere Untersuchungen sind jetzt notwendig, um zu verstehen, ob die Herunterregulierung der Sall4 Expression ein notwendiger und ausreichender Vorgang ist, um die EMT zu ermöglichen.

3 Introduction

3.1 The neural crest

The neural crest (NC) is an embryonic stem/progenitor cell population typical of vertebrate embryos. It is induced during neurulation at the border between the neuronal and non-neuronal ectoderm. Upon induction, NC cells undergo an epithelial to mesenchymal transition (EMT), delaminate from the dorsal neural tube and migrate extensively through the embryo. NC cells possess one of the broadest developmental potential in the vertebrate embryo. They are able to differentiate into a broad variety of cell types responsible for the generation of the peripheral nervous system (PNS), the enteric nervous system and the craniofacial skeleton, among others.

3.1.1 NC formation

The NC is induced at the border between the prospective neural and non-neural ectoderm. Signals from the ectoderm and from the underlying mesoderm create a complex gene regulatory network responsible for NC induction, delamination from the dorsal neural tube and the correct migration of NC cells throughout the developing embryo (Figure 1, Sauka-Spengler and Bronner-Fraser, 2008). In particular, bone morphogenetic protein (BMP), fibroblast growth factor (FGF) and Wnts regulate the expression of the neural tube specifiers Msx1, Msx2, Pax3, Pax7 and Zic1. Pax3 and Zic1, in turn, induce the expression of NC specifiers including Snail1, Snail2, Sox9, Sox10, AP-2, Twist, c-Myc, Id and FoxD3, in the dorsal neural tube in a Wnt-dependent manner. Upon NC induction, NC cells undergo EMT, during which the cells loose their apical-basal cell polarity, reorganize their cytoskeleton, upregulate adhesion molecules and delaminate from the neural folds (Sauka-Spengler and Bronner-Fraser, 2008). NC cells then vastly migrate through the embryonic body following migratory paths defined and regulated mostly by inhibitory molecules such as the SEMA3F-NPL2 and the Slit-Robo signaling molecules (Gammill et al., 2007; Jia et al., 2005). Chemoattractant molecules can, however, also guide migratory NC cells, such as the glial-cell-derived neurotrophic factor (GDNF) that regulates the migration of vagal NC cells to the developing enteric nervous system (Young et al., 2001; Sauka-Spengler and Bronner-Fraser, 2008).

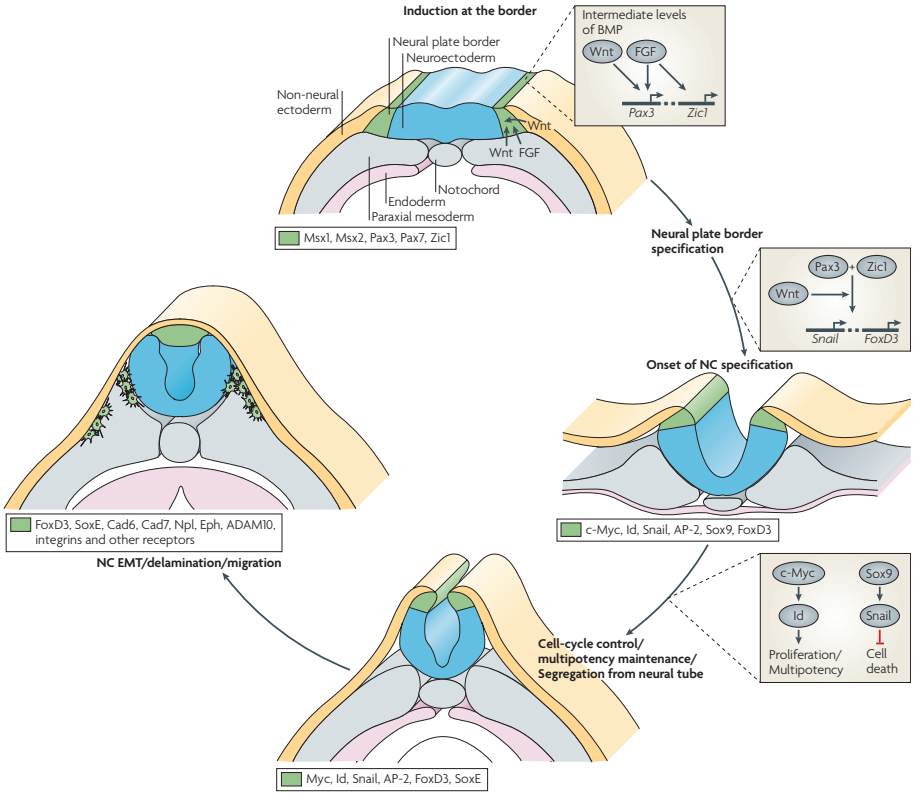

Figure 1. The regulatory network that controls NC formation

BMP, FGF and Wnts are the key regulators of the neural tube specifiers Pax3 and Zic1. The neural tube specifiers Pax3 and Zic1, in turn, induce NC specification in the dorsal neural tube through activation of Snail and FoxD3. Once the NC is segregated from the dorsal neuroepithelium, NC cells undergo EMT and migrate through the vertebrate embryo and differentiate into a broad range of diverse cells types (adapted from: Sauka-Spengler and Bronner-Fraser, 2008).

3.1.2 The NC populations

Figure.2 NC functional domains

The schematic drawing depicts the cranial (blue), the cardiac (green), the vagal (yellow) and the trunk (orange) NC.

The NC is subdivided into four groups depending on the rostro-caudal axis level from which the NC cells delaminate.

Cranial NC cells (Figure 2, in blue) emigrate from the neuroepithelium before neural tube closure and give rise to the osteocytes and the chondrocytes

that build up the craniofacial skeleton of the vertebrate embryo. In particular, cranial NC cells give rise to the pharyngeal apparatus (PA), a transient embryonic structure, which is eventually remodeled into the final structures of the jaws (Cordero et al., 2011). Cranial NC cells also differentiate into sensory neurons, Schwann cells, smooth muscle cells and the melanocytes of the head.

The cardiac NC (Figure 2, in green) originates from the area between the otic vesicle and the third somite. These cells differentiate into the smooth muscle cells of the cardiac outflow tract and give rise to the aorticopulmonary septum (Jiang et al., 2000; Sieber-Blum, 2004).

The vagal NC (Figure 2, in yellow) originates between somites 1 and 7 and gives rise to the enteric nervous system (Heanue and Pachnis, 2007).

Finally, the trunk NC (Figure 2, in orange) arises at somite 7 level until the most caudal region of the neural tube. After delamination from the dorsal neural tube trunk NC cells migrate ventrally to differentiate into various cell types: autonomic neurons and glia of the sympathetic ganglia (SG), glia cells of the ventral root (VR) and sensory neurons and glia of the dorsal root ganglia (DRG). Trunk NC cells that migrate on the dorsal lateral pathway (DLP) give rise to the melanocytic lineage of the skin (Figure 3). Moreover, the chromaffin cells of the adrenal glands also originate from the trunk NC (Crane and Trainor, 2006).

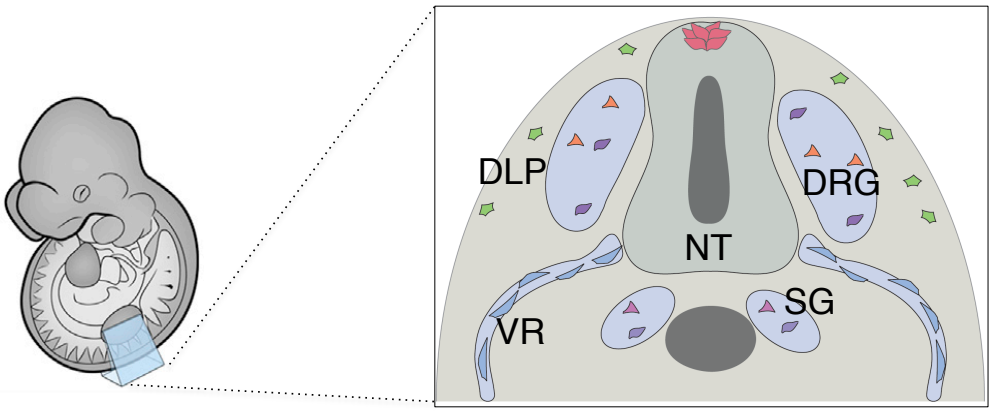

Figure 3. The derivatives of the trunk NC.

After delamination from the dorsal neural tube trunk NC cells give rise to a vast range of different cell types. At the forelimbs level the trunk NC creates the entire peripheral nervous system, including neuronal and glial cells of the DRG and of the SG, glial cells of the VR. Moreover, trunk NC cells that migrate along the DLP generate the melanocytes of the skin.

3.1.3 The fate of NC cells

Initial studies that investigated the developmental fate of NC cells were conducted performing quail-chick transplantations of premigratory NC cells. The NC of quail embryos was grafted at different levels along the rostro-caudal axis of the chick embryos (Couly and Le Douarin, 1985). Subsequent analysis of the chimeras revealed that the fate of the NC cells was not dependent on the rostro-caudal domain from where the cells were isolated, but rather on local cues provided from surrounding tissue at the site of transplantation. This result was one of the first indications for the multipotency of NC cells in vivo (Couly and Le Douarin, 1985; Dupin and Le Douarin, 2014). First evidence for the multipotency of the NC was generated by pioneer lineage tracing studies in the chick embryo in which single premigratory trunk NC cells were labeled by intracellular injection of a vital dye (Bronner-Fraser and Fraser, 1988; Bronner-Fraser and Fraser 1989). The majority of labeled trunk NC cells was located in multiple NC derivatives and it was, thus, assumed that these cells were able to differentiate into diverse cell types. Similarly, lineage tracing of mouse trunk NC cells by intracellular injection of vital dye suggested that this observation was also true for mammals (Serbedzija et al., 1990). Consistent with these results, in vitro investigations proved that NC cells were multipotent and able to self-renew (Stemple and Anderson, 1993).

More recent studies further investigated the developmental fate of the NC in vivo. Kalcheim and colleagues used a semi-open book preparation to mark single premigratory trunk NC cells by either vital dye microinjection or plasmid electroporation in the chick embryo (Krispin et al., 2010). Interestingly, they found that NC cells were restricted in their differentiation potential and that they were segregated inside the dorsal NT in a spatio-temporal manner. Accordingly single NC cells were restricted to a specific lineage and the fate of each cell could be anticipated depending on its location inside of the dorsal neural tube and the time of its emigration (Krispin et al., 2010a; Krispin et al., 2010b). However, such an early restriction of the premigratory NC and spatio-temporal segregation inside the dorsal neural tube could not be confirmed by neither time-lapse nor two-photon microscopic imaging of fluorescent dye labeled chick NC cells (McKinney et al., 2013).

The discrepancies of these results could be explained by stage differences at the moment of cell labeling or by technical differences in the injection procedures (Dupin and Sommer, 2012).

Recent work from our lab addressed this issue investigating the trunk NC in a mammalian embryo. Using genetic multicolor single cell tracing in the mouse,

combined with lineage differentiation analysis and extensive biostatistical examination, we revealed for the first time the broad developmental potential of NC cells in a mammalian system in vivo. Indeed, the vast majority of premigratory and, surprisingly, also migratory NC cells was able to generate sensory and autonomic neurons, glia and melanocytes (Baggiolini et al., 2015; Bronner, 2015; 4.1 Premigratory and migratory neural crest cells are multipotent in vivo).

3.1.4 NC-derived stem cells

The NC is a multipotent transient embryonic cell population. However, NC-derived stem cells exist in several NC derivatives and persist at later developmental stages and in the adult organism (Shakhova and Sommer, 2008).
$p75^{NTR+}/P_0^-$ cells can in fact be isolated from the sciatic nerve of rat embryos at embryonic day (E) 14.5. These cells show self-renewal capacity both in vitro and in vivo and can differentiate into neurons, glia and myofibroblasts in vitro (Morrison et al., 1999). Similarly, NC-derived precursor cells exist in the adult DRG (Li et al., 2007; Nagoshi et al., 2008), bone marrow (Nagoshi et al., 2008), gut (Kruger et al., 2002), heart (Tomita et al., 2005; El-Helou et al., 2008), cornea (Yoshida et al., 2006; Brandl et al., 2009), and finally also in the bulge region of the hair follicle in the skin (Toma et al., 2001; Wong et al., 2006).

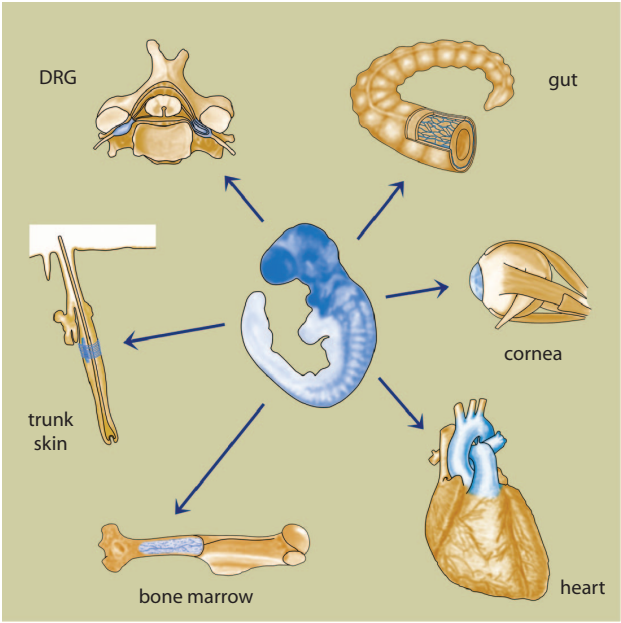

Figure 4. NC-like stem cells.
NC-derived precursor cells exist also in the adult organism. Cells with NC-like properties like self-renewal capacity and differentiation potential exist in almost all NC-derived structures.

These precursor cells can be found in the adult DRG, gut, skin, cornea, bone marrow and heart (adapted from: Shakhova and Sommer, 2008).

3.1.5 NC as a hallmark of vertebrate evolution

Vertebrates, together with Tunicates and Cephalocordates, belong to and represent the vast majority of the phylum of Chordates. In fact, vertebrates seem to have had a considerable evolutionary advantage compared to the other members of the Philum. The major trait that distinguished the vertebrates from the other Chordates was the appearance of the NC. All vertebrates possess a premigratory NC that arises in the dorsal neural tube, or at least adjacent to it. Moreover, the gene regulatory network controlling NC induction is very conserved among vertebrates (Sauka-Spengler and Bronner-Fraser, 2008). In all vertebrates, NC cells undergo EMT, delaminate from the neuroepithelium and migrate extensively through the embryo to give rise to a vast variety of cell types and structures.
In particular, the NC allowed the formation of a craniofacial skeleton and the appearance of a novel sensory system, which availed the vertebrates of a “New Head”; a concept that was coined by Gans and Northcutt (1983) to define the contributions of the NC to the vertebrates. These innovations enabled the vertebrates to develop from filter feeders to predators (Green et al., 2015) and, thus, to drastically change their life style and diet. Beyond the innovations of the jaws and of the sensory system, other NC-derived traits arose including pigment cells, pharyngeal cartilage and muscles, chromaffin cells and the outflow tract of the heart. All these evolutionary new features enabled vertebrate animals to adopt a more active behavior and furthermore profoundly changed their perception of environment. Finally, a change in metabolism, blood circulation and respiration definitively set vertebrates apart and rendered them unique (Green et al., 2015).

3.1.6 NC and disease

During development NC cells are induced in the dorsal neural tube and eventually delaminate from the dorsal neuroepithelium and migrate through the embryonic body to reach diverse locations where they have to differentiate, proliferate and survive. Whenever one or more of these processes are not correctly accomplished, organ defects and dysplasias may arise. Such developmental anomalies of the NC are termed neurocristopathies.

Many neurocristopathies are birth defects such as Hirschsprung disease, cleft lip/palate malformations, heart malformations and congenital nevi (Etchevers et al., 2006).

Congenital nevi occur in one of every 100 newborns and it is a dermal hyperplesia of the melanocytes, which arises during embryonic development. Congenital nevi are caused by the gain-of-function $NRAS^{Q61K}$ mutation, which aberrantly activates the mitogen-activated kinase (MAPK) pathway (Bauer et al., 2006). Of importance, patients affected by congenital giant nevi are more prone to develop melanoma (3.2 Melanoma), due to the constitutive activation of NRAS and the aberrant number of melanocytes, and need to be kept under observation (Lyon, 2010).

Besides congenital birth defects various cancer types can arise from NC-derived cells. Those malignancies include among others neuroblastoma, one of the most common childhood tumors derived from the symphatetic compartment of the PNS; and schwannoma, that arises from the glia of the sympathetic nervous system. Furhtermore, medullary thyroid carcinoma arises form the tyroid gland. Pheochromocytomas arise from the chromaffin cells of the adrenal medulla and paragangliomas derive from the non-chromaffin cell chemoreceptors of the head and neck. Moreover melanoma, a highly aggressive cancer deriving from the melanocytic lineage, also belongs to the acquired neurocristopathies (3.2 Melanoma; Etchevers et al., 2006).

3.2 Melanoma

3.2.1 Epidemiology of cutaneous melanoma

Cutaneous melanoma is an aggressive cancer that arises from the abnormal behavior of the melanocytic lineage. Cutaneous melanoma is the most aggressive skin cancer and it is responsible of 75% of the skin cancer-related deaths. It is a disease particularly common in the Western world (Figure 5) affecting 15-25 per 100'000 individuals (Schadendorf and Hauschild, 2014) every year. Cutaneous melanoma affects principally individuals with fair skin, blue eyes and red hair, while more pigmented populations from e.g. Africa or Asia are more likely to develop other types of melanoma, such as the more rare acral and mucosal melanomas (Schadendorf et al., 2015).

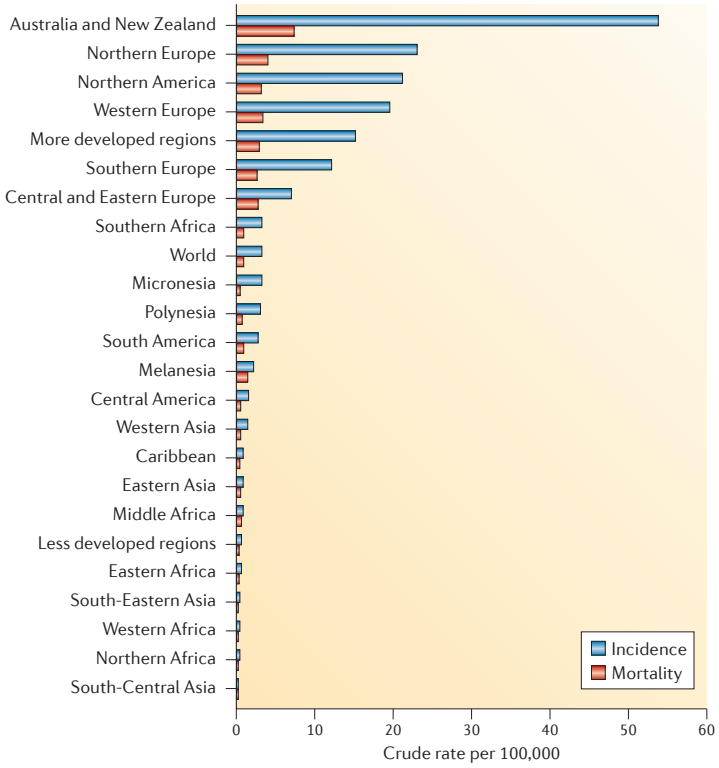

Figure 5. Worldwide incidence and mortality rates of cutaneous melanoma.
Incidence and mortality rates of cutaneous melanoma vary among countries, being the Western countries the most affected (adapted from: Schadendorf et al., 2015).

Beyond individual genetic susceptibility, such as fair skin and red hair, familial genetic background can also play a role. Familial melanoma, which accounts for 8% of all melanoma cases, is mostly caused by a germline mutation in the Cyclin-

Dependent Kinase Inhibitor 2A (CDKN2A) locus (FitzGerald et al., 1996). However, sporadic melanoma, which represents 90% of all melanoma cases, can not exclusively be explained by genetics. It is rather caused by a combination of frequent low-risk alleles together with environmental mutagenic factors (Eggermont et al., 2014). One of the highest environmental risk factors is the exposure to UV light. UVA and UVB light indeed play a mutagenic role and cause UV-signature mutations such as the C>T (UVB-induced) or G>T (UVA-induced) transitions (Hodis et al., 2012) that in turn can also account for some driver gene mutations. For example the activating mutation of $RAC1^{P29S}$ that leads to the downstream activation of PAK (p21-activated protein kinase) signaling, and the loss-of-function mutation of cell cycle regulator $p16^{Ink4a}$, express a UV-signature (Hodis et al., 2012).

3.2.2 Driver mutations in melanoma

However, not all mutations in melanoma show a UV-signature. Most of the mutations that affect the mitogen-activated protein kinase (MAPK) cascade indeed do not express a typical UV-signature, even though a role of UV damage can not be completely excluded. Among these oncogenic mutations there are common mutations such as $BRAF^{V600E}$, which is present in 50% of all melanomas, and $NRAS^{Q61R}$ and $NRAS^{Q61L}$, which affect between 15-20% of all melanomas (Hodis et al., 2012). Interestingly, BRAF and NRAS mutations, as well as mutations of other MAPK members, are mostly mutually exclusive.

The MAPK signaling pathway is initiated by RTKs (receptor tyrosine kinases, e.g. KIT), which activate the small GTPase RAS (HRAS, KRAS or NRAS), which in turn regulates the downstream kinases RAFs (ARAF, BRAF or CRAF). This results in activation of the MAP/ERK kinase (MEK1 and MEK2) and MAPKs (also known as ERK2 and ERK1) (Figure 6). Upon phosphorylation ERK translocates to the nucleus and regulates transcription factors responsible for cell growth, survival, cell motility and metabolism (Schadendorf et al., 2015). Under disease conditions, the MAPK signaling pathway is constitutively active resulting in aberrant regulation of the cell cycle and tumor growth (Figure 6). Moreover, eventual loss of PTEN aberrantly activates phosphatidylinositol 3-kinase (PI3K)-AKT signaling, which leads to further loss of control of normal cellular functions (Cristofano et al., 1998; Podsypanina et al., 1999).

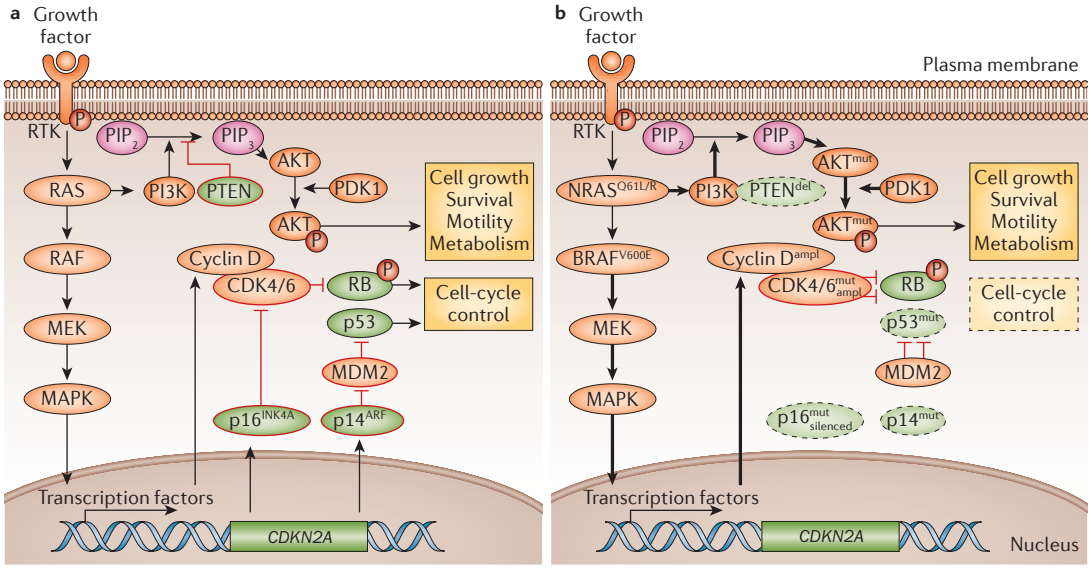

Figure 6. Major signaling pathways in melanoma.

(a) The MAPK and (PI3)-AKT signaling pathways normally control cellular functions by regulating cell growth, survival, motility and metabolisms. (b) However, under conditions of malignancy, such as melanoma, these pathways are constitutively activated (indicated by the thick arrows), which leads to aberrant cellular behavior (adapted from: Schadendorf et al., 2015).

3.2.3 Melanoma formation and progression

Classically melanoma has been explained as a linear and stepwise process. The Clark model for melanoma progression (Clark et al., 1984) describes how epidermal melanocytes undergo a neoplastic transformation that results in the formation of benign nevi. Eventually, upon further genetic mutations, some benign nevi develop into a dysplatic nevus. The Clark model further predicts that dysplatic nevi first undergo a radial growth phase and subsequently a vertical growth phase of tumor growth characterized by invasion of the dermis. Ultimately, the vertical growth phase results in metastases formation (Clark et al., 1984). Even though the Clark model may correctly depict the development of some melanomas, not all melanomas follow such a linear model of progression. Indeed, melanoma formation and progression to metastasis is often much more complex and less linear (Figure 7). A normal epidermal melanocyte does not always follow all the sequential steps described by the Clark model to progress into a primary tumor. Similarly, also metastasis formation is not necessarily the result of a vertical tumor growth phase, but can also occur at different steps of tumor development (Figure 7). Thus, a tumor can metastasize without previous progression through the vertical growth phase (Lomuto et al., 2004;

Taran and Heenan, 2001). Remarkably, 4-12% of patients have a metastasis burden without any detectable primary tumor (Giuliano et al., 1980; Norman et al., 1990; Reintgen et al., 1983), suggesting that disseminating capacities of malignant melanocytes may be independent of previous formation of an advanced primary melanoma. Of note, even benign melanocytes can be detected in lymph nodes from non-melanoma patients (Bautista et al., 1994; Carson et al., 1996; Fisher et al., 1994). The fact that some cells of the melanocytic lineages possess such an extraordinary migratory capacity elicits the comparison to the great migratory capacity of the NC cells during embryonic development (Damsky et al., 2014).

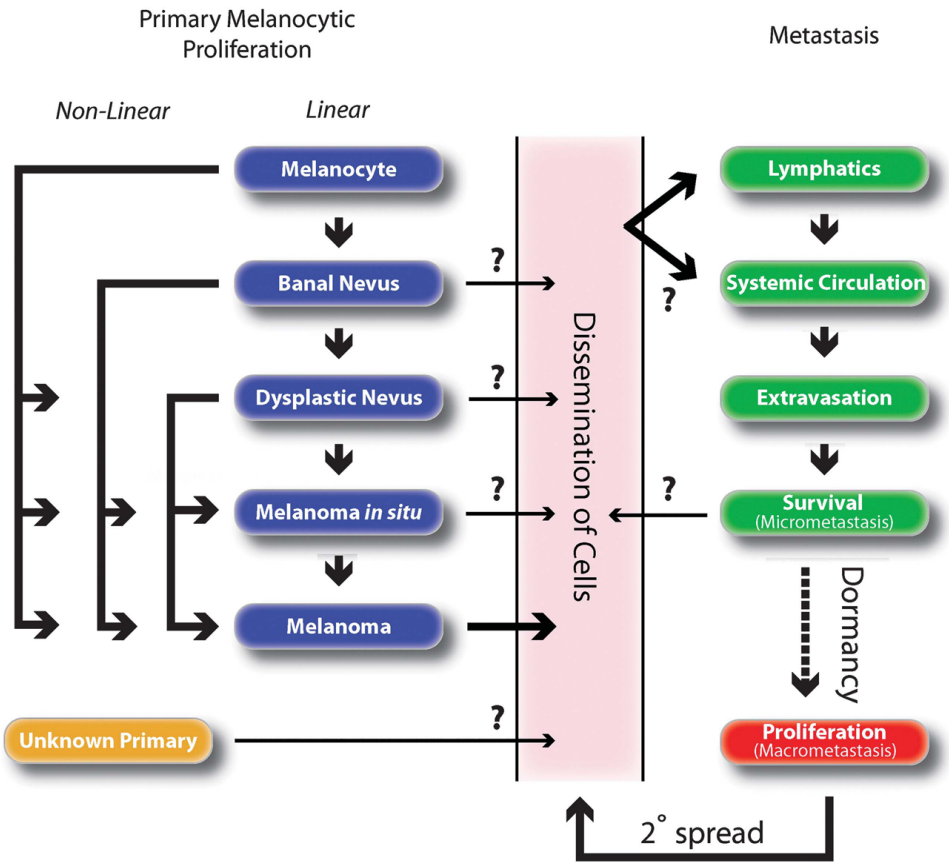

Figure 7. Linear and non-linear model of melanoma formation and progression.
The Clark's model depicts the linear progression of some melanomas. However, melanoma often follows a more complex non-linear model of progression and it eventually bypasses some steps of the Clark's model before progressing to an advanced primary tumor. Similarly, a tumor can metastasize before reaching the vertical growth phase and in some patients metastases are observed without any detectable primary tumor (adapted from: Damsky et al., 2014).

3.3 Sall4 in development

The homeotic spalt (sal) gene family was first identified in *Drosophila melanogaster* (Jürgens et al., 1988). In the fly it is required for patterning of the wing and of the embryonic termini (de Celis and Barrio 2009). The spalt gene family is highly conserved from invertebrates to humans (Figure 8) and its members encode transcription factors characterized by multiple double zinc finger motifs of the C2H2 type.

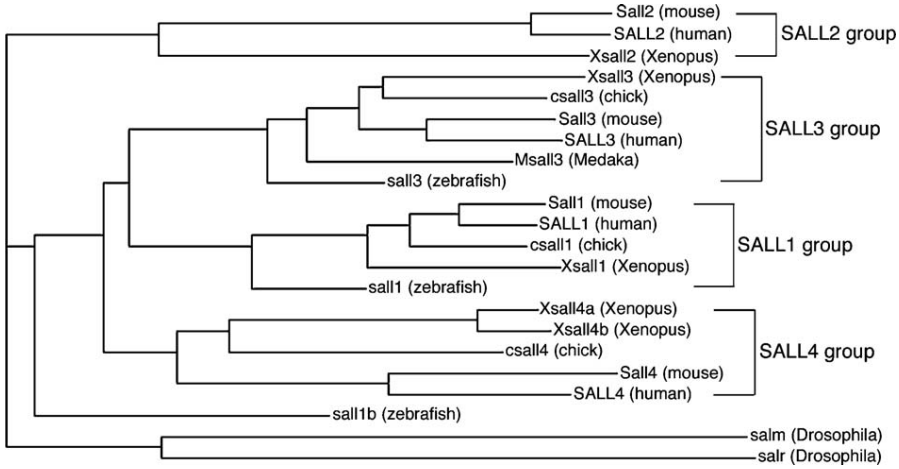

Figure 8. The spalt gene family in invertebrates and vertebrates.
The sal gene family can be divided into four different groups based on sequence comparison, named after the human gene: SALL1, SALL2, SALL3 and SALL4 group. (adapted from Sweetman and Münsterberg, 2006).

Four Sal-like genes are known in humans (*SALL1-4*) and mice (*Sall1-4*). Sall4 is ubiquitously expressed in the embryo and particularly enriched in the inner cell mass, where it plays a critical role in maintaining the pluripotency of ES cells (Zhang et al., 2006).

During development *Sall4* is required for embryo patterning as well as for limb and organ development (de Celis and Barrio, 2009). In vertebrate embryos, *Sall4* regulates NC cells that populate the sensory ganglia and it is also expressed in the branchial arches (Barembaum and Bronner-Fraser, 2004). Additionally, *Sall4* controls the invagination of the sensory placodes (Barembaum and Bronner-Fraser, 2007).

In adult animals, however, Sall4 is present in adult stem or stem like cell compartments, in particular it is enriched in the e.g. bone marrow, testis and ovary (Sweetman and Münsterberg, 2006).

3.3.1 Sall4 in embryonic stem cells

In the blastocyst, a first lineage commitment leads to the development of the inner cell mass and of the trophectoderm. The trophectoderm then generates the trophoblast that is responsible for providing nutrients to the embryo and to build up the extraembryonic tissues. Embryonic stem (ES) cells derive from the inner cell mass and they are able to differentiate into all embryonic germ layers. They are characterized by their pluripotency and ability to propagate (self-renewal).

Sall4 is enriched in ES cells and it was found to be a crucial factor in the mechanisms that regulate ES cell pluripotency. Sall4 interacts with Nanog and regulates Oct4 expression by directly activating the *Pouf5f1* promoter (Figure 9).

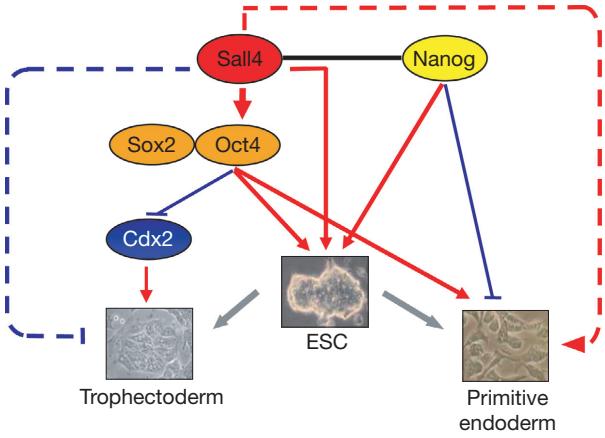

Figure 9. Schematic summary of the role of Sall4 in maintaining ES cell self-renewal and pluripotency. Sall4 directly regulates Oct4 by binding and transcriptionally activating the *Pou5f1* promoter. Sall4, Oct4 and Nanog are required for the maintenance of ES cell self-renewal and to prevent ES cell differentiation into trophectoderm or primitive endoderm. Positive regulation is indicated in red; repression is indicated in blue (adapted from: Zhang et al., 2006).

Moreover, genome-wide analysis demonstrated that Sall4 is a major transcriptional regulator of pluripotency in mouse ES cells (Yang et al., 2008). Interestingly, Sall4 can bind many more annotated genes within the promoter region than Oct4 or Nanog (Tanimura et al., 2013; Yang et al., 2008) (Figure 10), and it regulates a range of pathways that have explicit roles during development (Figure 11).

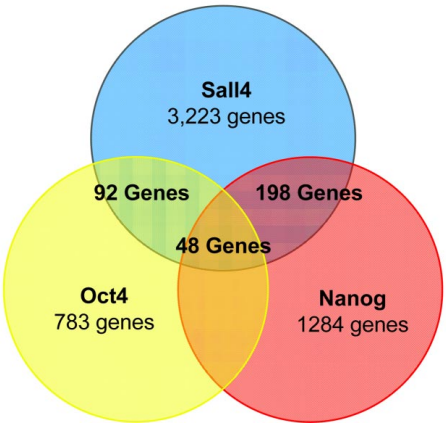

Figure 10. Target genes that are bound within the promoter region by Sall4, Oct4 and Nanog.

The Venn diagram illustrates that Sall4, Oct4 and Nanog share several target genes in common (adapted from: Yang et al., 2008).

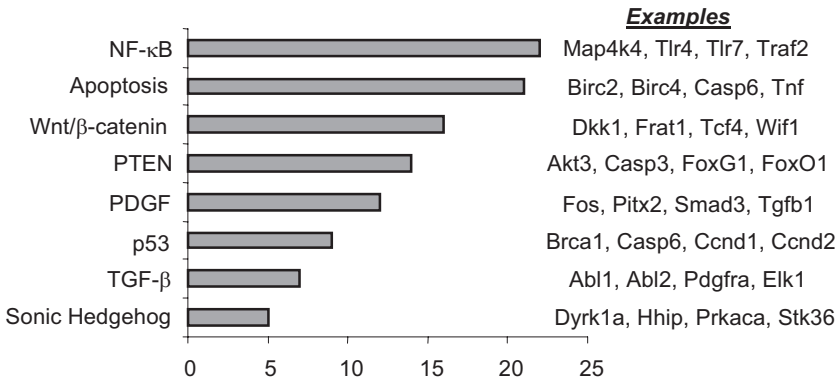

Figure 11. Sall4 regulates several pathways important for embryonic development.

Sall4 binds at the promoter region of a large number of genes that have distinct functions in maintaining ES cell pluripotency and in regulating differentiation (adapted from Yang et al., 2008).

3.3.2 Sall4 isoforms in ES cells

Sall4 exists in two isoforms, Sall4a and Sall4b (Figure 12), which are generated by different internal splicing of exon 2.

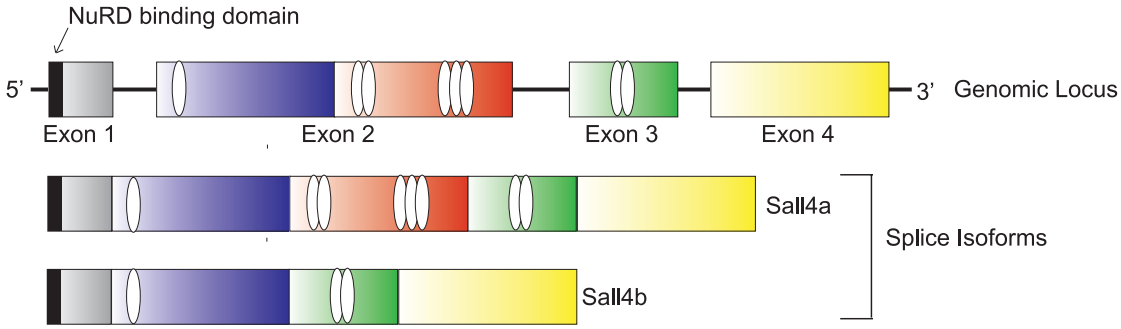

Figure 12. Genomic structure of the *Sall4* gene and its two protein isoforms.
Structure of the genomic locus of *Sall4* and of the protein isoforms Sall4a and Sall4b. Both isoforms contain a N-terminal NuRD binding domain (black rectangle) and Zinc finger domains (ovals) (adapted from: Rao et al., 2010).

Sall4a and Sall4b can build homo- and heterodimers with each other. Both isoforms can interact with Nanog to maintain ES cells pluripotency, even though they have slightly different functions. Sall4b builds homodimers or heterodimers together with Sall4a to positively regulate pluripotency genes (Figure 13). Sall4a, on the other hand, builds homodimers to regulate differentiation genes (Figure 13). Sall4b alone, but not Sall4a, can maintain pluripotency in mouse ES cells. Sall4a$^-$ Sall4b$^+$ ES cells indeed show a partially rescued pluripotency, although not all differentiation markers are completely inhibited. On the other side, Sall4a$^+$ Sall4b$^-$ ES cells lose pluripotency features and differentiate (Rao et al., 2010).

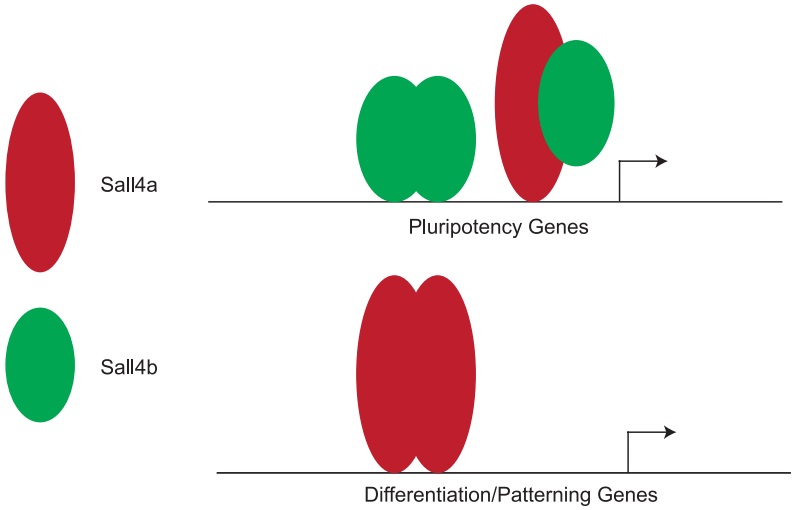

Figure 13. Sall4a and Sall4b homodimers and heterodimers have different functions.
Sall4b homodimers and Sall4a/Sall4b heterodimers regulate pluripotency genes, while Sall4a homodimers regulate differentiation genes (adapted from: Rao et al., 2010).

3.3.3 SALL4 in epigenetics

SALL4 can be a positive or negative regulator of gene expression depending on its interactions with the epigenetic machinery (Figure 14).

Sall4 is known to actively bind and activate the *Pouf5f1* promoter to positively regulate Oct4 expression. However, Sall4 can also act as a repressor through direct binding to the Mi2/NuRD HDAC complex. The Sall4-HDAC complex can prevent ES cell differentiation into trophectoderm through repression of the *Cdx2* promoter (Yuri et al., 2009), epigenetically inhibit somatic cell genes in primordial germ cells (Yamaguchi et al., 2015). SALL4 can also epigenetically repress the transcription of SALL1 and PTEN (Lu et al., 2009). In particular, SALL4 has been shown to regulate the epigenetic machinery by directly recruiting DNA methyltransferases (DNMT), HDAC1 and HDAC2 (Yang et al., 2012). Moreover, in hematopoietic stem cells SALL4 interacts with LSD1 (histone lysine-specific demethylase 1) to regulate stem cell proliferation and differentiation (Liu et al., 2013) (Figure 14).

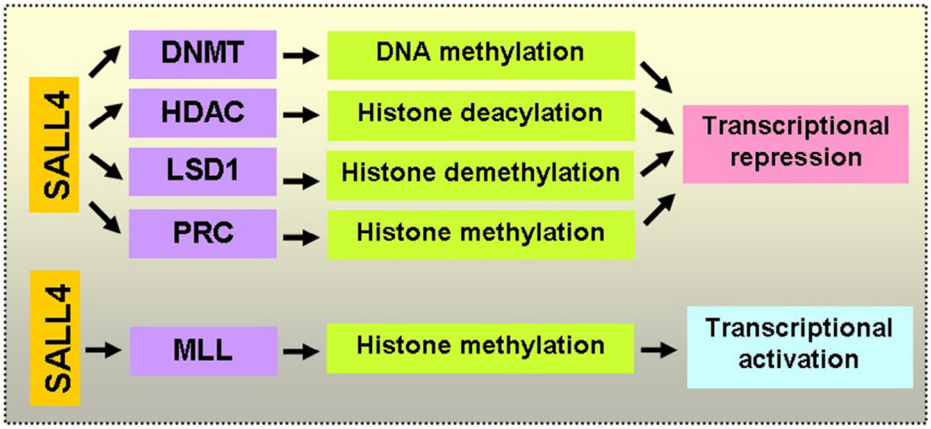

Figure 14. SALL4 regulation of the epigenetic machinery.
SALL4 represses transcription by actively recruiting DNA methyltransferases (DNMT), Mi-2/nucleosome remodeling and deacetylase (NuRD) complex, the histone demethylase LSD1 and the polycomb repression complex (PRC). SALL4 acts also as a transcriptional activator through regulation of the histone methyltransferase MLL (mixed-lineage leukemia) (adapted from: Zhang et al., 2015).

Similarly, in cancer SALL4 expression was correlated to HDACs activity in hepatocellular carcinoma (Zeng et al., 2014) and it has been shown to promote leukomogenesis by repressing PTEN through its direct binding to the HDAC complex (Gao et al., 2013).

Moreover, SALL4 has been shown to play a role in the regulation of H3K27 methylation. It can activate the transcription of BMI-1, a polycomb group member, in hematopoietic stem cells and in leukemia (Yang et al., 2007) and it is known to bind to several genes that are targeted by PRC1 and PRC2 (Yang et al., 2008) (Figure 14).

3.3.4 Sall4 in DNA damage response

ES cells have a higher genomic stability compared to somatic cells, which prevents the passage of aberrant information to the progeny. The mechanisms that conserve ES cell genomic stability and that react upon DNA damage are characterized by Sall4 modulation of the epigenetic machinery (Xiong et al., 2015). Sall4 is in fact associated to heterochromatin and upon DNA damage it is relocated to the γ-H2AX sites around DNA double strand breaks (DSBs) (Figure 15).

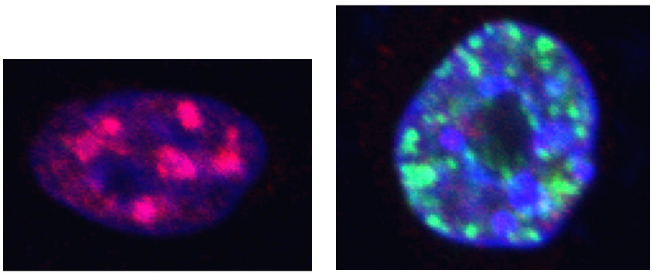

Figure 15. Sall4 relocation upon DNA damage.
In ES cells, Sall4 (red) is relocated from the heterochromatin to sites of DNA DSBs characterized by γ-H2AX (green) formation (adapted from Xiong et al., 2015).

In detail, Sall4 interacts with Rad50, which stabilizes the Mre11-Rad50-Nbs1 complex. Consecutively the Mre11-Rad50-Nbs1 complex recruits and activates the Ataxia Telangiectasia Mutated (ATM) response to DNA damage, by autophosphorylation of ATM at Ser1987. Sall4 is recruited to the sites of DNA DSBs by interaction with Baf60, which is a member of the SWI/SNF ATP-dependent chromatin remodeling complex. Finally, ATM phosphorylation activates the p53-mediated response to DNA damage (Xiong et al., 2015) (Figure 16).

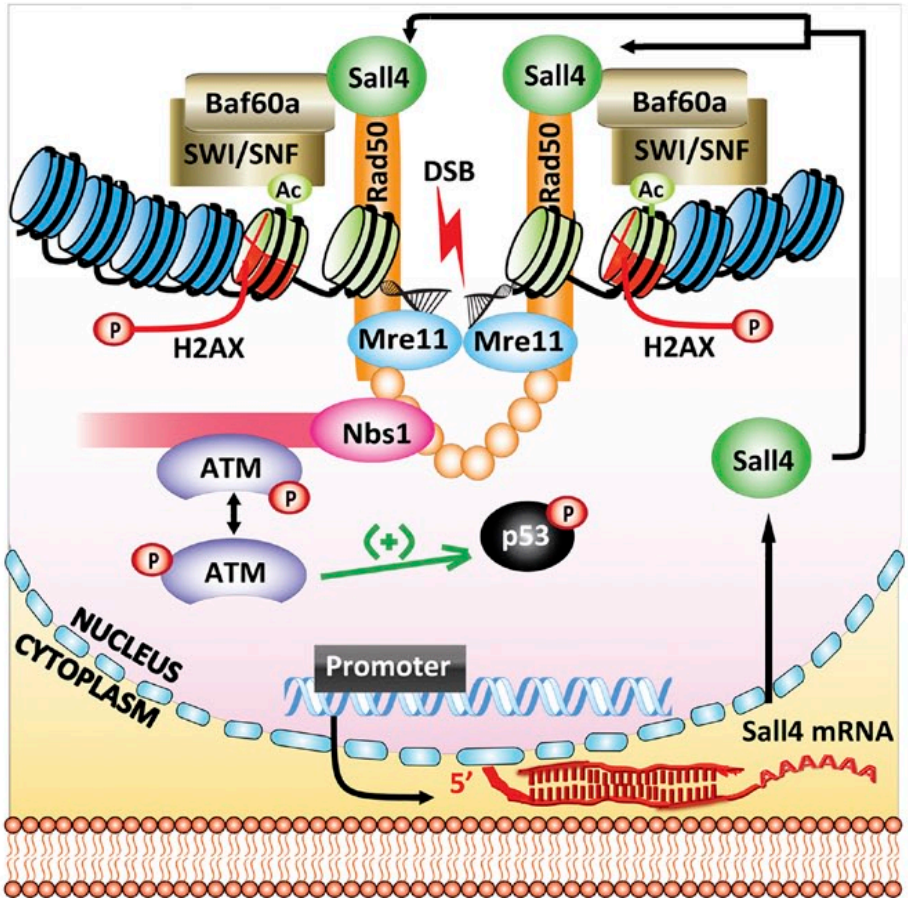

Figure 16. Sall4-mediated response upon DNA damage.
Sall4 activates ATM as a cellular response to DSBs in mouse ES cells. This mechanism protects ES cells from DSB-induced cytotoxicity and preserves their genomic stability (Adapted from: Xiong et al., 2015).

Sall4 function in the maintenance of genomic stability and the fact that Sall4 is aberrantly expressed in some tumorigenic cells, could suggest a potential role of Sall4 in the development of resistance to chemotherapy (Leslie 2015).

3.3.5 Sall4 in cell proliferation

In ES cells, Sall4 controls cell proliferation and its loss results in impaired cell proliferation characterized by a prolonged G1 phase and a shorter S phase (Sakaki-Yumoto et al., 2006, Yuri et al., 2009).
Similarly, SALL4 has been shown to be pro-proliferative and to activate BMI-1, which in turn inhibits $p16^{INK4a}$ and induces aberrant proliferation in leukemia (Yang et al., 2007). Additionally, SALL4 loss has been shown to reduce tumor proliferation in a

range of various tumor types suggesting SALL4 as a potentially interesting therapeutic target (Kobayashi et al., 2011; Li et al., 2015; Zhang et al., 2014a).

3.4 SALL4 in disease

3.4.1 SALL4 in developmental disorders

Mutations of the *SALL4* gene located on chromosome 20q13.13–q13.2 result into the autosomal dominantly inherited Duane-radial ray syndrome (Okhiro syndrome). This syndrome comprises the Duane anomaly that affects ocular motility as well as radial sided hand malformations (Kohlhase et al., 2002) (Figure 17). The disease often occurs accompanied by anal stenosis, heart, kidney and ears defects, facial asymmetry and pigmentation abnormalities (Al-Baradie et al., 2002; Kohlhase et al., 2002).

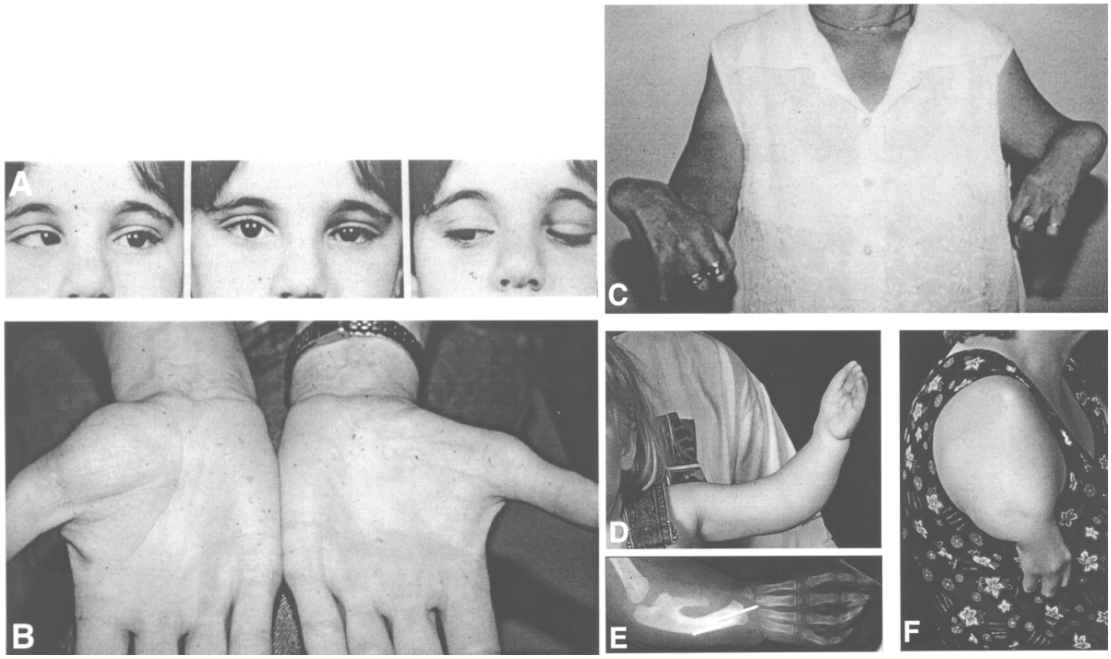

Figure 17. Patients affected by the Okihiro Syndrome.
(A) The patient suffers from a defect in ocular mobility characterized by the unability of abducting the eyes without closing of the palpebra. (B-C) Hand and (D-F) limb malformations in patients with the Okihiro Syndrome (adapted from: Kohlhase et al., 2002).

In particular, in regards to the ear malformation and defect, data obtained in chick embryos suggest that Sall4 plays an important role during the invagination of the sensory placodes and it may, thus, be involved in ear development (Barembaum and Bronner-Fraser, 2007).

3.4.2 SALL4 in cancer

SALL4 up-regulation has been reported in various types of tumor as in germ cell tumors, e.i. testicular germ cell tumor, in yolk sac tumor (Bai et al., 2013; Cao et al., 2009), in gastrointestinal carcinonoma (Zhang et al., 2014a), in glioma (Zhang et al., 2014b), in hepatocellular carcinoma (Yong et al., 2013), in endometrial cancer (Li et al., 2015), in colorectal cancer (Forghanifard et al., 2013), in breast cancer (Kuribayshi et al., 2011), in lung cancer (Fujimoto et al., 2014; Kobayashi et al., 2011), in chronic myeloid leukemia (Gao et al., 2011; Lu et al., 2011), in acute myeloid leukemia (Ma et al., 2006) and in B cell lymphoma (Ueno et al., 2014). SALL4 regulates a variety of cellular functions that are responsible for tumor initiation and progression and high levels of protein expression have been associated with worse survival prognosis in the tumor types mentioned above (Figure 18). High SALL4 levels have been indeed linked to increased levels of BMI-1 (Yang et al., 2007), of CyclinD1 (CCND1) and D2 (CCND2), and overall to increased tumor proliferation and, thus worse prognosis. Interestingly, SALL4 loss leads to decreased cellular proliferation and is linked to improved survival (Kobayashi et al., 2011; Li et al., 2015; Yang et al., 2007; Zhang et al., 2014a). Moreover, high SALL4 levels are correlated to an EMT signature that is characterized by elevated levels of mesenchymal cell markers such as TWIST and N-cadherin (CDH2) as well as diminished expression of epithelial cell markers such as E-cadherin (CDH1). Hence, high SALL4 levels account for increased number of metastases resulting in worse survival expectancy, while loss of SALL4 reduces cellular motility and decreases metastasis formation (Cao et al., 2009; Forghanifard et al., 2013; Itou et al., 2013; Zhang et al., 2014a).

Of note, SALL4 expression has also been linked to the acquisition of pluripotency features such as expression of EpCAM in hepatocellular cancer (Zeng et al., 2014), and of SOX2, BMI-1, CD133 and LIN28B in gastric cancer (Zhang et al., 2014a).

Furthermore, high SALL4 levels have been linked to the development of chemoresistance in several types of cancer, such as leukemia (Hupfeld et al., 2013), hepatocellular cancer (Oikawa et al., 2013) and endometrial cancer (Li et al., 2015; Liu et al., 2015).

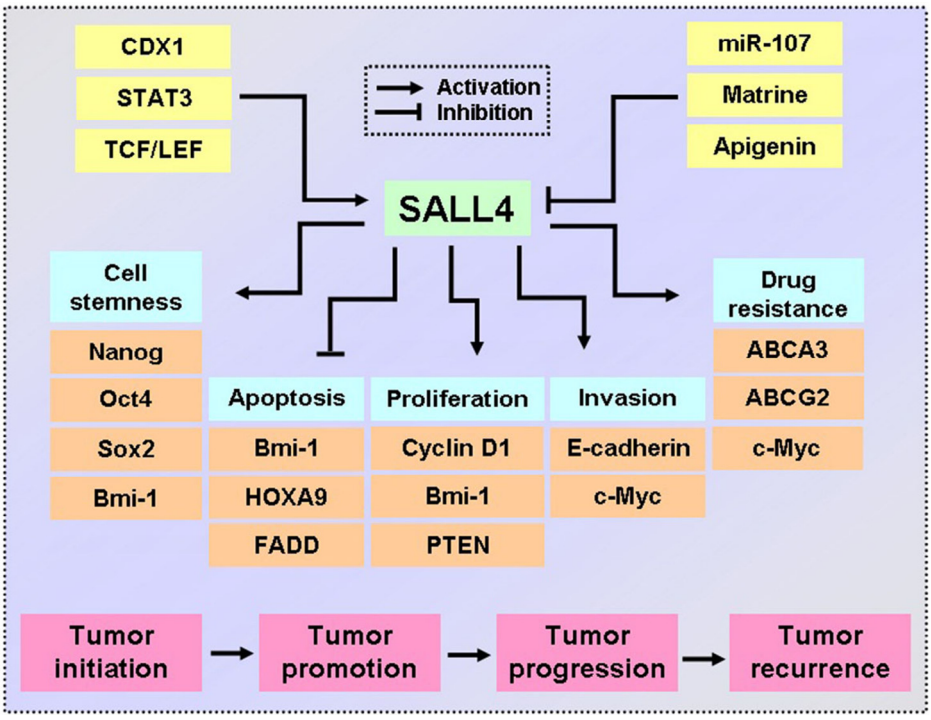

Figure 18. SALL4 regulates several signaling pathways during tumorigenesis.
SALL4 can be activated by CDX1, STAT3 and TCF/LEF. In turn, SALL4 positively or negatively regulates a number of signaling pathways that control cell stemness, apoptosis, proliferation, invasion and drug resistance. SALL4 is, thus, an important factor in cancer initiation and progression (adapted from: Zhang et al., 2015).

3.4.3 SALL4 in melanoma

SALL4 function has been extensively investigated both in development as well as in cancer. However, whether SALL4 may also play a role in the formation and progression of melanoma has not been studied so far, opening the possibility to future novel investigations (4.2 The roles of Sall4 in melanoma).

4 Results

4.1 Premigratory and Migratory Neural Crest Cells are Multipotent In Vivo

Cell Stem Cell **5**: 314-22; 2015

Arianna Baggiolini[1], Sandra Varum[1], José María Mateos[2], Damiano Bettosini[1], Nessy John[1], Mario Bonalli[1], Urs Ziegler[2], Leda Dimou[3], Hans Clevers[4], Reinhard Furrer[5], Lukas Sommer[1].

[1]Institute of Anatomy, University of Zurich, 8057 Zurich, Switzerland

[2]Center for Microscopy and Image Analysis, University of Zurich, 8057 Zurich, Switzerland

[3]Department of Physiological Genomics, Ludwig Maximilian University of Munich, 80336 Munich, Germany

[4]Hubrecht Institute, KNAW and University Medical Center Utrecht, Uppsalalaan 8, 3584 CT Utrecht, The Netherlands

[5]Institute of Mathematics, University of Zurich, 8057 Zurich, Switzerland

4.1.1 My contribution to this work

- Design of the experiment with inputs from Sandra Varum and Prof. Lukas Sommer
- Execution of all the experiments and collection of the data
- Breeding of the mice used in the study, including genotyping, time mating and collection of the embryos
- Production of all the figures
- Design of the paper outline together with Prof. Lukas Sommer. Writing of the manuscript with inputs and corrections provided by Sandra Varum and Prof. Lukas Sommer

4.1.2 In brief

The neural crest (NC) gives rise to a broad variety of neural and non-neural cell types during vertebrate development, but whether NC cells are multipotent or rather a heterogeneous population of restricted progenitors is unclear. In this study, we performed an in vivo lineage tracing analysis of single premigratory and migrating NC cells and demonstrated that the majority of NC cells are multipotent in vivo (Baggiolini et al., 2015; Figure 19).

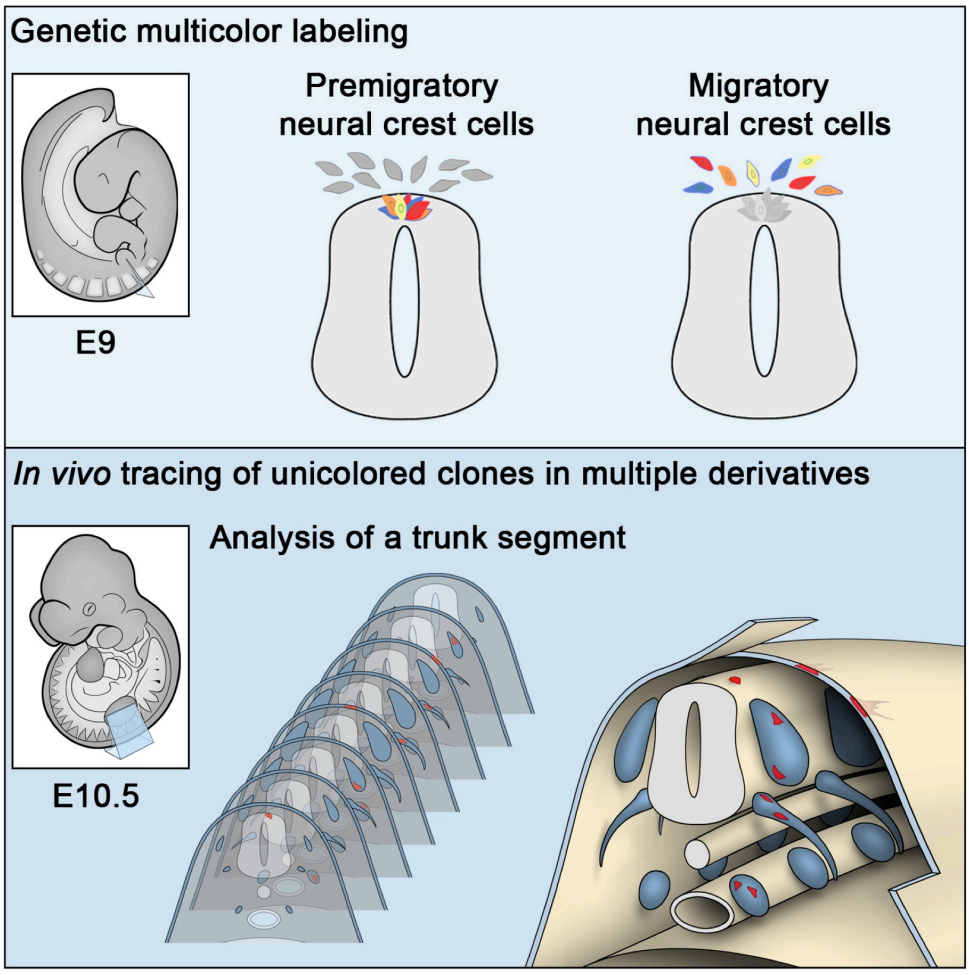

Figure 19. In vivo lineage tracing of premigratory and migratory NC cells.

We used mouse genetics to label NC cells at the premigratory and migratory stage in an inducible way in vivo at E9. The recombined clones were analyzed at E10.5 by determination of color, location and expression of differentiation markers.

4.1.3 Summary

The neural crest (NC) is an embryonic stem/progenitor cell population that generates a diverse array of cell lineages, including peripheral neurons, myelinating Schwann cells, and melanocytes, among others. However, there is a long-standing controversy as to whether this broad developmental perspective reflects in vivo multipotency of individual NC cells or whether the NC is comprised of a heterogeneous mixture of lineage-restricted progenitors. Here, we resolve this controversy by performing in vivo fate mapping of single trunk NC cells both at premigratory and migratory stages using the R26R-Confetti mouse model. By combining quantitative clonal analyses with definitive markers of differentiation, we demonstrate that the vast majority of individual NC cells are multipotent, with only few clones contributing to single derivatives. Intriguingly, multipotency is maintained in migratory NC cells. Thus, our findings provide definitive evidence for the in vivo multipotency of both premigratory and migrating NC cells in the mouse.

4.1.4 Introduction

Neural crest (NC) cells are a defining feature of vertebrates that give rise to many of the cell types that imbue them with their unique characteristics, such as jaws and peripheral nervous system. They represent an important population from the perspective of regenerative medicine, since they contribute to many critical cell types that are prone to both developmental birth defects and metastatic transformation in adults. In the embryo, NC cells arise from the dorsal margin of the neural plate border during neurulation (Le Douarin et al., 2008), undergo an epithelial to mesenchymal transition (EMT), and migrate extensively throughout the embryo to populate numerous derivatives. In fact, NC cells have one of the broadest developmental potentials of any vertebrate cell type.

This has raised the important question of what underlies this remarkable ability to contribute to so many diverse derivatives, ranging from craniofacial cartilage to neurons and glia to melanocytes. One model suggests that the entire NC cell population is “multipotent” and capable of forming many or all of the potential derivatives. At the opposite extreme, the NC might instead represent a heterogeneous mixture of “predetermined” cells, each fated to form a particular derivative. Finally, the NC may be comprised of a mixture of these two types of precursor cells.

Over several decades, there has been considerable controversy regarding the correct answer to this pivotal question (Dupin and Sommer 2012). Early studies concluded that NC cells were multipotent *in vivo* (Bronner-Fraser and Fraser, 1988; Bronner-Fraser and Fraser, 1989; McKinney et al., 2013; Serbedzija et al., 1990) and *in vitro* (Baroffio et al., 1988; Dupin et al., 2010; Stemple and Anderson, 1992). However, other publications instead reported that the NC was comprised of heterogeneous populations of restricted progenitor cells (Harris and Erickson, 2007; Henion and Weston, 1997; Krispin et al., 2010; Luo et al., 2003; Ziller et al., 1983). In particular, recent studies using vital dye microinjection or electroporation of a GFP-reporter proposed that premigratory NC cells are fate-determined prior to delamination and organized according to a spatio-temporal pattern in the dorsal neural tube (dNT) of chick embryos (Krispin et al., 2010; Nitzan et al., 2013). In this model, each NC cell gives rise only to a specific cell type, depending on the timing of emigration and the site of origin in the dNT.

Despite technical differences potentially explaining these discrepancies, it has so far not been possible to reconcile these studies (Dupin and Sommer, 2012). Early *in vivo* lineage tracing studies lacked the ability to identify specific cell types other than by location in various derivatives. Whereas clonal analysis *in vitro* circumvents these problems, the culture techniques analyze cells outside of their endogenous environment and expose cells to culture media, which may alter cell behavior. Moreover, there is very little information regarding the developmental potential of NC cells in mammalian model systems. Lineage-tracing studies were originally performed in chicken embryos by vital dye injection, which is very challenging to carry out in mouse embryos (Serbedzija et al., 1990). With the advent of modern transgenic technology, it is now possible to resolve the controversy regarding NC potentials in the mammalian embryo. Recently, transgenic mouse models have been established that allow genetic lineage tracing in mammalian embryos and adult organs (Lescroart et al., 2010; Mathis et al., 1997; Tzouanacou et al., 2009). One of these models is the *R26R-Confetti* mouse (Snippert et al., 2010), which has proved very useful for mapping fates of single cells in adult tissues. Here, we use this approach to perform genetic *in vivo* fate mapping of NC cells. Our results definitively show that the vast majority of murine NC cells, both prior to and during migration, are multipotent.

4.1.5 Results

4.1.5.1 Multicolor labeling of premigratory and migratory NC cells

To achieve temporal tracing of NC cells, we used the CreER loxP system, by which activation of CreER recombinase can be induced in embryos in a cell type- and stage-dependent manner upon tamoxifen (TM) injection of pregnant females. CreER-mediated genomic recombination of reporter alleles leads to marker expression that can be tracked in CreER-expressing cells and all of their daughter cells, allowing fate mapping of these cells in vivo. To trace the fate of premigratory NC cells, we made use of *Wnt1-CreERT* animals. Accordingly, *CreERT*-induced b-galactosidase expression in *Wnt1-CreERT* embryos carrying the *CreERT*-reporter allele *R26R-Rosa* was observed in the dNT and in all NC derivatives (Figures 20A and 20B) (Soriano, 1999; Zervas et al., 2004). To trace NC cells that have already emigrated from the dNT, we used the *Sox10-CreERT2* line (Simon et al., 2012). In the mouse, Sox10 expression follows Wnt1 expression and marks virtually all NC cells immediately after their delamination from the dNT (Hari et al., 2012). Therefore, TM-induced recombination at E.9.0 in *Sox10-CreERT2 R26R-Rosa* embryos resulted in b-galactosidase expression in all NC derivatives, but not the dNT (Figures 20C and 20D).

Upon *CreER* activation and recombination across sets of loxP sites in the *R26R-Confetti* reporter mouse, one out of four fluorescent reporter proteins, nuclear GFP, cytoplasmic YFP, cytoplasmic RFP, or membrane-bound CFP, is expressed. To increase the colors available for the tracing, we used animals homozygous for the *R26R-Confetti* allele. In these animals, both alleles are recombined, which leads to expression of two out of the four available fluorescent proteins, allowing a total of 10 color combinations (Figure 21). In both *Wnt1-CreERT R26R-Confetti* (hereafter called *Wnt1-CreERT)* (Figures 20E–20J) and in *Sox10-CreERT2 R26R-Confetti* (Sox10-CreERT2) embryos (data not shown), expression of the following single color combinations was readily detectable: red (rfp, Figure 20E); yellow (yfp, Figure 20F); and blue (cfp, Figure 20G). In addition, we observed the expression of mixed color combinations, such as red and blue (rfp cfp, Figure 20H), red and yellow (rfp yfp, Figure 20I), and yellow and blue (yfp cfp, Figure 20J). In contrast, color combinations with the fluorescent protein GFP were extremely rare, indicating that not all theoretically possible color combinations were equally represented.

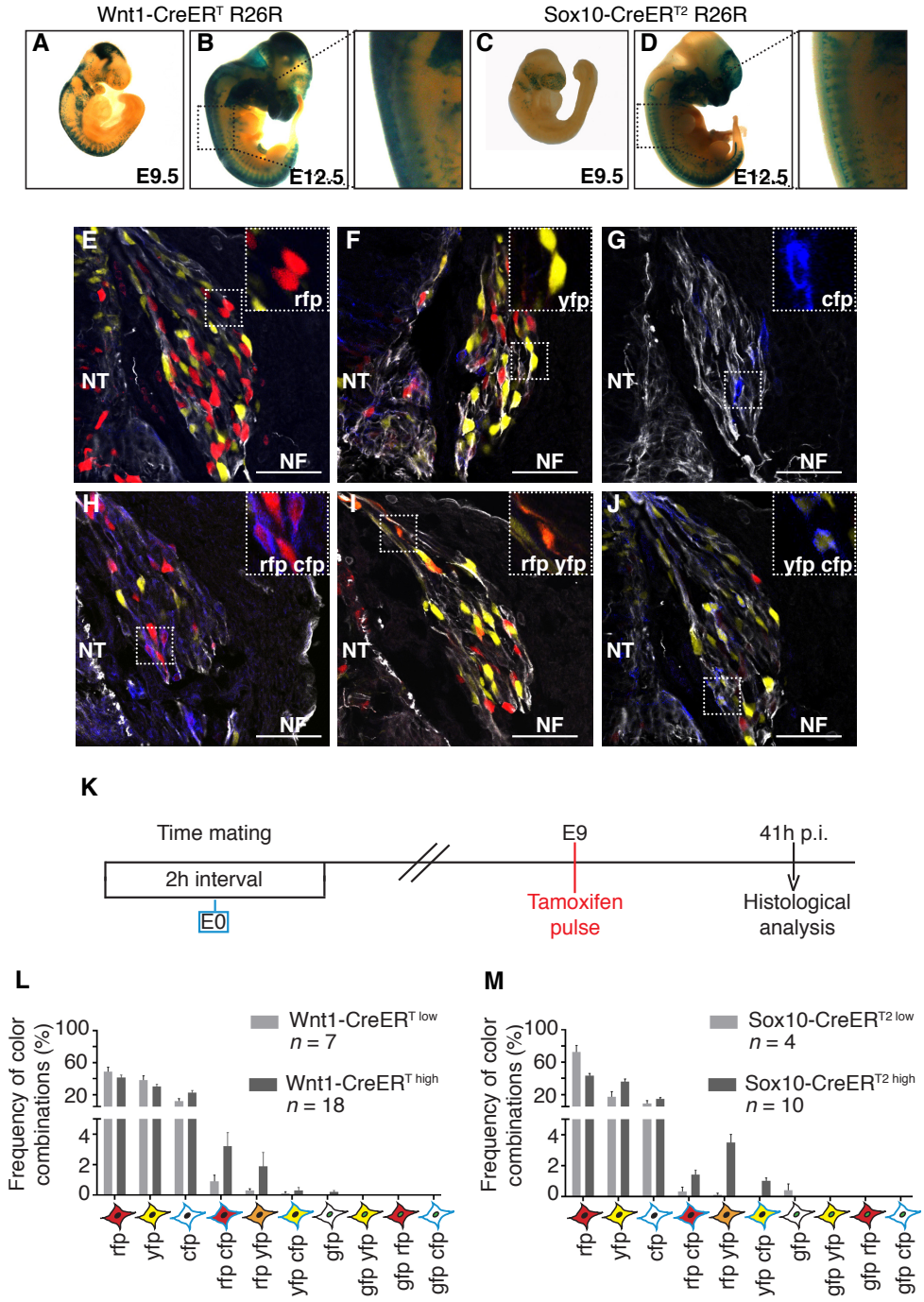

Figure 20. Multicolor tracing of premigratory and migratory NC Cells (A–D) (A and B) b-galactosidase expression in premigratory NC cells in E9.5 and E12.5 *Wnt1-CreERT R26R* embryos and in migratory NC cells in *Sox10-CreERT2 R26R* embryos ([C] and [D]). (E–J) In vivo expression of the single-color combinations rfp (E), yfp (F), and cfp (G) and of the mixed color combinations rfp cfp (H), rfp yfp (I), and yfp cfp (J). Neurofilament staining (NF, in white) delineates the structure of the dorsal root ganglia (DRG).

(K) Experimental outline for the multicolor lineage tracing approach. E0, embryonic day 0; p.i., post injection of TM. (L and M) Frequencies of the color combinations in the four cases analyzed (Wnt1-CreERT and *Sox10- CreERT2* at low and high recombination densities). For numbers of analyzed embryos, see 4.1.7 Experimental Procedures. Scale bars: 50 mm. See also Figure 21 and Table 1.

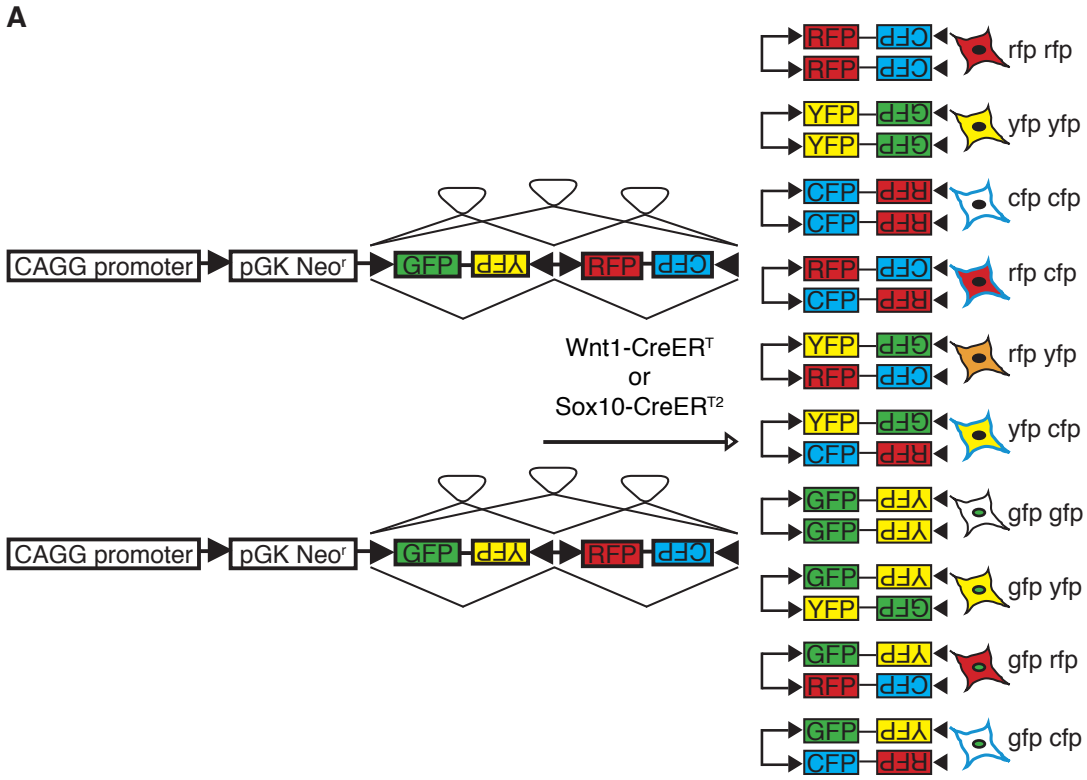

FIGURE 21: The R262-Confetti construct.

(A) Confetti construct inserted in the *Rosa26* locus. Upon *Wnt1-CreERT* or *Sox10- CreERT2* activation, recombination occurs across different pairs of *loxP* sites and results in expression of one out of the four possible fluorescent reporter proteins: nuclear GFP, membrane-associated CFP, cytoplasmic RFP, cytoplasmic YFP. Recombination in embryos homozygous for the *R26R-Confetti* allele allows up to ten different fluorescent proteins combinations. For the single color combinations, rfp, yfp and cfp, the recombination of only one of the two *R26R-Confetti* alleles cannot be excluded, since limiting dosages of TM were used.

4.1.5.2 Multicolor output depends on promoter activity and recombination density

The frequency of color combinations observed upon *CreER*- mediated recombination of a multicolor *Cre* reporter influences the probability of whether a cohort of cells marked by a single color derives from one or more founder cells. Therefore, we examined the frequency of different colors expressed in E10.5 *R26R-Confetti* embryos of both *CreER* lines (Figure 20K). A single limiting dose of TM resulted in few recombination events. Quantification of low-TM-dose-treated E10.5 *Wnt1-CreERT R26R-Confetti* embryos (Wnt1-CreERT low) revealed that the mixed color combinations were expressed in only 0.1%–0.9% of the recombined NC cells (Figure 20L; Table 1). Similarly, in low-TM-dose-treated *Sox10-CreERT2 R26R-Confetti* embryos (Sox10-CreERT2 low), mixed colors were found at very low frequencies (Figure 20M; Table 1). In contrast, the pure colors red, yellow, or blue were consistently expressed in recombined NC cells in both *CreER* lines (Figures 20L and 20M; Table 1).

These findings prompted us to increase the level of recombination for both *CreER* lines, in order to obtain more NC cells expressing rare color combinations. For the *Wnt1-CreERT R26R-Confetti* line, higher recombination density achieved by elevating the TM dose (Wnt1-CreERT high) resulted in increased, but still low, occurrence of the rare color combinations (0.3%– 3.2% of all recombined cells) (Figure 20L; Table 1). Similarly, elevating the TM concentration in the *Sox10-CreERT2 R26R-Confetti* line (Sox10-CreERT2 *high)* allowed increased representation of the mixed color combinations (1.0%–3.5%) (Figure 20M; Table 1). Summarizing, in our system we were able to trace NC cells not only at two different developmental stages, namely at the premigratory and at the migratory stage, but also at two different recombination densities producing different color outputs. The most frequent color combinations allowed clonal tracing when only few recombination events occurred. Rare fluorescent marker combinations, on the other hand, could be used to discern single clones at both low and high recombination densities.

	Wnt1-CreER$^{T\ low}$		Wnt1-CreER$^{T\ high}$		Sox10-CreER$^{T2\ low}$		Sox10-CreER$^{T2\ high}$	
	Average%	SEM (+/-)	Average%	SEM (+/-)	Average%	SEM (+/-)	Average%	SEM (+/-)
rfp 	48.69	5.47	41.48	2.91	72.69	7.91	43.50	2.64
yfp 	37.89	5.55	30.24	2.57	17.35	6.57	35.94	3.27
cfp 	12.06	2.87	22.62	2.52	9.18	3.28	14.58	1.69
rfp cfp 	0.95	0.37	3.25	0.85	0.33	0.33	1.43	0.29
rfp yfp 	0.28	0.13	1.93	0.90	0.07	0.07	3.53	0.45
yfp cfp 	0.12	0.10	0.30	0.18	n.o.	n.o.	1.01	0.21
gfp 	n.o.	n.o.	0.17	0.11	0.38	0.38	n.o.	n.o.
gfp rfp 	n.o.	n.o.	n.o.	n.o.	n.o.	n.o.	n.o.	n.o.
gfp yfp 	n.o.	n.o.	n.o.	n.o.	n.o.	n.o.	n.o.	n.o.
gfp cfp 	n.o.	n.o.	n.o.	n.o.	n.o.	n.o.	n.o.	n.o.

TABLE 1: Frequency of color representations in NC cells traced by *R26R-Confetti.* Frequency of the different color combinations represented in the Figure 20L and 20M for *Wnt1-CreERT* and *Sox10-CreERT2* embryos analyzed at low and high recombination densities. To calculate the color densities for the *Wnt1-CreERT* line we analyzed 7 embryos (14 DRG-units, 4 litters) and 18 embryos (36 DRG-units, 7 litters) at low and at high recombination densities respectively. To measure the color frequencies for the *Sox10-CreERT2* line we analyzed 4 embryos (9 DRG-units, 2 litters) and 10 embryos (22 DRG-units, 5 litters) at low and high recombination densities respectively. n.o. indicates not observed situations.

4.1.5.3 Representation frequencies of recombined NC cells in trunk derivatives

NC cells in the trunk of mouse embryos give rise to several structures, such as dorsal root ganglia (DRG), Schwann cells associated with peripheral nerves as, for instance, evident in the ventral root (VR), sympathetic ganglia (SG), and finally cells that migrate along the dorsal lateral pathway (DLP) to generate melanocytes. As expected, all these derivatives were marked in *Wnt1-CreERT* and *Sox10-CreERT2* embryos (Figures 22A–2F; data not shown). Moreover, tracing NC cells at the premigratory stage with the *Wnt1-CreERT* line allowed the observation of recombined cells in the dNT, which we defined as the most dorsal three cell layers of the neural tube (Figures 22A and 22B).

The likelihood to detect daughter cells of a NC progenitor cell in different target structures is possibly dependent on the relative sizes of these structures: The bigger a given compartment, the more likely it might be for a daughter cell to end up in this compartment. In *Wnt1-CreERT* embryos, we observed 7.6%– 14.0% of recombined cells in the dNT (Figure 22G; Table 2), while no recombined cells were found in the dNT of *Sox10- CreERT2* embryos. In all conditions, the majority of recombined cells were found in the biggest trunk NC derivative, the DRG (Figures 22C and 22G; Table 2). The SG and the VR were populated by comparable numbers of recombined NC cells, while the DLP was the derivative with the lowest number of recombined cells (Figures 22D–22G; Table 2). Given the number of possible cell divisions in a time window of 41 hr (Figure 20K), the elevated numbers of some recombined cells of the same color in certain derivatives cannot be explained only by differential proliferation in these derivatives. Therefore, the fact that the majority of recombined cells were present in the bigger derivatives is likely due to higher numbers of migratory NC cells populating these derivatives.

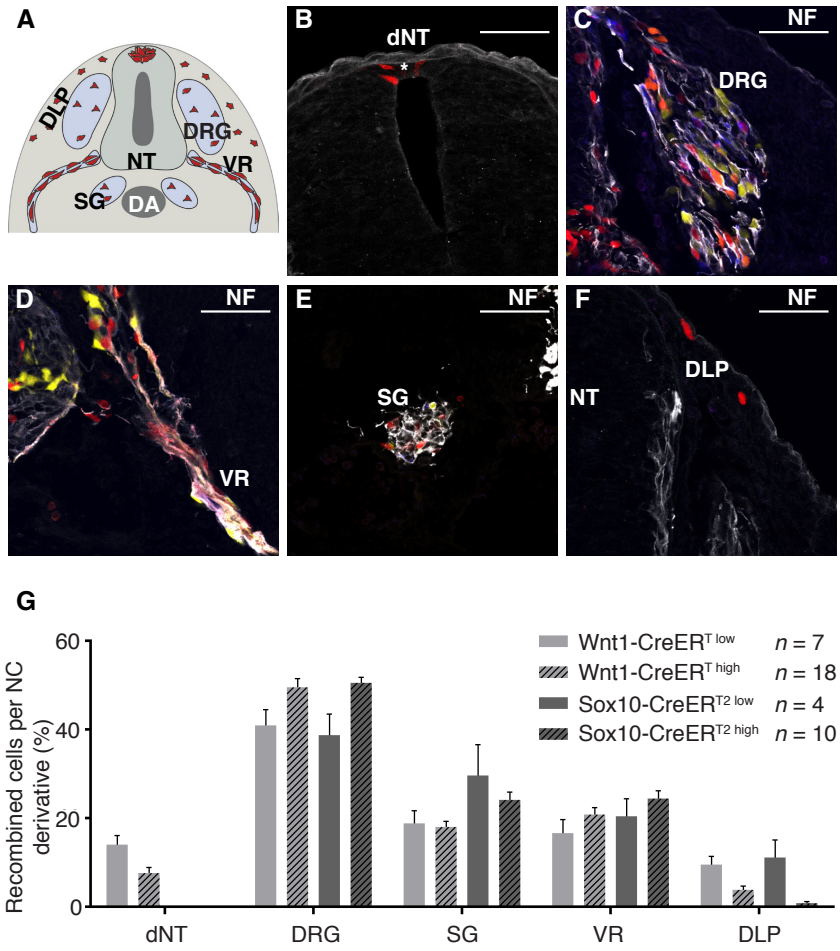

Figure 22. Frequencies of genetically traced cells in trunk derivatives of the NC. (A–F) (A) Schematic drawing of a transverse section with NC cells (in red) in the dorsal lateral pathway containing cells of the melanocytic lineage (DLP), sensory dorsal root ganglia (DRG), sympathetic ganglia (SG), and ventral root with Schwann cells (VR). Recombined NC cells are found in vivo in the dNT (B), DRG (C), VR (D), SG (E), and DLP (F). (G) Percentages of recombined cells per derivative in *Wnt1-CreERT* and Sox10-CreERT2 embryos at low and high recombination densities, respectively. For numbers of analyzed embryos, see 4.1.7 Experimental Procedures. Scale bars: 50 mm. See also Table 2.

	Wnt1-CreER$^{T\ low}$		Wnt1Cre-ER$^{T\ high}$		Sox10-CreER$^{T2\ low}$		Sox10-CreER$^{T2\ high}$	
	Average%	SEM (+/-)	Average%	SEM (+/-)	Average%	SEM (+/-)	Average%	SEM (+/-)
dNT	14.02	2.11	7.64	1.28	n.o.	n.o.	n.o.	n.o.
DRG	40.91	3.62	49.58	1.87	38.70	4.77	50.55	1.30
SG	18.88	2.78	18.01	1.26	29.66	6.91	24.13	1.80
VR	16.63	3.10	20.88	1.53	20.44	4.00	24.48	1.74
DLP	9.55	1.83	3.88	0.86	11.19	3.90	0.84	0.40

TABLE 2: Derivative representations upon *R26R-Confetti*-mediated NC cell tracing. Percentage of recombined cells per NC derivatives for each of the four experimental setups. To calculate the percentage of recombined cells per derivative in the *Wnt1-CreERT* line we analyzed 7 embryos (14 DRG-units, 4 litters) and 18 embryos (36 DRG-units, 7 litters) at low and at high recombination densities, respectively. For the *Sox10-CreERT2* line we analyzed 4 embryos (9 DRG-units, 2 litters) and 10 embryos (22 DRG-units, 5 litters) at low and high recombination densities, respectively. n.o. indicates not observed situations.

4.1.5.4 Qualitative assessment of multicolor fate mapping of single premigratory NC cells

Our data reveal that *CreER*-mediated recombination of the *R26R-Confetti* allele allows tracking of NC cells by different color combinations at defined frequencies. We next exploited this system to track the fate of individual NC cells, with a first emphasis on premigratory cells. E10.5 embryos were collected 41 hr post-TM injection (Figure 20K). As previously demonstrated, the mean cell-cycle length of E9.5 NC cells is 10.6 hr (Gonsalvez et al., 2013). The literature does not provide exact error intervals for the cell division rate, and it is likely that during 41 hr of NC development the cell-cycle length varies and becomes cell type and derivative specific. Since these variations are unknown and can hardly be determined, we first applied a fixed assumption that NC cells could divide three times between TM-induced recombination and the time point of analysis. Hence, we initially considered only equally colored cohorts of cells with a minimum of two and a maximum of eight cells, with the goal that such a stringent analysis would serve as a basis to establish and assess a statistical method able to discern between multipotency and cell fate restriction.

For the analysis of putative clones, we focused on the forelimbs area, taking into account cells of the same color that were present in a unit defined by a trunk segment spanning the width of one DRG (10–14 transverse sections of 10 mm thickness each) (Figure 23). 3D reconstruction confirmed that our recombination protocol allowed marking of a small number of equally colored NC daughter cells disseminating over various trunk derivatives (Figure 23; data not shown).

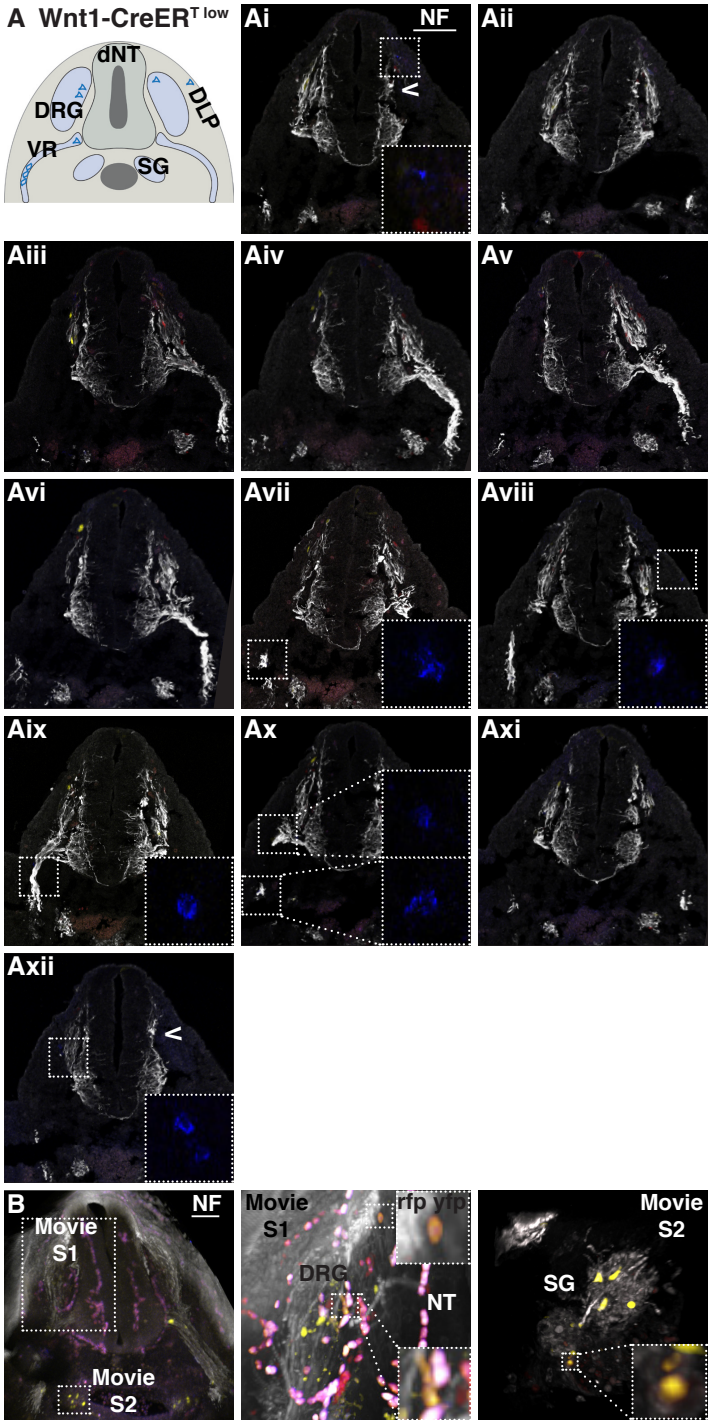

FIGURE 23: DRG-unit and clone representations.

(A) Schematic summary of an 8-cells cfp+ clone analyzed in an E10.4 *Wnt1-CreERT* low embryo. (Ai-Axii) Pictures of all transversal embryonic sections spanning the entire DRG-unit, in which the cfp+ clone was observed. Arrows in Ai and Axii indicate the beginning and the end of the DRG-unit. (B) Z 316.7 µm stack of the trunk segment of an E10.5 *Wnt1-CreERT high* embryo (data not shown). Scale bars: 100 µm.

Consecutive transverse sections at the level of the forelimbs were imaged (Figure 23Ai–23Axii), and the number and location of equally colored recombined cells per trunk segment were assessed (Figure 24). For the different conditions used, the density of putative clones ranged between 0.8 ± 0.1 and 1.0 ± 0.3 clones per unit, with most units analyzed containing 0 or 1 clone (Table 3). *Wnt1-CreER* embryos displayed many putative clones with progeny in multiple derivatives, including sometimes the dNT and DLP (Figures 24A and 25A). To corroborate these results, we analyzed *Wnt1-CreERT* high embryos, in which we observed cohorts of cells (two to eight cells) expressing rare mixed color combinations (Figures 24A and 25C). Strikingly, putative clones were mostly spread over multiple derivatives (Figures 24A and 25C).

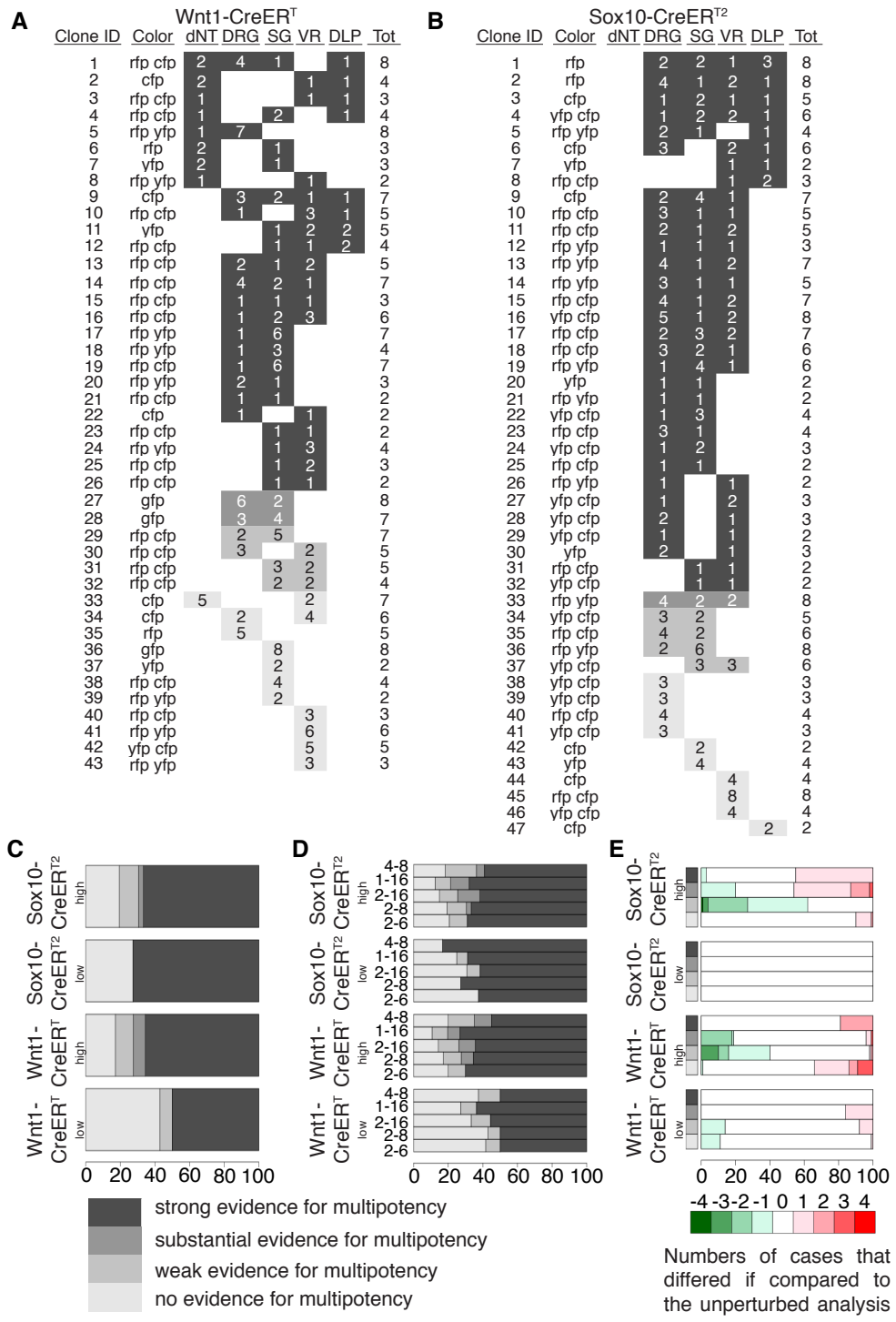

Figure 24. Lineage tracing analysis of premigratory and migratory NC cells and mathematical evaluation of fate determination in NC cells

(A and B) List of the clonal frameworks for premigratory (A) and migratory (B) NC cells ordered by degree of evidence of multipotency. Both conditions of low and high recombination densities were pooled to compare exclusively premigratory versus migratory NC.

(C) Percentages of clones expressing no, weak, substantial and strong evidence of multipotency for both premigratory and migratory NC cells at low and high recombination densities. (D) Degrees of evidence of multipotency when the minimum and the maximum size of a clone were changed for premigratory and migratory NC at low and high recombination densities. (E) Sensitivity assay of the statistical evaluation method. Each of the 16 barplots shows the proportion of cases that changed (ranging from loss of four clones up to gain of four clones) upon 100 different simulations. White indicates no change, red cases that were added and green cases that were lost. For numbers of analyzed embryos, see 4.1.7 Experimental Procedures.

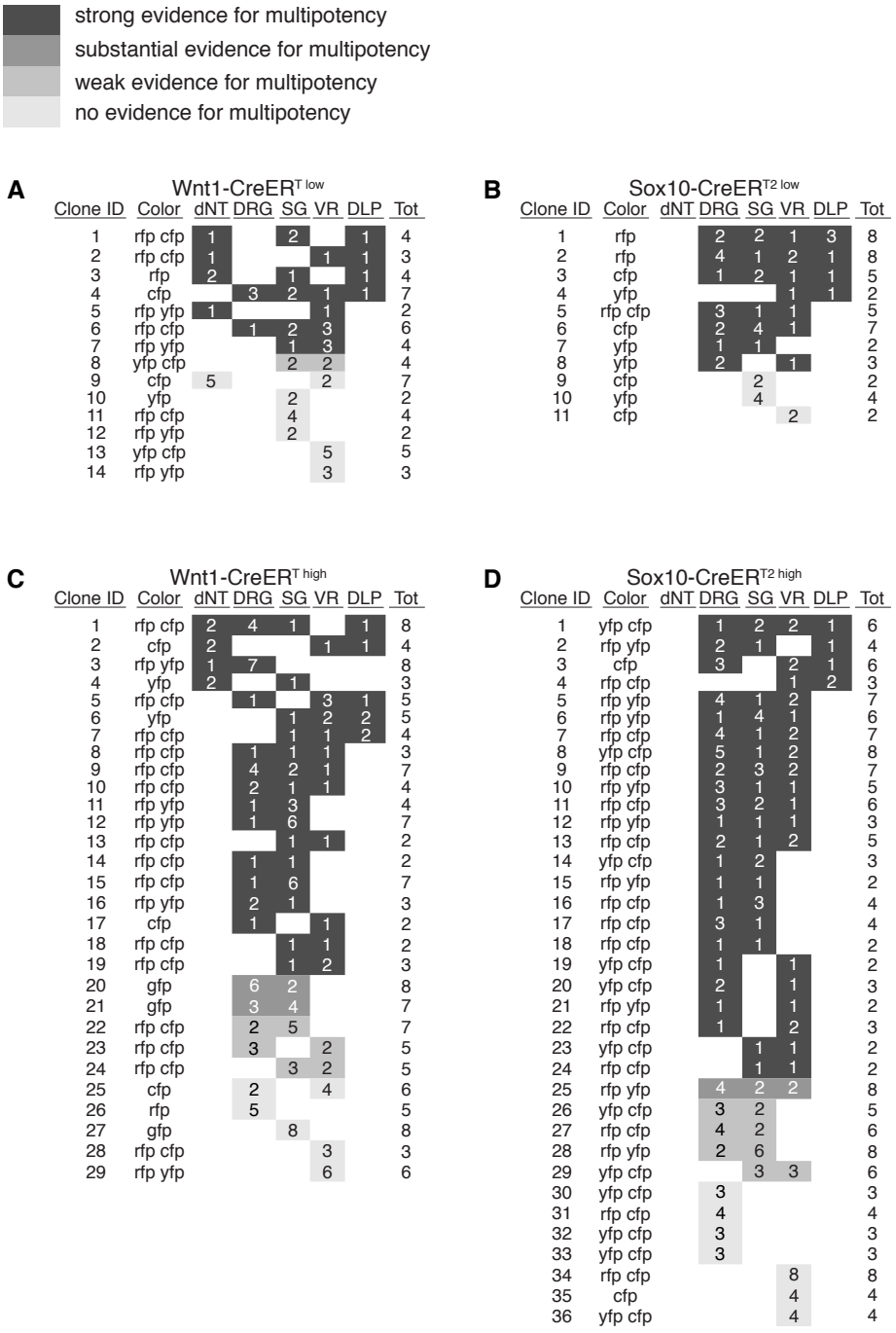

FIGURE 25: Clonal observations upon lineage tracing of premigratory and migratory NC cells.

Lists of the 2-8 cell clones observed in the *Wnt1-CreERT* and *Sox10-CreERT2* embryos both at low (25A, 25B) and high (25C, 25D) recombination densities. For each clone the following information is provided: category of statistical evidence for multipotency, derivatives where the clone was observed, number and color of the cells comprising the clone. The clones observed in the *Wnt1-CreERT* line were obtained analyzing 7 *Wnt1-CreERT low* embryos (14 DRG-units, 4 litters, 25A) and 18 *Wnt1-CreERT high* embryos (36 DRG-units, 7 litters, 25C). The clones observed in the *Sox10-CreERT2* line were obtained analyzing 4 *Sox10-CreERT2*

low embryos (9 DRG- units, 2 litters, 25B) and 10 *Sox10-CreERT2 high* embryos (22 DRG-units, 5 litters, 25D).

Clonal density for 2-8 cell cohorts

	Nr of clones	Nr of units	Nr of embryos	Nr of litters	Clones per unit
Wnt1-CreER$^{T\ low}$	14	14	7	4	1.0 ± 0.3
Wnt1-CreER$^{T\ high}$	29	36	18	7	0.8 ± 0.1
Sox10-CreER$^{T2\ low}$	11	9	4	2	2.2 ± 0.2
Sox10-CreER$^{T2\ high}$	36	22	10	5	1.6 ± 0.2

Clonal distribution per DRG-unit

Nr of clones per unit	0	%	1	%	2	%	3	%	>3	%	Total of units
Wnt1-CreER$^{T\ low}$	4	28.6	8	57.1	0	0	2	14.3	0	0	14
Wnt1-CreER$^{T\ high}$	16	44.4	11	30.6	9	25.0	0	0	0	0	36
Sox10-CreER$^{T2\ low}$	1	11.1	5	55.6	3	33.3	0	0	0	0	9
Sox10-CreER$^{T2\ high}$	2	9.1	8	36.4	8	36.4	4	18.1	0	0	22

TABLE 3: Clonal density analysis for cohorts of 2-8 cells. The total number of clones, of DRG-units, of embryos, and of litters analyzed for each of the four experimental setups, *Wnt1-CreERT* and *Sox10-CreERT2* line both at low and at high recombination densities, are listed. The data refer to Figures 24 and 25. The average of clones per unit is provided ± SEM. To indicate the observed clonal distribution per DRG-unit, we listed the absolute numbers and the respective percentages of numbers of clones per DRG-unit.

4.1.5.5 Multicolor fate mapping of single migratory NC cells

Our findings prompted us to ask whether multipotency might be a unique characteristic of premigratory NC cells or whether this developmental potential is retained upon NC delamination and migration. Therefore, we analyzed the fate of NC cells in *Sox10-CreERT2* embryos (Figure 20K). The clonal density found in *Sox10-CreERT2* embryos was again low (Table 1). Surprisingly, in *Sox10-CreERT2* low embryos, many equally colored cell cohorts were dispersed over multiple NC derivatives, in a similar manner to what had been observed in *Wnt1-CreERT* embryos (Figures 24B and 25B). Similar results were acquired for the *Sox10-CreERT2 high* embryos, suggesting that these observations are independent of the recombination density and the color of the cell cohort (Figures 24B and 25D).

4.1.5.6 Statistical evaluation of cell fates adopted by premigratory and migratory NC cells

Our observations suggested that the majority of NC cells are multipotent both at the premigratory stage and, intriguingly, also at the migratory stage. To verify our results, we analyzed each data set considering the color of the observed putative clone, the derivative where we observed it, and its size. Defining the exact cell-cycle length and its variation during a period of 41 hr for each specific derivative would have been extremely difficult and prone to mistakes. Thus, we applied a static framework instead of a complete dynamic modeling approach. To distinguish between a predetermined and a multipotent framework for both *Wnt1-CreERT* and *Sox10-CreERT2* embryos, at low and high recombination levels, we calculated the respective probabilities of observing the specific clone configuration. Because the statistical model is based on count data, these probabilities are equivalent to likelihoods and thus twice the negative log of the likelihood ratio (deviance) was used to discriminate between the two frameworks (see 4.1.8 Supplemental Experimental statistical explanation). To simplify the interpretation, the numerical values of the deviance were discretized into no, weak, substantial, and strong evidence for a framework of multipotency (Figure 24).

Based on this statistical evaluation, we first analyzed the cell cohorts (composed of two to eight cells from the same color) obtained with the *Wnt1-CreERT* embryos, pooling the data for low and high recombination densities. Strikingly, 65.1% (28 cases out of 43) of all unicolored cell cohorts represented clones of the categories strong or substantial evidence for multipotency (Figures 24A and 24C). 27.9% (12 cases out of 43) of all cohorts analyzed were multipotent clones with more than two fates. In 18.6% (8 cases out of 43) of the clones, a progeny remained in the dNT. Half of these clones also contained cells in ventral structures as well as the DLP, demonstrating the broad developmental potential of the corresponding mother cells. Moreover, all unicolored cell cohorts with derivatives in the DLP (18.6%, 8 cases out of 43) belonged to the category strong evidence for multipotency and contained NC-derived cells in at least one additional structure. Of all the cases analyzed, only 25.6% (11 cases out of 43) were belonging to the category no evidence for multipotency, indicating that lineage-restricted progenitor cells represent a minor fraction of premigratory NC cells (Figures 24A and 24C).

Unexpectedly, clones with strong or substantial evidence for multipotency were by far the most frequent categories also in the *Sox10-CreERT2* embryos (70.2%, 33 cases

out of 47) (Figures 24B and 24C). 31.9% (15 cases out of 47) of all cohorts analyzed were multipotent clones with progeny in only two derivatives (bi-fated) and 38.3% (18 cases out of 47) were clones with progeny in more than two derivatives; 24.2% (8 cases out of 33) of the unicolored cell cohorts with substantial or strong evidence for multipotency contributed to the DLP (Figure 24B). Of note, all of these were multipotent clones with cells in the DLP and in at least one other structure, and half of the DLP-clones contained cells in as many as three additional NC derivatives. Similar to premigratory NC cells, fate-restricted migratory NC cells showing no evidence for multipotency were 21.3% (10 out of 47) of all clones (Figures 24B and 24C).

To assess the robustness of our statistical evaluation, we performed a sensitivity analysis by altering various parameters in the calculation of the multipotency likelihoods. When the minimum and maximum clone sizes were varied (rather than considering only clones of two to eight cells), the resulting clone categories were still predominantly strong and substantial evidence for multipotency (Figure 24D). Furthermore, we perturbed the values of color frequency (rcolor) and derivative size (dderiv) (see 4.1.8 Supplemental statistical evaluation) by multiplying the probabilities and fractions by a random number between 1/3 and 3 (uniformly distributed), followed by rescaling. The analysis was carried out as described in 4.1.8 Supplemental statistical evaluation, and the differences with respect to the evidence classification shown in Figures 24A and 24B were recorded. Figure 24E shows the results for 100 of such simulations and reveals that in both *Wnt1-CreERT* and *Sox10-CreERT2* embryos, the categorization of the clones into no, weak, substantial, and strong evidence for multipotency was not (low recombination densities) or only moderately changed (high recombination densities). Thus, even when challenged by modulating various parameters, our statistical evaluation consistently revealed that the majority of premigratory and migratory NC cells were multipotent rather than fate restricted.

The statistical analysis presented in Figure 24 was performed under the stringent criteria that the maximum clone size was eight cells. However, this clone size might not fully recapitulate the heterogeneity of embryonic cell populations, since it does not take into account the possibility that faster dividing cells might be present in distinct locations. Moreover, parameter modulation in our statistical analysis not only provided clear evidence for multipotency of NC cells but also predicted that cell cohorts larger than the chosen range of two to eight cells could also be actual clones. Therefore, we performed a further analysis, in which we considered all unicolored cell cohorts found in defined trunk segments of *Wnt1-CreERT* and *Sox10-CreERT2*

mice. To increase the probability of clonal tracing, we restricted this analysis to cell cohorts expressing rare colors only. The clonal density was low, ranging from 0.1 ± 0.1 to 1.7 ± 0.3 clones per unit (Table 4B).

Clonal density for cohorts of cells belonging to the rare color category

	Nr of clones	Nr of units	Nr of embryos	Nr of litters	Clones per unit
Wnt1-CreER$^{T\ low}$	11	14	7	4	1.7 ± 0.3
Wnt1-CreER$^{T\ high}$	64	77	36	14	0.8 ± 0.1
Sox10-CreER$^{T2\ low}$	1	9	4	2	0.1 ± 0.1
Sox10-CreER$^{T2\ high}$	63	45	18	9	1.4 ± 0.2

Clonal distribution per DRG-unit

Nr of clones per unit	0	%	1	%	2	%	3	%	>3	%	Total of units
Wnt1-CreER$^{T\ low}$	7	50.0	5	35.7	0	0	2	14.3	0	0	14
Wnt1-CreER$^{T\ high}$	32	41.5	31	40.3	9	11.7	5	6.5	0	0	77
Sox10-CreER$^{T2\ low}$	8	88.9	1	11.1	0	0	0	0	0	0	9
Sox10-CreER$^{T2\ high}$	12	26.7	13	28.9	10	22.2	10	22.2	0	0	45

TABLE 4: Clonal density analysis for cohorts of cells belonging to the rare color category (rfp cfp, rfp yfp, yfp cfp, gfp).
List of the total number of clones, of DRG-units, of embryos, and of litters analyzed for both *Wnt1-CreERT* and *Sox10-CreERT2* line at low and high recombination densities. The data refer to Figures 26 and 27. The average of clones per unit is provided ± SEM. The clonal distribution per DRG-unit is given by the absolute numbers and the respective percentages of numbers of clones observed per DRG- unit.

By applying the statistical analysis mentioned above, we observed that the vast majority of the clones fell into the categories of strong or substantial evidence for multipotency, both in the *Wnt1-CreERT* line (76.4%, 42 cases out of 55) and in the *Sox10-CreERT2* line (75%, 36 cases out of 48) (Figure 26). Thus, including larger clones into our analysis did not affect the proportion of multipotent clones originating from premigratory and migratory NC cells, respectively, further demonstrating the robustness of our statistical analysis.

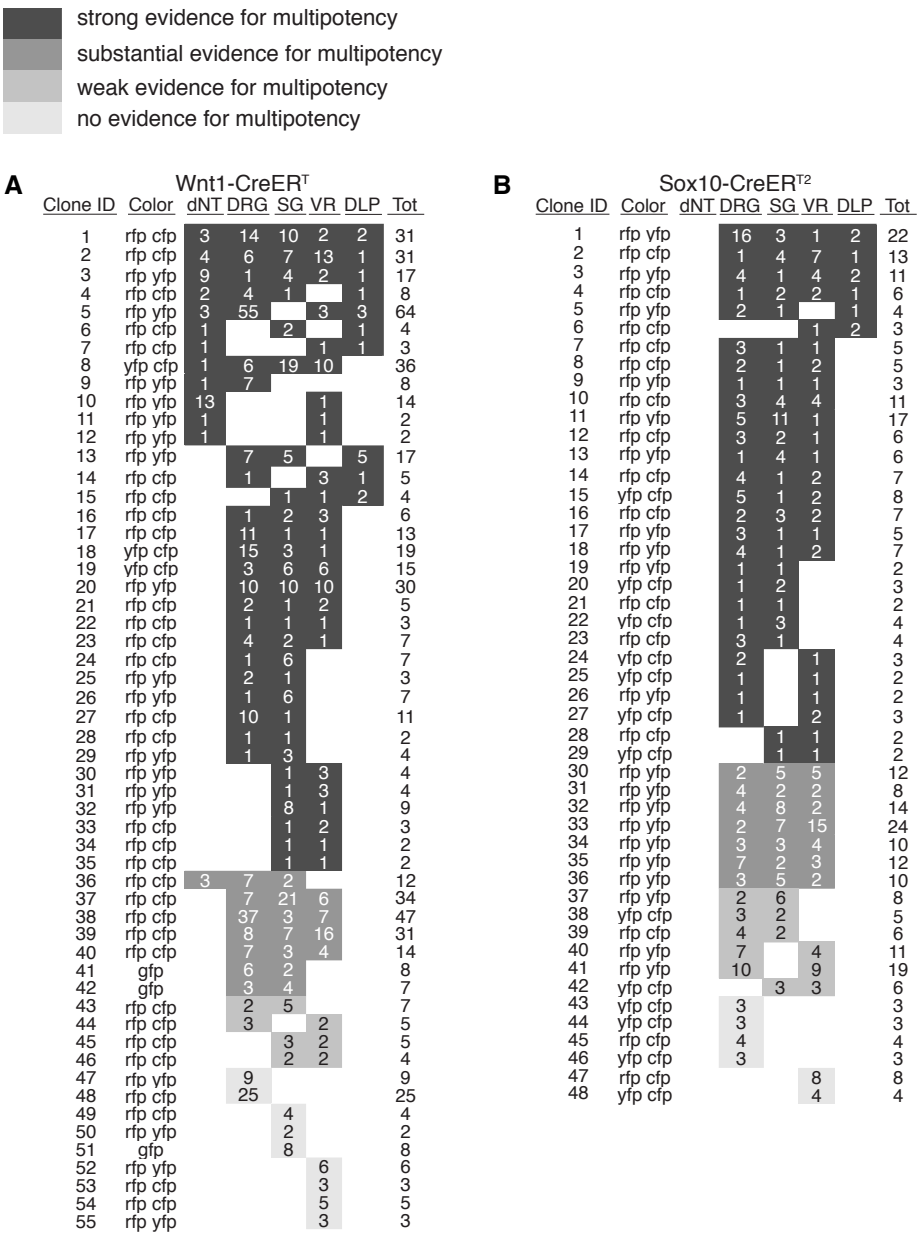

FIGURE 26: Mathematical evaluation of NC cell fate determination for all the clones of the rare color category without size restriction.

List of the clonal frameworks for premigratory (26A) and migratory (26B) NC cells ordered by degree of evidence for multipotency. Both conditions of low and high recombination densities were pooled to compare the potentials of premigratory versus migratory NC cells. We listed and analyzed statistically all the clones with rare colors (rfp cfp, rfp yfp, yfp cfp, gfp) that were observed in 25 *Wnt1-CreERT* embryos (50 DRG-units, 11 litters) and in 14 *Sox10-CreERT2* embryos (31 DRG-units, 7 litters), respectively.

4.1.5.7 Multipotency assessed by differentiation marker analysis

During NC development, fate segregations are accompanied by spatial segregations of the resulting cell lineages. Therefore, a clone simultaneously located to multiple structures represents the progeny of a multipotent mother cell (Figures 24 and 26). However, additional fate decisions are made within certain NC-derived structures, such as the DRG and SG, where neuronal lineages segregate from satellite glia. A multipotent clone with cells in DRG and SG could thus be a neuron-only clone consisting of different types of neurons (sensory, autonomic), a glia-only clone with distinct types of glia (Woodhoo and Sommer, 2008), or a mixed neuron-glia clone. To address this issue, we performed an additional clonal analysis, taking into consideration not only the location of unicolored NC cells but also the expression of well-defined differentiation markers, such as Brn3a for sensory neurons, tyrosine hydroxylase (TH) for autonomic neurons, and Sox10 for glial and melanocytic cells. Groups of cells belonging to the rare color category were considered, without clonal size restriction (Figure 27). Only 4 out of 20 clones (Wnt1-CreERT embryos) and 2 out of 16 clones (Sox10-CreERT2 embryos) were lineage restricted, respectively, meaning that these clones were not only confined to a single derivative, but they were also expressing only one marker of differentiation. Of note, of the 16 clones in *Wnt1-CreERT* embryos that were not lineage restricted, only one clone contained only neurons and no glia (clone ID 11; Figure 27A), while the other 14 clones were mixed neuron-glia clones. Likewise, one clone in *Sox10-CreERT2* embryos contained sensory and sympathetic neurons but no glia (clone ID 11, Figure 27C), while all other multipotent clones were mixed neuronal and glial. Intriguingly, some of the cases that would have been considered to represent lineage-restricted clones based on their location, turned out to be at least bipotent, expressing multiple markers of differentiation (Figure 27A, clone IDs 13, 14, 15, and 16; Figure 27C, clone IDs 13 and 14). These data substantiate our findings that single premigratory, as well as single migratory NC cells, mostly generate daughter cells that localize to distinct target structures and acquire different fates.

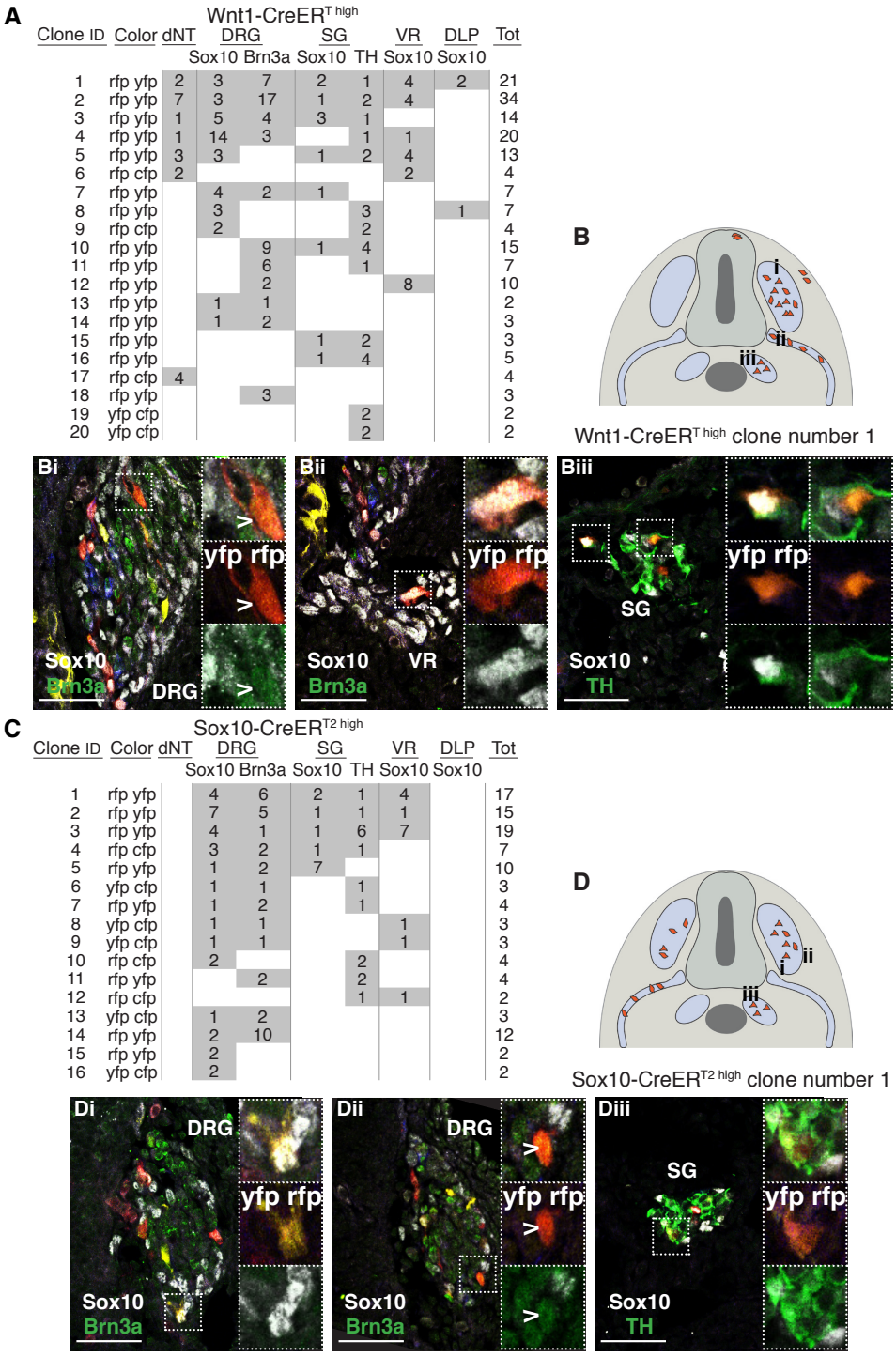

Figure 27. Quantitative clonal assays combined with differentiation marker analysis

(A and C) Lists of the clonal frameworks for premigratory (A) and migratory (C) NC cells ordered by degree of evidence for multipotency. Only clones belonging to the rare color category where analyzed, and no size restriction was applied. Each single clone was analyzed in regard to its location and expression of the following differentiation markers: Brn3a, a sensory neuron marker; TH, a sympathetic neuron marker; and Sox10 that at this

developmental stage labels glial and melanocytic lineages. (B and D) Schemes summarizing the distribution of entire clones respectively found in *Wnt1-CreERT* and *Sox10-CreERT2* embryos at high recombination densities. (Bi–Biii and Di–Diii) Examples of embryonic sections through NC derivatives that comprise rare color-expressing cells belonging to the clones shown in (B) and (D), respectively. For numbers of analyzed embryos, see 4.1.7 Experimental Procedures. Scale bars: 50 mm.

4.1.6 Discussion

A fundamental question in developmental biology is how the distinct cell types of a given organ are established. Although it is thought that organ formation and homeostasis rely on the activity of organ-specific multipotent stem cells, several recent publications demonstrated that heterogeneous populations of restricted progenitor cells, instead of multipotent mother cells, are often involved in the formation of vertebrate body structures (Lehoczky et al., 2011; Park et al., 2012). This issue is of particular interest with respect to the NC, because this structure represents one of the cell populations in the vertebrate embryo with the broadest developmental potential (Le Douarin et al., 2008). Several studies demonstrated that at least upon isolation, the majority of NC cells display stem cell features, being multipotent and able to self-renew (Dupin and Sommer, 2012). Others, however, reported the presence of many lineage-restricted cells in NC cell cultures (Harris and Erickson, 2007; Henion and Weston, 1997), suggesting that multipotency might be dependent on or even induced by culture conditions. The recent establishment of transgenic mouse lines allowing low-density genetic recombination makes it possible to trace the lineage of single cells without the need to expose the cells to varying conditions. For instance, the *R26R-Confetti* reporter was used to track cells in the postnatal gut (Snippert et al., 2010). Here we applied this system to demonstrate that in vivo the NC cell population is primarily composed of multipotent cells rather than of a mixture of lineage-restricted precursors.

The *R26R-Confetti* mouse model offers the possibility to distinguish several clones from each other in the same specimen. Importantly, clonal analysis can be made in this system without prior cell isolation, transplantation, or any disturbance of the cellular microenvironment that might reactivate a ‘‘stemness’’ program (Snippert and Clevers, 2011). However, like in all retrospective lineage-tracing studies, redundant recombination events have to be excluded in the *R26R-Confetti* system to ensure clonal identification. To this end, we took advantage of the fact that theoretically equiprobable fluorescent protein combinations were expressed at different frequencies. In *Wnt1-CreERT* mice, we were able to monitor the development of single premigratory NC cells at a low clonal density in vivo and to compare their fates with those of migratory *Sox10-CreERT2*-traced NC cells. Surprisingly, the range of fates and clonal distribution was very similar for these two settings. Most clones were distributed over several NC target structures and only in a minority of cases premigratory and migratory NC cells were fate restricted. Importantly, our statistical evaluation revealed a very high probability for multipotency, independent of color

expression and recombination density. Moreover, subjecting our statistical evaluation to a sensitivity assay by altering multiple parameters, such as expected clone sizes and dimensions of the NC derivatives, confirmed the robustness of our method and the finding that most NC cells are multipotent.

Furthermore, the vast majority of clonal derivatives were not only spread over distinct locations but also acquired distinct fates within given target structures. In particular, combining quantitative clonal assays with expression analysis of differentiation markers showed that the majority of NC cells, at least at the early stages analyzed, can neither be divided into ‘‘sensory-only’’ versus ‘‘sympathetic-only,’’ nor into ‘‘neuron-only’’ versus ‘‘glia-only’’ precursors.

In chicken embryos, DLP-colonizing NC cells are separate from ventrally migrating cells and belong to a late emigrating population (Erickson et al., 1992; Henion and Weston, 1997). We did not address here whether late emigrating NC cells exclusively destined to the DLP exist in mice. However, all clones with DLP contribution were multipotent in our study and contained cells in at least one ventral derivative. Thus, even after their emigration from the dNT, at least some mouse NC cells that will generate DLP derivatives maintain the potential to produce ventral neural cells.

Previous studies proposed that premigratory NC cells of the trunk are fate restricted (Krispin et al., 2010; Nitzan et al., 2013). This result differed from earlier work that indicated the presence of multipotent premigratory NC cells, including ‘‘resident’’ precursor cells for both CNS and NC in the dorsal neuroepithelium (Bronner-Fraser and Fraser, 1988; Bronner-Fraser and Fraser, 1989). These discrepancies might have been due to technical challenges and to differences in the stages and location of the labeled premigratory NC cells in the dNT. Although we cannot exclude differences in mechanisms of lineage segregation between avian and mammalian systems, our findings support the model in which the majority of NC cells are multipotent not only at the population but also at the single cell level and that multipotency is maintained in NC cells even after their emigration from the neural tube. However, we cannot rigorously exclude the existence of fate-restricted NC cells, as we found a minority of NC cells that appeared to give rise to only one derivative. It is therefore possible that the NC cell population contains a fraction of fate-restricted cells.

Even though most NC cells were multipotent in our study, the actual cell type composition varied in each clone, with some multipotent clones acquiring all possible fates and others producing only two cell types. This reflects the heterogeneous behavior of NC cells also seen in cell culture conditions permissive for multiple fates,

where multipotency is frequently observed, but not fully realized by all cells (see e.g., Dupin et al., 2010; Stemple and Anderson, 1992). This heterogeneous behavior can be switched to a virtually homogeneous response when NC cells are exposed to instructive growth factors either in vitro (Shah et al., 1994) or in vivo (Hari et al., 2012). It remains to be shown whether, normally, fate choices by multipotent NC cells in vivo are purely stochastic.

Of note, we did not observe a pattern of restricted fate choices when we compared migratory with premigratory NC cells, speaking against gradual lineage restriction during NC development (Krispin et al., 2010; Le Douarin et al., 2008) at least during the time window analyzed. Therefore, the multiple and variable fates adopted by NC cells appear to reflect the dynamic behavior of stem cells in vertebrates as opposed to more deterministic lineage acquisitions observed in species such as *C. elegans* (Morrison et al., 1997).

Upon recombination at the premigratory stage, we found clones with recombined cells retained in the dNT, in addition to cells in NC derivatives. This may suggest an asymmetric division of NC cells and that a resident ‘‘stem cell’’ population is established in the dorsal midline. Moreover, multipotency was maintained in migratory NC cells. Together, these findings are consistent with the hypothesis that NC stem cells (NCSCs) as originally characterized in cell culture (Stemple and Anderson, 1992) might not only be in vitro stem cells (Smith, 2006) but actually exist in vivo. In support of this hypothesis, undifferentiated NC- derived cells in the sciatic nerve were shown before to be able to self-renew in vivo and to maintain their multipotency as revealed upon isolation (Morrison et al., 1999). However, to demonstrate self-renewal and maintenance of multipotency by single NC cells in vivo without cell isolation or disturbing the cellular microenvironment would be technically challenging due to the dissemination of NC cells within a short time period. Concluding, our study demonstrates that the majority of NC cells are multipotent, both at the premigratory and at the migratory stage.

4.1.7 Experimental procedures

4.1.7.1 Mice

Mice homozygous for the *R26R Confetti* allele (Snippert et al., 2010) were crossed with the two inducible mouse lines *Wnt1-CreERT* (Zervas et al., 2004) and *Sox10-CreERT2* (Simon et al., 2012). All the embryos used in the analyses were derived from a 2 hr time-mating. Lineage tracing of premigratory NC cells at low and high recombination densities was achieved with pregnant *Wnt1-CreERT R26R-Confetti* homozygous females, injected at E9.0. The animals were injected intraperitoneally (i.p.) with a single limiting dose of 7.5 mg and 50 mg TM/g body weight for low and high recombination densities, respectively. Similarly, to recombine migratory NC cells, we injected i.p. pregnant *Sox10-CreERT2 R26R-Confetti* homozygous animals at E9.0 with a single dose of 50 mg or 150 mg TM/g body weight to induce low or high recombination densities, respectively. Finally, embryos were collected at E10.5, 41 hr post- TM injection. Animal experiments were approved by the veterinary office of the Canton of Zurich, Switzerland.

Embryo numbers Number of embryos used for data presented in Figure 20

To calculate the color densities for the *Wnt1-CreERT* line we analyzed 7 embryos (14 DRG-unit, 4 litters) and 18 embryos (36 DRG-unit, 7 litters) at low and at high recombination densities, respectively. To measure the color frequencies for the *Sox10-CreERT2* line we analyzed 4 embryos (9 DRG-units, 2 litters) and 10 embryos (22 DRG-units, 5 litters) at low and high recombination densities, respectively.

Number of embryos used for data presented in Figure 22

To calculate the percentage of recombined cells per derivative in the *Wnt1-CreERT* line we analyzed 7 embryos (14 DRG-units, 4 litters) and 18 embryos (36 DRG-units, 7 litters) at low and high recombination densities, respectively. For the *Sox10-CreERT2* line we analyzed 4 embryos (9 DRG-units, 2 litters) and 10 embryos (22 DRG-units, 5 litters), respectively.

Number of embryos used for data presented in Figure 24

The clones observed in the *Wnt1-CreERT* line were obtained analyzing 7 *Wnt1-CreERT low* embryos (14 DRG-units, 4 litters) and 18 *Wnt1-CreERT high* embryos (36 DRG-units, 7 litters). The clones observed in the *Sox10-CreERT2* line were obtained analyzing 4 *Sox10-CreERT2 low* embryos (9 DRG-units, 2 litters) and 10 *Sox10- CreERT2 high* embryos (22 DRG-units, 5 litters).

Number of embryos used for data presented in Figure 27

The clones of the *Wnt1-CreERT* line were obtained by analyzing 18 *Wnt1-CreERT high* embryos (41 DRG-units, 7 litters). The clones of the *Sox10-CreERT2* line were obtained by analyzing 8 *Sox10-CreERT2 high* embryos (23 DRG-units, 4 litters).

4.1.7.2 Immunofluorescence, whole mount staining and SeeDB clearing

For immunohistochemistry, 10µm-thick cryosections were processed as previously described (John et al., 2011). Primary antibody was used as follows: mouse anti-NF160 (1:300; Sigma, N-5264), rabbit anti-Sox10 (1:250; Abcam, ab27655), mouse anti-Brn3a (1:100; Millipore, MAB1585), mouse anti-tyrosine hydroxylase (1:200; Sigma, T1299). As a secondary antibody the DyLight 649 Donkey anti-mouse IgG (H+L) (1:300; Jackson, 715-495-150), DyLight 649 Goat anti-rabbit (1:300; Jackson, 111-495-003), Alexa Fluor 488 Goat anti-mouse (1:300; Invitrogen, A-11029). *lacZ* reporter gene expression was detected as previously described (Hari et al., 2012). For 3D imaging the whole mount staining with anti-NF160 (1:250; Sigma, N-5264) and the SeeDB clearing protocol were applied as previously described (Ke et al., 2013).

4.1.7.3 Microscopy

Images were acquired using a Leica CTR600 microscope and a Confocal Laser Scanning Microscopy (Leica CLSM SP5). For the Rosa four-color imaging, scans were performed in a series for fluorescent protein excitation as described in Snippert et al. (2010).

4.1.7.4 Data Analysis

The data analysis was performed using R version 3.1.1. R Development Core Team (http://www.R-project.org).

4.1.8 Supplemental statistical explanation

4.1.8.1 Assumptions of the statistical model

The statistical analysis is based on the following assumptions:

1. Within each mouse line and recombination density, each embryo is independent
2. Within each embryo, each DRG-unit is independent
3. The development and migration is color-independent
4. Each mother cell leads to at least two cells

5. There is at most one mother cell per color and corresponding derivative(s)

These are typical assumptions and essentially imply: By 1 and 2, the individual sections from all embryos (within a particular mouse line and recombination) can be taken as replicates. The available data does not show any indication against these assumptions. By 3, we can – by appropriately taking into account the relative color frequencies – use each color individually. At our current state of knowledge there is no competition between the individual colored cells. Assumption 4 implies that no mother cell gets lost or dies and that there is at least one replication. Assumption 5 is justified as we restrict the analysis to at most eight cells per color (for larger cell numbers see below).

In the following we describe in some detail how the probabilities of observing a particular configuration of cell counts (Figure 24, all the cohorts of 2-8 cells) in the five derivatives (dNT, DRG, SG, VR, DLP, Table 2) for each color (Table 1) under the respective framework (predetermination or multipotency) was calculated. The different colors appear with different relative expression frequencies, denoted by *rcolor.* Similarly, the derivative sizes vary and the relative derivative sizes are denoted by *dderiv.* These two quantities are unknown and we estimated their values from frequency tables (Figures 20L, 20M, 22G, and Table 1, 2). We assumed that each embryo and DRG-unit are independent from one another, and that embryonic development and cell migration are color-independent as well and thus the product *rcolor dderiv* is the probability of observing the particular color in the particular derivative. We represented each configuration of cell counts as a quintuple (corresponding to the five derivatives) with binary entries, which equaled one if cells were observed in the corresponding derivative and zero otherwise. We denoted such a binary “observed” value with *ocolor.deriv* for any of the colors and five derivatives.

To calculate the probability of observing a particular configuration, we considered cases of mother cell configurations that lead to the corresponding configuration. Not all mother cell configurations develop with equal probability into the particular configuration and hence this probability has to be taken into account (this approach is formally termed the of law of total probability). In the case of predetermination, the mother cell configuration is identical to the derivative configuration and thus, one only needs to calculate the probability of observing an identical mother cell configuration. This probability consists of the product of the probabilities of having a colored cell in the derivative whenever we observed one and of one minus that probability whenever we did not observe one:

P(configuration) = P(mother cell configuration) = Πderiv (rcolorderiv)ocolor.deriv (1-rcolorderiv)(1-ocolor.deriv),

where *rcolor, deriv* and *ocolor.deriv* are as above.

In the case of multipotent cells, it has to be taken into account that the clones migrate to the derivatives with probabilities according to the estimated derivative size (Figure 22 and Table 2). The probability to observe a mother cell with a specific color is proportional to the relative expression frequency of that color (Figures 20L and 20M, Table 1). Hence,

P(configuration) = P(observing mother cell) P(migration to derivatives) = rcolor Πderiv derivocolor.deriv (1-deriv)(1-ocolor.deriv)

where *rcolor, deriv* and *ocolor.deriv* are as above. The precise stochastic assumptions of the model, a sensitivity analysis of the involved parameters and further technical insights are given below.

4.1.8.2 Sensitivity Analysis

The cutoffs to classify the deviance (twice the negative log of the likelihood ratio) are -2log(.1), -2log(.01), -2log(.001) resulting in the (approximate) bins (-∞, 4.6), (4.6, 9.2), (9.2, 13.8) and (13.8, ∞) for “no”, “weak”, “substantial” and “strong” evidence. Choosing slightly different cutoffs does not change the result. In many cases, the weak and substantial bins are empty. Note that a zero deviance is equivalent to equal probabilities of both frameworks and thus a “no”-evidence case does not imply that a predetermined case was more likely. Figure 24D summarizes and compares the likelihoods when the minimum/maximum clone sizes are varied according to the pairs 4-8, 1-16, 2-16, 2-8, 2-6. The results do virtually not depend on these sizes.

We have also perturbed the values of the relative color frequencies (rcolor) and relative derivative size (deriv) by multiplying them by a random number between 1/3 and 3 (uniformly distributed) followed by a rescaling. The analysis has been carried out as described above and the differences with respect to the classification for the evidence of multipotency has been recorded. Figure 24E shows the results for 100 of such simulations. Each of the 16 barplots shows the proportion of the 100 cases that changed, white indicates no change, redish to red cases that are added and greenish to green cases that are lost. For the low recombination rates, the results are virtually the same (white dominates the barplots). For the high recombination rates moderate changes occur. For example, for the results of the analysis of the *Sox10-CreERT2* high embryos, 1/36 of the cases are classified as substantial evidence (clone ID 25, Figure 25D). In one third of the perturbed cases this proportion has not changed. In

one fifth of the cases there is no case marked as substantial evidence and in 33% (10%, 2%) there are 2/36 (3/36 and 4/36) cases marked as substantial evidence, respectively.

4.1.8.3 Additional Comments

The presented methodology is “frequency based”. Naturally, a Bayesian framework would be possible. In such a framework, priori information about our beliefs in multipotency needs to be specified and then enters the calculations. A fully Bayesian specification would imply that all other parameters (relative color frequencies, relative derivative sizes, etc.) would need to be considered as random and would be equipped with a priori distribution. We do not have any priori knowledge about these parameters and “uniform”/uninformative priors would be the only possible choice. Such a uniform priori would essentially lead to the same result as a frequency setting.

The calculation of the configuration probabilities for both the predetermined and multipotency cases can be unified through the use of the law of total probability. More precisely, these probabilities can be expressed as follows.

$P(\text{ configuration }) = \Sigma k\ P(\text{ configuration } | \text{ mother cell configuration } k\ )\ P(\text{ mother cell configuration } k\ )$

In the case of predetermination, the mother cell configuration is identical to the derivative configuration; hence the conditional probabilities are equal to one in the case the derivative configuration is equal to the mother cell configuration and zero otherwise. A particular mother cell configuration is characterized by having or not having the colored cell in a particular derivative. Therefore,

$P(\text{ configuration }) = P(\text{ same mother cell configuration })$

$= \Pi \text{deriv } (rcolordderiv)ocolor.deriv\ (1-rcolordderiv)(1-ocolor.deriv),$

where *rcolor, dderiv and ocolor.deriv* are as in the main text.

In the case of multi-fated cells, the mother cell configuration is derivative independent and consists of a particularly colored clone (all other colored cells lead to zero conditional probability). It has to be taken into account that the clones migrate to the derivatives with probabilities according to the estimated derivative size. This migration is color independent. Hence

$P(\text{ configuration }) = P(\text{ configuration } | \text{ mother cell with appropriate color }\ )\ P(\text{ mother cell with appropriate color }\ ) = \Pi \text{deriv } dderivocolor.deriv\ (1-dderiv)(1-ocolor.deriv)\ rcolor$

where *rcolor, dderiv* and *ocolor.deriv* are as above.

Assumption 5 excludes the possibility of several mother cells in the case of multipotency as well. These cases are (statistically) very rare compared to one single mother cell. Among these few cases, some would be manifested as predetermination and could not be used to discern the frameworks. All others would slightly increase the probability of observing multipotency and thus shift the deviances in direction towards “strong evidence”. Hence, we can safely ignore these rare cases.

4.2 The Roles of Sall4 in Melanoma

Unpublished data

Arianna Baggiolini[1], Johanna Diener[1], Sandra Varum[1], Jessica Häusel[1], Gaetana Restivo[1], Phil Cheng[2], Mitchell P. Levesque[2], Mathias Treier[3], Reinhard Dummer[2], Lukas Sommer[1].

[1]Institute of Anatomy, University of Zurich, 8057 Zurich, Switzerland

[2] Department of Dermatology, University Hospital Zurich, 8091 Zurich, Switzerland.

[3] Max Delbrück Center for Molecular Medicine, 13125 Berlin-Buch, Germany.

4.2.1 My contribution to this work

- Design of the experiments
- Execution of all experiments and collection of data, with exception of Figure 28 which was performed together with Sandra Varum in the frame of her project; Figure 29B, C, D and Figure 30A, B, C which were produced by Johanna Diener and Gaetana Restivo
- Breeding of mice used in the study, including genotyping, tamoxifen injection and collection of mouse material
- Production of the figures

4.2.2 In brief

Sall4 is a zinc-finger transcription factor crucial for ES cell self-renewal and pluripotency. SALL4 has been shown to play a role in several cancer types, but its role in melanoma formation and progression has not been investigated so far. By combining mouse genetics and in vitro analysis of human melanoma cell lines, we found first indications suggesting that SALL4 may be an important factor in primary melanoma and metastasis formation.

4.2.3 Summary

Sall4 is a zinc-finger transcription factor crucial for the maintenance of self-renewal and pluripotency of ES cells. Moreover, SALL4 has been be related to tumorigenesis and high expression of SALL4 is linked to worse patient survival and metastasis formation in several cancer types.

SALL4 function in melanoma, however, has so far been unknown. In this study, we show that Sall4 is necessary for primary melanoma formation in the *Tyr::NRas*^{Q61K} *Ink4a*$^{-/-}$ melanoma mouse model, but that surprisingly Sall4 loss is linked to worse survival performance. Interestingly, SALL4 was downregulated both *in vitro* and in xenotransplants during EMT and SALL4 knockdown in a proliferative human melanoma cell line induced an EMT signature. Thus, our findings suggest a novel role of SALL4 in tumorigenesis that is characteristic of melanoma.

4.2.4 Introduction

Melanoma is a malignancy of the melanocytes, which are the pigment-producing cells of NC-origin. During development melanocytes migrate extensively through the embryonic body and find location mostly in the skin, as well as in the iris and the rectum. Cutaneous melanoma, which originates from the melanocytes of the skin, is a common malignancy in the Western world. Cutaneous melanoma is one of the most aggressive cancers and it is indeed responsible for 75% of deaths related to skin cancer (Schadendorf et al., 2015). One of the characteristics that makes melanoma particular aggressive is its high metastatic potential. Melanoma cells can in fact often metastasize to proximal and distant organs and their invasive capacity is to some extents reminiscent to the great migratory and invasive properties of the NC cells. This has contributed to the hypothesis that NC-derived malignant cells may exploit developmental regulatory programs to gain an advantage over normal non-malignant cells and to progress to more advanced stages of the disease. Indeed, several studies on melanoma showed that malignant cells reactivate or exploit genes such as *Snail*, *Twist* and *Sox10* (Shakhova et al. 2012; Shirley et al. 2012; Weiss et al. 2012), which are key transcription factors in the gene regulatory network controlling NC induction and migration (Sauka-Spengler and Bronner-Fraser, 2008).
First we performed a microarray analysis on isolated mouse NC cells as well as on NC cells 6 hour primed for differentiation towards the mesenchymal, the neuronal and the glial lineage (Varum et al., unpublished). We obtained a list of 53 transcription factors that were specifically expressed in the NC and that were downregulated in the primed NC counterparts. We decided to further study Sall4 as one of these 53 genes, since the zinc-finger transcription factor was known to be responsible for the great self-renewal and pluripotency capacities of ES cells (Zhang et al., 2006).
Beyond its role in development, SALL4 was described to play a key function in a large number of cancers (Zhang et al., 2015). High levels of SALL4 are related to increased tumor proliferation, acquisition of pluripotency features, increased metastasis formation and overall to a worse patient outcome (Zhang et al., 2015).
Whether SALL4 is expressed in melanoma and may play a role in this malignancy has not been investigated so far. In this study we now show that SALL4 is expressed in some proliferative human melanoma cell lines, while being absent in more invasive melanoma cell lines. Moreover, SALL4 is downregulated upon EMT induction both *in vitro* and in xenotransplants. Additionally, siRNA specific for SALL4 induces an EMT signature in proliferative melanoma cells. Interestingly, Sall4 loss in the

Tyr::NRas^{Q61K} Ink4a$^{-/-}$ melanoma mouse model (Ackermann et al., 2005) prevents primary tumor formation, but unexpectedly results in worse survival of the cKO animals and in detection of recombined cells in their lymph nodes and lungs.

Further investigations are now required to understand whether SALL4 loss is necessary and sufficient to allow EMT and whether SALL4 upregulation may prevent invasion.

4.2.5 Results

4.2.5.1 Sall4 is a zinc-finger transcription factor expressed in NC cells

We were initially interested in discovering new transcription factors responsible for the multipotency of the NC. To do this we dissected the neural tubes of wild type E9 NRMI embryos and we derived NC explants (Figure 28A). NC cells were then cultured at the presence of different instructive factors for 6 hours. In particular we instructed NC cells to differentiate into the mesenchymal lineage (by application of TGF-b), the neuronal lineage (by BMP-2) and the glial lineage (by heregolin and forskolin). We then performed a microarray analysis compering the isolated NC cells (0 hours) to the NC cells that were primed for 6 hours towards a specific fate (Figure 28B). We obtained a total of 53 transcription factors that were specifically expressed in NC cells and that were commonly downregulated upon the 6 hours of differentiation conditions (Figure 28C) (Varum et al., unpublished).

Out of these 53 transcription factors we selected Sall4, that was one of the top ten mostly downregulated factors upon differentiation. Sall4 is known to be a crucial factor in the maintenance of the pluripotency and self-renewal of ES cells. Although, little is known about the function of Sall4 in NC biology, for exception of its role on the competence of the cranial NC cells to populate sensory ganglia (Barembaum et al., 2004).

To reveal the function of Sall4 in the NC, we produced *Wnt1-Cre Sall4* $^{lox/lox}$ embryos in which Sall4 was specifically deleted in the premigratory NC cells. The embryos were not viable and they died at E 15.5 most likely by heart failure (data not shown). NC derivatives showed minor defects that were mostly rescued at later developmental stages for exception of the melanocytic lineage that was significantly reduced (data not shown). Most likely, the moderate phenotype was due to compensatory mechanisms by other members of the Sall family, phenomenon already documented in other contexts as during neural tube closure (Böhm et al., 2008).

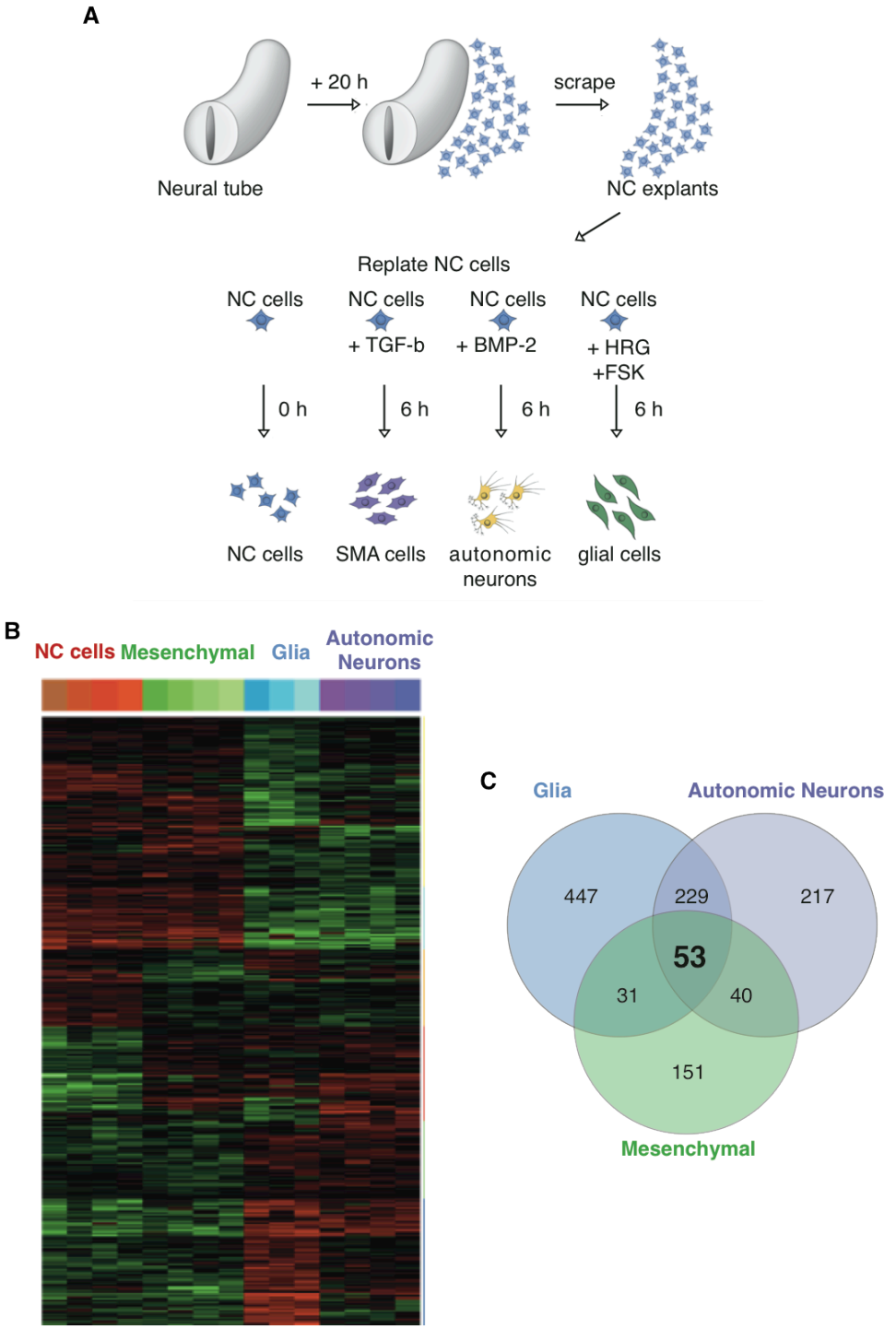

Figure 28. Sall4 is a transcription factor expressed in the NC cells and that is downregulated upon differentiation.

(A) NC explants were isolated from the dorsal neural tube at E9. The NC cells were incubated for 6 hours at the presence of different instructive growth factors that induced their differentiation into the smooth muscle fate (TGF-b), the autonomic neuronal fate (BMP-2) and the glial fate (heregulin, HER, and forskolin, FSK). (B) Microarray analysis of NC cells and NC

cells previously incubated for 6 hours under differentiation conditions. (C) Summary of the microarray data indicating a total of 53 genes that were expressed in the NC cells and that were downregulated upon all three differentiation conditions.

4.2.5.2 Increased SALL4 expression is associated with poor melanoma patient survival

Previous results demonstrated that melanoma cells can exploit NC-specific regulatory programs and that these processes play an important role in melanoma formation and progression (Shakhova et al., 2012). Moreover, Sall4 loss during development seems to have a specific effect on the melanocytic lineage (data not shown), suggesting a possible role in melanoma. To investigate the relevance of SALL4 expression in skin cutaneous melanoma patients we analyzed the RNAseq and clinical data from the The Cancer Genome Atlas (TCGA, http://cancergenome.nih.gov/). Interestingly, when we compared SALL4 expression levels in primary tumors and lymph nodes, the patients with low levels of SALL4 expression (SALL4 low group, 120 patients, median survival of 3587 days, Figure 29A) showed a significantly better overall survival compared to patients with high SALL4 levels of expression (SALL4 high group, 120 patients, median survival of 1960 days, Figure 29A), suggesting a potential role of SALL4 in melanoma.

4.2.5.3 SALL4 is differentially expressed in human melanoma cell lines

Intrigued by the fact that SALL4 expression levels may affect patient survival, we tested several human melanoma cell lines for its level of expression. Initially, we measured mRNA SALL4 levels in human melanoma cell lines and compared them to a human melanocytic cell line. SALL4 mRNA levels were remarkably higher in proliferative melanoma cell lines (defined by the Heurisic Online Phenotype Prediction (HOPP) analysis (Widmer et al., 2012); as e.g. M130423, M080423, M010817)) than in more invasive melanoma cell lines (M080310, M080214, M080201) when compared to SALL4 basal level of expression in a human melanocytic cell line (Figure 29B).
Protein expression was reflecting mRNA levels and some highly proliferative melanoma cell lines expressed SALL4 protein (Figure 29C), while more invasive melanoma cell lines showed poor expression of its protein (Figure 29D).

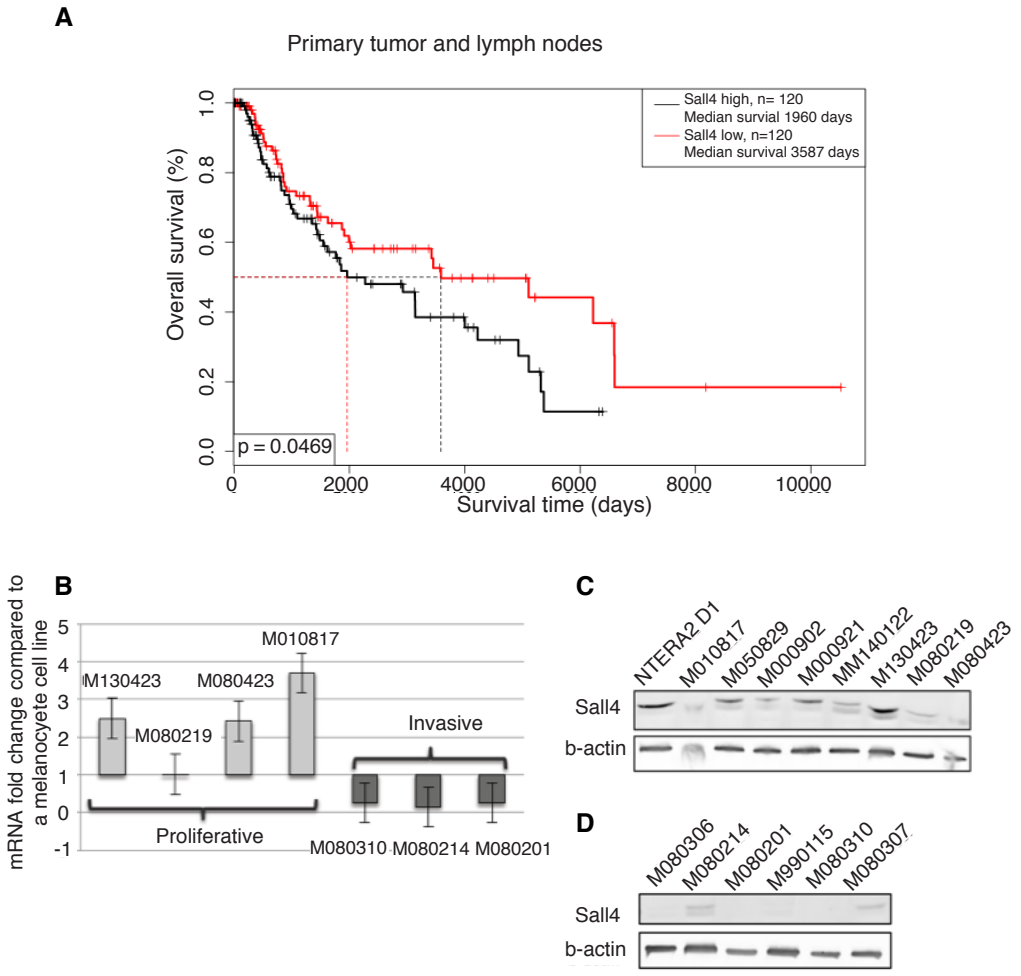

Figure 29. Overall survival of skin cutaneous melanoma patients related to SALL4 transcript levels and SALL4 expression in human melanoma cell lines.

(A) Kaplan-Meier curves comparing overall survival of melanoma patients depending on the SALL4 transcript levels (primary melanoma and lymph node metastases) based on TCGA. (B) SALL4 transcript levels in human melanoma cell lines compared to a human melanocytic cell line. (C-D) SALL4 protein expression in human proliferative (C) and in invasive (D) melanoma cell lines. As a positive control we used the NTERA D1 cell line.

4.2.5.4 SALL4 is downregulated *in vitro* and in xenotransplants during EMT

The characteristic expression of SALL4 prompted us to investigate whether its expression would change in a human proliferative melanoma cell line, as M010817, under conditions that would induce EMT. We thus treated the M010817 line with TGFb-1, which is a known EMT inducer (Xu et al., 2009). Interestingly, concomitant with an increase in the transcript levels of N-cadherin and p75 neurotrophin receptor

(p75^{NTR}) (data not shown), we observed a significant decrease in SALL4 expression. These data suggest that during the process of EMT a proliferative human melanoma cell line downregulates SALL4.

To corroborate our results, we analyzed SALL4 expression in M010817 upon overexpression of the EMT inducer p75^{NTR} (Restivo et al., unpublished data). We infected the M010817 line with an empty vector (CMVTO) and with a vector overexpressing p75^{NTR} (CMVTO p75^{NTR}) and we then xenotransplanted these cells into nude mice. The analysis of the xenotransplants showed that the tumor originating from CMVTO M010817 cells was expressing SALL4 protein (Figure 30B), while the xenotransplant overexpressing p75^{NTR} (CMVTO p75^{NTR}) completely lost SALL4 expression (Figure 30C).

These data suggest that human proliferative melanoma cell lines that express SALL4 lose its expression upon EMT induction.

4.2.5.5 SALL4 loss is sufficient to induce an EMT signature

We next investigated whether SALL4 downregulation was a functional event during EMT. For this purpose, we transfected the M010817 line with RNAi specific for SALL4 (siSALL4) and we analyzed the cells at different time points after transfection (Figure 30D-K). At 24 hours post siSALL4 treatment we analyzed the mRNA levels of transcription factors as ZEB1, ZEB2 and TWIST1 that are dynamically regulated in the first phase of EMT (Caramel et al., 2013) (Figure 30D-E). Upon SALL4 knockdown, we observed a significant reduction in the ZEB2 transcript levels (Figure 30D) and a significant increase in ZEB1 and TWIST1 expression (Figure 30E). At 48 hours and 72 hours post transfection we observed a significant reduction in the transcript level of E-cadherin (CDH1) (Figure 30F-G) and a significant increase in the levels of N-cadherin (CDH2) and fibronectin (FN1) (Figure 30H). Interestingly, we detected a considerable increase in p75^{NTR} expression levels (Figure 30J-K), reaching almost 30-fold increase after 72 hours post RNAi treatment (Figure 30K). Overall, these data suggest that SALL4 loss upon EMT induction (Figure 30A-C) is rather a functional event that is sufficient to trigger EMT. Moreover, the extensive increase in p75^{NTR} expression upon SALL4 knockdown suggests the existence of a regulatory loop, in which p75^{NTR} can downregulate SALL4 (Figure 30B-C), and SALL4 can, in turn, directly or eventually through epigenetic mediators, inhibit p75^{NTR} (Figure 30J-K).

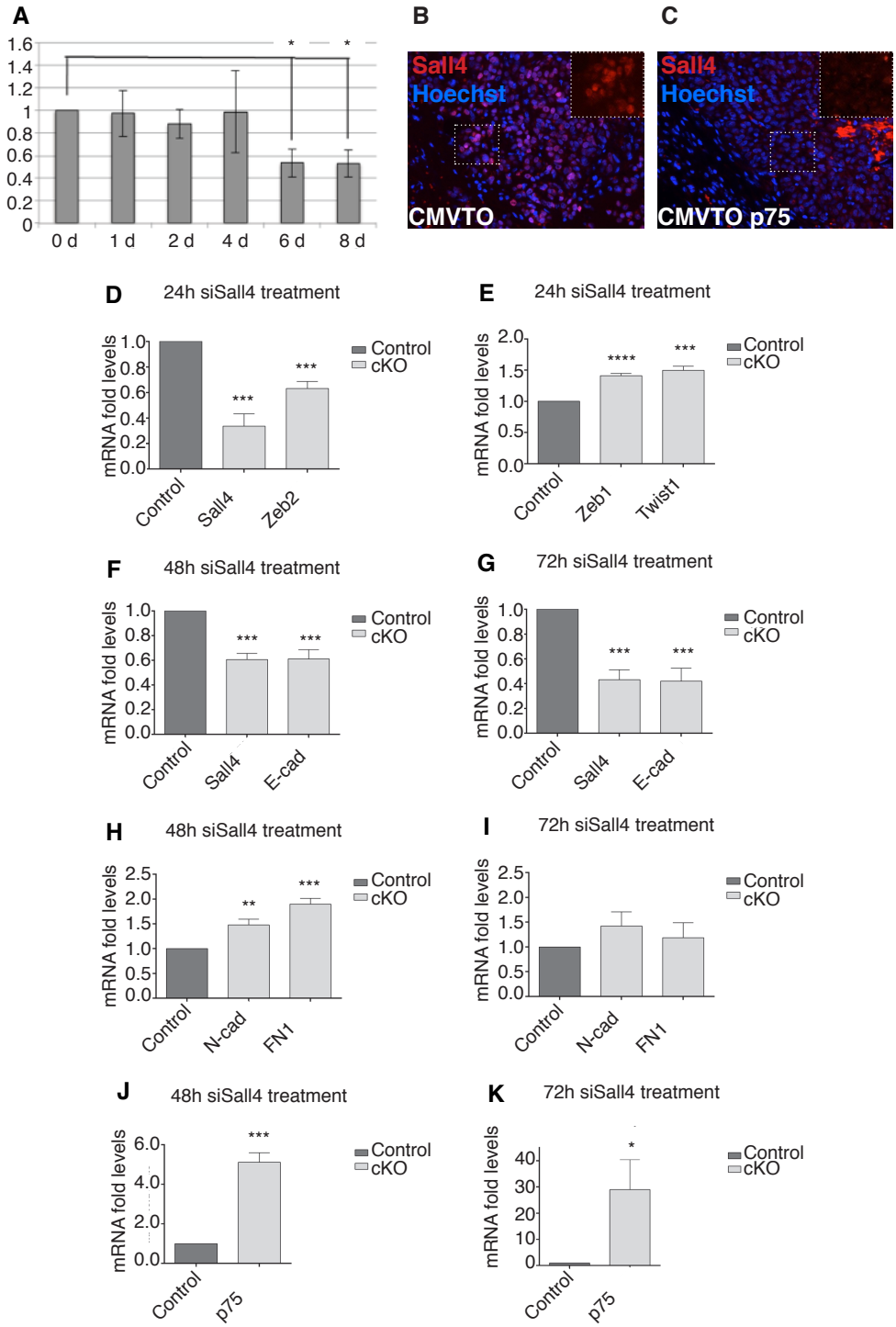

Figure 30. SALL4 expression in respect to EMT.

(A-C) M010817 treatment with TGFb-1 (A) or overexpression of $p75^{NTR}$ (B-C) induces EMT and decreases transcript (A) and protein levels (C) of SALL4. (D-K) RT-qPCR data for genes of the EMT signature upon SALL4 knockdown by RNAi in the M010817 line. Data are mean ± standard deviation. Statistic performed with N ≥ 3. P-values calculated with unpaired Student's t-test.

4.2.5.6 Sall4 expression in mouse wild type skin and in the Tyr::NRas^{Q61K}Ink4a$^{-/-}$ melanoma mouse model

Sall4 was weakly expressed in the Dct^{+} cells in the in the hair follicle of wild type (wt) mouse skin (Figure 31A) and in the hyperplastic lesions of the melanoma mouse model Tyr::NRas^{Q61K} Ink4a$^{-/-}$ (Figure 31B). In primary melanomas Sall4 was strongly expressed by a subpopulation of Dct^{+} cells. Future accurate quantifications are going to reveal the percentage of Sall4^{+} cells in the hyperplesia and in the primary tumors.

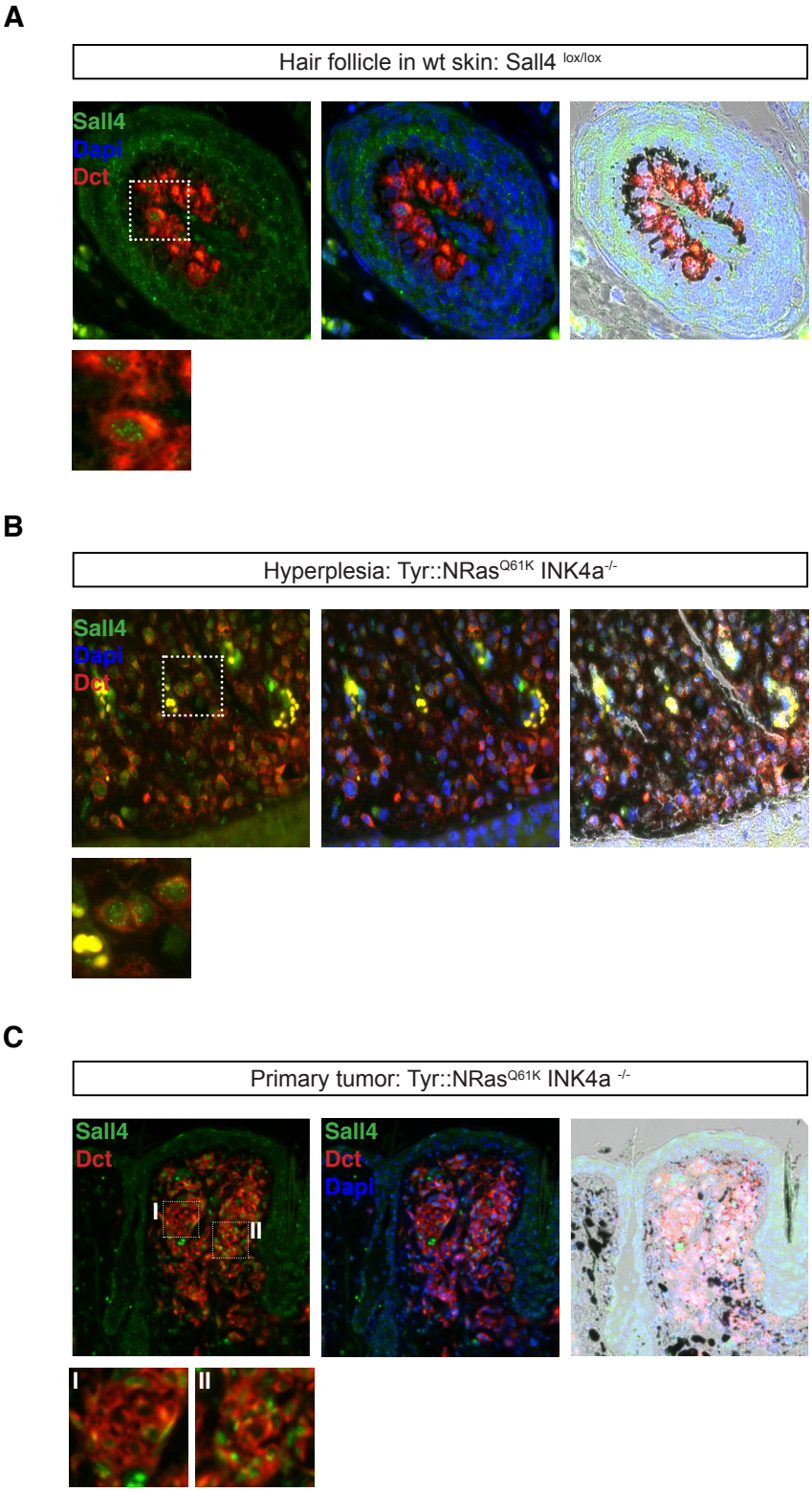

Figure 31. Sall4 staining in normal and tumorigenic mouse skin.

(A-C) Immunofluorescent staining on normal skin (mouse with Sall4 $^{lox/lox}$ genotype), hyperplastic lesion and primary melanoma (mouse with Tyr::NRas^{Q61K} Ink4a$^{-/-}$ genotype).

4.2.5.7 Sall4 is necessary for melanoma initiation

To examine the possibility that Sall4 may play a role in tumor initiation we conditionally deleted Sall4 by five consecutive intraperitoneal (i.p.) injections of tamoxifen (TM) in the melanoma mouse model *Tyr::NRas^{Q61K} Ink4a$^{-/-}$ Tyr::Cre^{ERT2} Sall4$^{lox/lox}$ R26R::GFP* at one month of age before any tumor initiation (cKO animals, Figure 32A, C). Control animals were not injected littermates (Figure 32B). The animals were sacrificed at the moment that the maximum tumor size was achieved (diameter of 5 mm) or that any atypical behavior and/or pain was assessed. As expected, around 5 to 6 months of age Control animals were developing primary tumors (diameter ≥ 2 mm, Figure 32D). However, cKO animals barely developed any tumors and the few observed were never recombined (Figure 32E, G). The skin of the cKO animals was hyperplastic and the animals were not greying suggesting that Sall4 loss was not influencing melanocytes survival.

However, the overall survival of the cKO animals was unexpectedly worse compared to the Control animals (Figure 32F), implying that Sall4 loss was having a negative effect on the survival outcome.

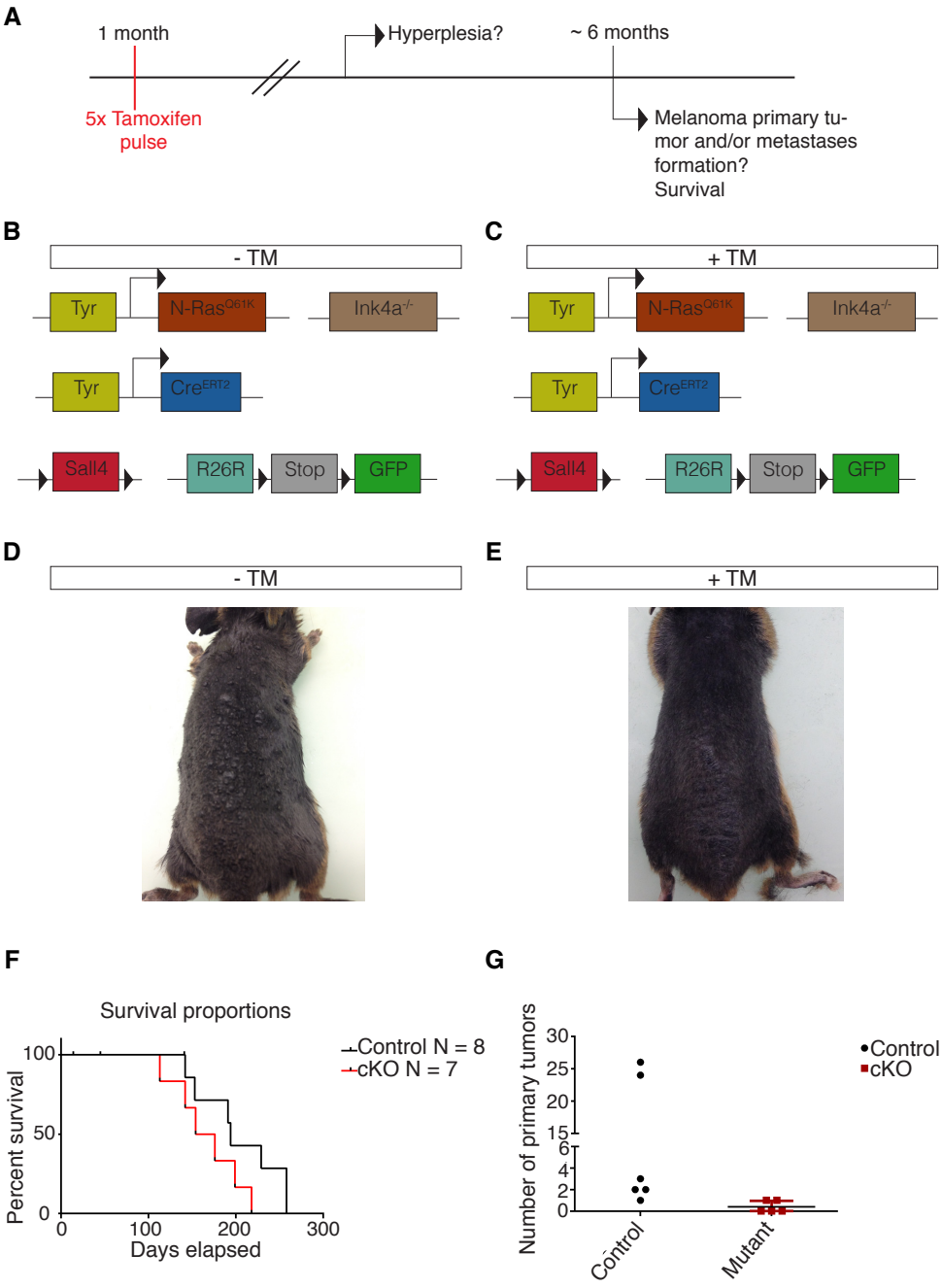

Figure 32. Sall4 function is essential for primary melanoma formation, but Sall4 loss is linked to worse overall survival.

(A) Experimental setup to analyze the function of Sall4 loss in the melanocytic lineage and its effect on melanoma formation. (B-C) Genotype strategy for the Control (- TM) animals and the cKO (+ TM) animals. (D-E) Macroscopic picture of a Control and of a cKO littermate at 5 months post TM injection. (F) Kaplan-Meier curve of the overall survival of Control and cKO

littermates. (G) Total number of primary skin melanoma observed in both Control and cKO littermates. In the cKO animals the total number of primary tumors is shown, independently whether recombination was observed.

4.2.5.8 Recombined melanocytes in the cKO animals

Intrigued by the previous results, we analyzed the skin of the cKO animals. Surprisingly, few recombined GFP^{+} cells were detected in the skin of the cKO animals (Figure 33 A-B). We could detect recombined cells only in the lymph nodes (Figure 33C) and in some lungs (data not shown) of the cKO animals.

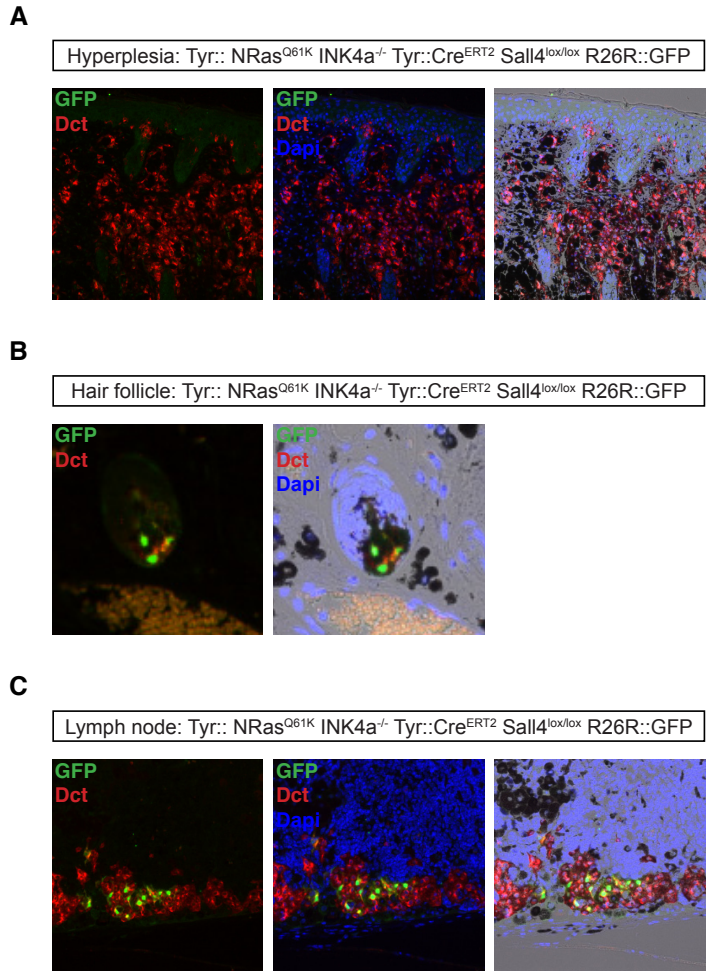

Figure 33. The effect of Sall4 loss in the cKO animals.

(A-B) Immunostaining for the melanocytic marker Dct (red) and for recombined cells (GFP, green) showed that very few recombined cells could be detected in the skin of cKO animals (hair follicle, B). (C) Recombined cells (green) in the lymph node of a cKO animal.

The limited number of recombined cells in the in the cKO animals could suggest that the recombination efficiency was low. However, we could exclude this possibility by injecting Control littermate Sall4 $^{wt/wt}$ animals (Figure 34). Recombination efficiency in these Control animals was in fact high (Figure 34A-B) and could confirm the validity of our experimental setup.

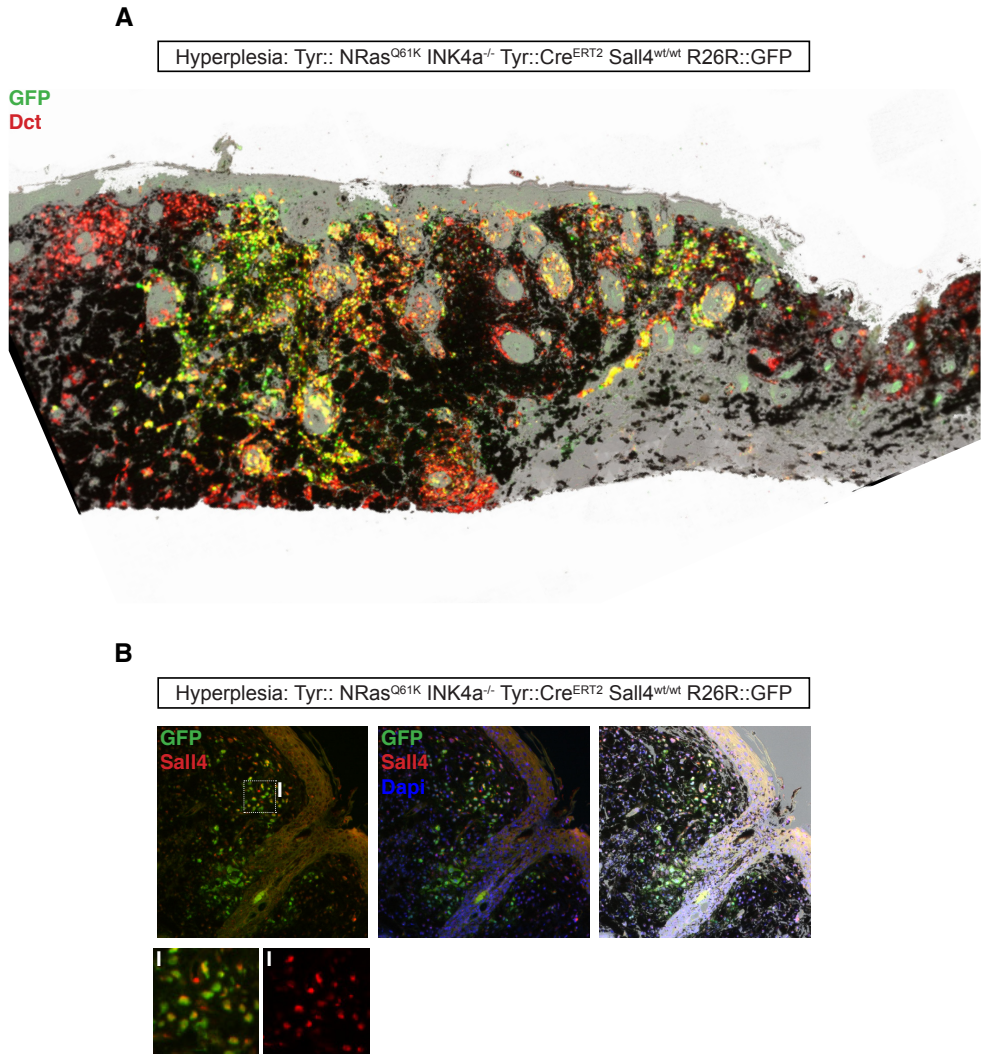

Figure 34. Recombination efficiency in the Tyr::NRas^{Q61K} Ink4a $^{-/-}$ Sall4 $^{wt/wt}$ R26R::GFP control animals.

(A) Immunofluorescent staining for Dct (red) and GFP (green) and (B) staining for GFP (green) and Sall4 (red) in injected Control animals demonstrates the efficiency of the recombination protocol.

Another possible explanation would be that Sall4 loss in the melanocytic lineage is lethal in vivo. However, this interpretation would not explain the presence of recombined cells in the hyperplesia and in the lymph nodes of the cKO animals (Figure 33 B, C).

To definitively rule out both possibilities we are going to analyze and quantify cKO animals sacrificed shortly after recombination before any cell dissemination may occur.

4.2.6 Discussion and Outlook

Sall4 is a crucial factor in the maintenance of pluripotency and self-renewal in ES cells. Moreover, SALL4 upregulation has been linked to worse survival, metastasis formation and acquisition of pluripotent characteristics in several types of tumor (Cao et al., 2009; Forghanifard et al., Gao et al., 2011; 2013; Yong et al., 2013; Zhang et al., 2015). In this study, preliminary results suggest that SALL4 may play an important unknown role in melanoma.

4.2.6.1 SALL4 expression in human melanoma cell lines and its influence on the survival rate of skin cutaneous melanoma patients.

SALL4 was expressed at both mRNA and at protein level in some proliferative human melanoma cell lines, while it was absent in more invasive melanoma cell lines. Interestingly, when invasiveness was induced in a proliferative melanoma cell line by TGFb-1 treatment (Figure 30A) or in xenotransplants by overexpressing $p75^{NTR}$ (Figure 30B-C) SALL4 expression was significantly reduced. Moreover, SALL4 knockdown by RNAi treatment induced an EMT signature in a proliferative melanoma cell line. At 24 hours post RNAi treatment we observed a significantly reduced expression of ZEB2 and a significant increase in ZEB1 and TWIST1 transcript levels (Figure 30D, E). After 48 hours and respectively 72 hours post RNAi treatment, we reported a reduction in the expression of the epithelial marker E-cadherin (CDH1) and an increase in the expression of mesenchymal markers as N-cadherin (CDH2) and fibronectin (FN1) (Figure 30F-I). Moreover, we observed a 30-folds increase in $p75^{NTR}$ (NGFR) transcript levels after 72 hours post RNAi treatment (Figure 30K) Overall these results suggest the presence of a regulatory loop in which SALL4 downregulation is a functional event that is also sufficient to induce EMT. However, further validations in additional melanoma cell lines are indispensable. Moreover, to test our hypothesis we plan to induce SALL4 overexpression combined with TGFb-1 treatment to investigate whether we could block, or partially inhibit, the EMT machinery. Furthermore, given that SALL4 can act as a transcriptional repressor through regulation of the epigenetic machinery by direct interaction with the NuRD complex, we plan to check whether SALL4 knockdown is related to a decrease in the HDACs activity, and whether, on the contrary, treatment of a proliferative melanoma cell line with a HDACs inhibitor would increase $p75^{NTR}$ expression.

The results obtained in vitro and with the xenotranplants (Figure 30), apparently contradict the overall survival rate produced by the TCGA analysis, in which patients of the SALL4 low group show a better survival than those of the SALL4 high group (Figure 28). A possible hypothesis explaining this discrepancy would be that it is the proliferation rate of the primary melanoma and mostly of the metastases the most severe factor affecting patients survival. Given that SALL4 is expressed in highly proliferative melanoma cell lines and it is downregulated upon EMT induction, we can speculate that SALL4 may be important for the maintenance of proliferation in melanoma. SALL4 decrease would thus reduce cell proliferation, as it has already been shown for other tumor types (Zhang et al., 2015), and have a positive effect on patient survival. Further analyses of the cell cycle upon SALL4 knockdown are required to confirm this point.

However in the mouse model, Sall4 loss can not be dynamically regulated. We are prompted, thus, to speculate that Sall4 loss may result in an even more severe outcome, characterized by a higher number of metastases (Figure 33).

In the literature, SALL4 overexpression is linked to worse prognosis, increased metastasis formation and increased tumor proliferation in tumors other than melanoma (Yong et al., 2013; Zhang et al., 2015). Although, our results don't suggest that high SALL4 expression is promoting a higher number of metastases, but actually the contrary, we have indications that SALL4 positively influences cell proliferation in melanoma (Figure 29B-D), as it has been proposed in other types of tumors (Kobayashi et al., 2011).

4.2.6.2 Sall4 function in the Tyr::NRas^{Q61K} Ink4a$^{-/-}$ melanoma mouse model

Preliminary results in vivo suggest that Sall4 is necessary for primary melanoma formation and that its loss inhibits tumor development (Figure 32D, E). These results would suggest a function of Sall4 in cell proliferation (Kobayashi et al., 2011; Li et al., 2015) and that its loss would unable tumorigenic cells to proliferate and give rise to primary tumors.

Sall4 is heterogeneously expressed in primary melanomas of the Tyr::NRas^{Q61K} Ink4a$^{-/-}$ mouse model (Figure 31C) and it would be interesting to investigate whether Sall4^{+} melanoma cells would have a survival advantage.

When we analyzed the cKO animals, we surprisingly observed few recombined cells in the skin. We could exclude that this result was due to low recombination efficiency because recombined Control littermates were showing good levels of recombination (Figure 34). We also excluded that Sall4 loss was affecting cell survival, because of

the results obtained in vitro and in the xenotransplants (Figure 30) and because we still recorded recombined cells after 5 month post recombination (Figure 33).
We then analyzed LNs and lungs of the cKO animals and we could always observe recombined cells in the LNs (Figure 33C), and in some cases in the lungs (data not shown). Whether cKO cells may really undergo EMT, invade the bloodstream and finally colonize distant organs needs extensive further investigations. To examine this hypothesis, we plan to produce doxycycline-inducible SALL4 overexpressing invasive human melanoma cell lines and to inject them into NSG mice. If it is correct that SALL4 loss is reducing cell proliferation and promoting metastases formation, we expect that SALL4 overexpression would decrease metastasis numbers when overexpressed shortly after injection, even though increasing primary tumor size. On the other side, we expect that SALL4 overexpression later after cells injection, once the cells have already metastasized, would produce bigger and more proliferative metastases.
A further experiment that we are planning to perform is to inject tumoral cells derived from a *Tyr::NRas^{Q61K} Ink4a$^{-/-}$ Tyr::Cre^{ERT2} Sall4$^{lox/lox}$ R26R::GFP* mouse into nude mice. Following tumor growth we plan to induce recombination. The derived recombined tumors should demonstrate whether recombined cells eventually die upon Sall4 loss in vivo, or whether they perform EMT, and provide material for gene expression analysis.

4.2.6.3 SALL4 as a putative therapeutic target

SALL4 is not expressed in the majority of normal adult tissues, with exception of the spermatogonia (Cao et al., 2009), but it is aberrantly upregulated in a vast number of tumors (Zhang et al., 2015). This led to the idea that SALL4 may be a good therapeutic target to treat cancer (Jones, 2013; Yong et al., 2013). High levels of SALL4 expression are indeed linked to a higher rate of tumor proliferation, acquisition of stem cell-like properties and high metastatic potential. These features result in an overall worse survival outcome, while low levels of SALL4 expression are correlated to lower proliferation rate, weaker metastasizing potential and better survival expectancy. Consequently, for some types of tumor, as hepatocellular carcinoma (Yong et al., 2013), it is now under discussion whether to use small-molecule drugs to target SALL4. These treatments could consist of SALL4-peptide-based inhibitors or other drugs, as HDAC inhibitors, that would inhibit SALL4-activated pathways.

These treatments could indeed be of interest to treat numerous types of cancer. However, on the basis of our preliminary results their efficacy on treating melanoma would be highly debatable. Our prediction would be in fact that inhibiting SALL4 in an already formed tumor would reduce cell proliferation, but would eventually promote metastasis formation. Further investigations are now needed to elucidate whether SALL4 may really play such a unique role that seems to be characteristic of melanoma.

4.2.7 Experimental procedures

4.2.7.1 Mice

The experimental animals *Tyr::NRas^{Q61K} Ink4a$^{-/-}$ Tyr::Cre^{ERT2} Sall4$^{lox/lox}$ R26R::GFP* were obtained by crossing the *Tyr::NRas^{Q61K}* and the *Ink4a$^{-/-}$* mouse line (Ackermann et al., 2005; Serrano et al., 1996) with the *Tyr::Cre^{ERT2}* (Bosenberg et al., 2006), the *Sall4 ^{lox}* (Elling et al., 2006) and the *R26R::GFP* (Simon et al., 2012) mouse lines (Table 5). Animals of both genders were put under experiment at one month of age. Animals were sacrificed around 5 to 6 months of age whenever affected by skin tumors > 5 mm, weight loss (< 15%), symptoms of pain as hunched back or any abnormal behavior. Animal experiments were approved by the veterinary office of the Canton of Zurich, Switzerland.

Table 5: Mouse genotyping primers

Allele	Forward sequence	Reverse sequence
Cre	AGGCTAAGTGCCTTCTCTACAC	ACCAGGTTCGTTCACTCATGG
Sall4^{lox}	CTCCACCAACTCTAGCTGCTAATGGC	ATGGCCTTTGCACATGTGTTCTGGAG
Sall4^{wt}	CTCCACCAACTCTAGCTGCTAATGGC	GTTACAGCAATACGGAGATACACAGC
Ink4a^{wt}	ATGATGATGGGCAACGTTC	CAAATATCGCACGATGTC
Ink4a^{-}	CTATCAGGACATAGCGTTGG	AGTGAGAGTTTGGGGACAGAG
GFP	CGCACCATCTTCTTCAAGGACGAC	AACTCCAGCAGGACCATGTGATCG

4.2.7.2 Tamoxifen injections and quantification of primary melanomas and metastases

Sall4 was conditionally ablated at one month of age in *Tyr::NRas^{Q61K} Ink4a$^{-/-}$ Tyr::Cre^{ERT2} Sall4$^{lox/lox}$ R26R::GFP* animals by i.p. injections of 2mg tamoxifen for five consecutive days. Tamoxifen (T5648, Sigma-Aldrich) was diluted in ethanol and sunflower oil (1:10) for a final concentration of 10mg/ml.
When the animals were sacrificed the numbers of melanoma and of metastases was assessed. Melanomas were defined as kin lesion with a diameter > 2mm. Metastases were detected at the binocular and checked whether they were recombined and expressing GFP^{+}.

4.2.7.3 Immunofluorescence

Mouse samples were fixed in 4% formaldehyde and embedded in paraffin. For immunohistochemistry, paraffin sections were processed as previously described (Shakhova et al., 2012). See Table 6 for the list of antibodies.

Table 6: Primary and secondary antibodies

Primary antibodies				
Antigen	Specificity	Company	Serial number	Dilution
DCT	human/mouse	Santa Cruz Biotechnology	sc-10451	1:250
Sall4	mouse	abcam	ab29112	1:200
GFP	mouse	Aves	GFP-1020	1:400

Secondary antibodies				
Fluorophore	Specificity	Company	Serial number	Dilution
DyLight 649	goat	Jackson	705-495-147	1:300
Cy3	rabbit	Jackson	711-165-152	1:300
DyLight 549	chicken	Jackson	703-505-155	1:300

4.2.7.4 Cell culture

Human melanoma lines were cultured with RPMI 1640 (42401, Life Technologies) with addition of 10% FCS (16140, Life Technologies), 4mM L-Glutamine (25030, Life Technologies), Penicillin-Streptomycin (15070, Life Technologies) and Fungizone (15290, Life Technologies).

4.2.7.5 Cell transfection

20 mM siRNA (Table 7) was applied to the cells in combination with jetPRIME siRNA Transfection Reagent (114-75, Polypus Transfection) according to manufacturer's guidelines.
The medium was exchanged after 24 hours and the cells were analyzed at 24, 48 and 72 hours post transfection.

Table 7: RNAi constructs

Target gene	siRNA name	Specificity	Company	Serial numbers
none	siCtr	human	Life Technologies	12935-112
SALL4	siSALL4	human	Life Technologies	HSS183741, HSS126094, HSS126095

4.2.7.6 RNA isolation and RT-qPCR

RNA was extracted and purified using the RNeasy Mini Kit (74104, Qiagen). Purified RNA was measured using the nanodrop. Reverse transcription was performed using the Maxima First Strand cDNA Synthesis Kit (K1641, Thermo Scientific) and cDNA was treated with RNase H /EN0202, Thermo Scientific). Quantitative real-time PCR (RT-qPCR) was perfomed using the LightCycler 480 System (Roche) and the LightCycler 480 SYBR Green I Master (4707516001, Roche). Primers are indicated in Table 8.

Table 8: Human RT-qPCR primers

Gene	Forward sequence	Reverse sequence
b-actin	CGA CAA CGG CTC CGG CAT GTG C	CGT CAC CGG AGT CCA TCA CGA TGC
E-cadherin	TGC CCA GAA AAT GAA AAA GG	GTG TAT GTG GCA ATG CGT TC
N-cadherin	ACA GTG GCC ACC TAC AAA GG	CCG AGA TGG GGT TGA TAA TG
Fibronectin (FN1)	TACCAAGGCTGGATGATGG	AGATGCACTGGAGCAGGTTT
$p75^{NTR}$	CCT ACG GCT ACT ACC AGG ATG	CAC ACG GTG TTC TGC TTG T
Twist1	GTC CGC AGT CTT ACG AGG AG	CCA GCT TGA GGG TCT GAA TC
Zeb1	GCA CAA CCA AGT GCA GAA GA	CAT TTG CAG ATT GAG GCT GA
Zeb2	CGC TTG ACA TCA CTG AAG GA	CTT GCC ACA CTC TGT GCA TT

5 Discussion

5.1 The NC to model and treat disease

The NC is a transient embryonic multipotent cell population that during development of the vertebrate embryo gives rise to a variety of cell types ranging from the neurons and the glia of the peripheral nervous system, to the melanocytes of the skin and to the craniofacial cartilage, among others (Baggiolini et al., 2015; Bronner-Fraser and Fraser, 1988). Aberrant control of the mechanisms regulating NC cells migration, differentiation and proliferation often results in the onset of neurocristopathies, such as pigmentation defects, craniofacial abnormalities and cancer. Most of the studies on the NC have been performed in model organisms as the mouse, chick and zebrafish. However, these models are not always the most appropriate to study the molecular mechanisms underlying human neurocristopathies and eventually to screen for therapeutic targets to prevent and treat human developmental defects.

A promising model to study disease mechanisms is the use of induced NC cells that can be derived from both human embryonic stem cells (hESCs) or from human induced pluripotent stem cells (iPSCs) (Lee et al., 2007; Lee et al., 2009). For instance, familial dysautonomia (FD), which is a NC-derived peripheral neuropathy caused by a point mutation in IKBKAP8, has been already modeled using patient-derived iPSCs (Lee et al., 2009). This resulted in a large-scale drug-discovery screen on iPSCs-derived NC cells for a total of 6,912 small-molecule compounds and the discovery of SKF-86466, a compound able to rescue IKAP protein level and to rescue the FD-caused loss of autonomic neurons (Lee et al., 2012).

The availability of patient-specific iPSCs-derived NC cells does not only provide material for molecular studies and drugs screening, but also opens the possibility to personalized cell-based therapy and cell replacement. However, because of the multipotent nature of the NC cells, it is still necessary to develop appropriate protocols to definitively commit NC cells in the required cell fate to avoid the appearance of undesired cell types or tumor development.

5.2 The NC to understand and fight cancer

Upon induction of the NC in the neural folds, NC cells undergo an epithelial to mensenchymal transition characterized by loss of cell-cell contacts, change of the actin cytoskeleton and loss of the apico-basal cell polarity. With the acquisition of the

mesenchymal features NC cells delaminate from the neural tube and migrate extensively through the embryonic body on defined paths to finally differentiate into varied cell types and proliferate. NC cells are, thus, highly invasive and mobile; characteristics that are essential during development, but that can be exploited by malignant cells at later stages. It is widely accepted indeed that tumoral cells may adopt embryonic programs to progress to further stages of malignancy (Maguire et al., 2015). For instance, in both the NC and in cancer, EMT occurs through a "cadherin switch" (Taneyhill, 2008) from E-cadherin to N-cadherin expression. Moreover in both systems the EMT master regulators Snail, Zeb and Twist are activated. NC cells activate during EMT also matrix metalloproteinases (MMPS) and domain-containing protein 10 (ADAM10) to break the basement membrane that separate the neural epithelium from the mesenchyme and to migrate through the developing embryo. Similarly, malignant cells upregulate MMPS and ADAMs too, to break the basement membrane and reach lymphatic and blood vessels and be able to metastasize. Furthermore, NC cells require the hypoxia inducible factor-1alpha (HIF-1alpha) to activate Twist and regulate the chemotaxis receptor CXCR4 (Barriga et al., 2013), which regulate NC cells migration. Similarly, malignant cells exploit HIF-1alpha and activate Twist to undergo EMT (Maguire et al., 2015).

Melanoma is a malignancy of the melanocytes, which are NC-derived. NRAS and especially BRAF mutations are the most occurring genetic aberrations in melanoma. Both mutations result in a constitutive activation of the MEK/ERK signaling pathway and in consequent cell proliferation and survival (Schadendorf et al., 2015). Melanoma cells activate as well EMT regulators known from development; in particular melanoma cells perform a switch from SNAIL2/ZEB2 to TWIST1/ZEB1 expression (Caramel et al., 2013) and downregulate E-cadherin (CDH1). That melanoma cells adopt NC-mechanisms during malignancy is also evident from transplantation studies in which aggressive melanoma lines were injected in chick embryos. As a result, aggressive melanoma cells, but not less aggressive melanoma cells or melanocytes, could respond to signals in the developing embryos and migrate to the embryonic target structure (Kulesa et al., 2006).

The fact that cancer cells exploit many mechanisms typical of NC development suggests that a deep understanding of NC biology may significantly contribute to treatment of this malignancy. On this line, a trancriptome analysis of premigratory and migratory NC cells isolated from the chick embryo has been performed and compared to neuroblastoma microarray data. The comparison resulted in the discovery of 27 genes that are NC-specific and relevant to neuroblastoma formation (Rabadán et al., 2013).

Similarly, our laboratory has recently performed a microarray analysis of isolated mouse NC cells and compared it to the microarray data of NC cells primed towards differentiation (Varum et al., unpublished). We obtained a list of 53 trancription factors that were specifically expressed in the NC and that were downregulated upon differentiation. Some of these factors, including Sall4 (4.2 The roles of Sall4 in melanoma), have already demonstrated to have an influence on melanoma formation and progression (Varum et al., unpublished). The ongoing investigations are going to enlighten more similarities between development and cancer and hopefully to bring deeper understanding of how we should apply our knowledge on embryogenesis to treat this malignancy.

6 References

Ackermann, J., Frutschi, M., Kaloulis, K., McKee, T., Trumpp, A., and Beermann, F. (2005). Metastasizing Melanoma Formation Caused by Expression of Activated N-RasQ61K on an INK4a-Deficient Background. Cancer Res *65*, 4005–4011.

Angeles Rabadán, M., Usieto, S., Lavarino, C., and Martí, E. (2013). Identification of a putative transcriptome signature common to neuroblastoma and neural crest cells. Devel Neurobio *73*, 815–827.

Baggiolini, A., Varum, S., Mateos, J.M., Bettosini, D., John, N., Bonalli, M., Ziegler, U., Dimou, L., Clevers, H., Furrer, R., et al. (2015). Premigratory and Migratory Neural Crest Cells Are Multipotent In Vivo. Cell Stem Cell *16*, 314–322.

Bai, S., Wei, S., Ziober, A., Yao, Y., and Bing, Z. (2013). SALL4 and SF-1 Are Sensitive and Specific Markers for Distinguishing Granulosa Cell Tumors From Yolk Sac Tumors. INT J SURG PATHOL *21*, 121–125.

Al-Baradie, R., Yamada, K., St. Hilaire, C., Chan, W.-M., Andrews, C., McIntosh, N., Nakano, M., Martonyi, E.J., Raymond, W.R., Okumura, S., et al. (2002). Duane Radial Ray Syndrome (Okihiro Syndrome) Maps to 20q13 and Results from Mutations in SALL4, a New Member of the SAL Family. The American Journal of Human Genetics *71*, 1195–1199.

Barembaum, M., and Bronner-Fraser, M. (2004). A novel spalt gene expressed in branchial arches affects the ability of cranial neural crest cells to populate sensory ganglia. Neuron Glia Biol. *1*, 57–63.

Barembaum, M., and Bronner-Fraser, M. (2007). Spalt4 mediates invagination and otic placode gene expression in cranial ectoderm. Development *134*, 3805–3814.

Baroffio, A., Dupin, E., and Douarin, N.M.L. (1988). Clone-forming ability and

differentiation potential of migratory neural crest cells. PNAS *85*, 5325–5329.

Barriga, E.H., Maxwell, P.H., Reyes, A.E., and Mayor, R. (2013). The hypoxia factor Hif-1α controls neural crest chemotaxis and epithelial to mesenchymal transition. J Cell Biol *201*, 759–776.

Bauer, J., Curtin, J.A., Pinkel, D., and Bastian, B.C. (2006). Congenital Melanocytic Nevi Frequently Harbor NRAS Mutations but no BRAF Mutations. J Invest Dermatol *127*, 179–182.

Baumann, K. (2015). Stem cells: Linking stemness to low DNA damage. Nat Rev Mol Cell Biol *16*, 205–205.

Bautista, N.C., Cohen, S., and Anders, K.H. (1994). Benign melanocytic nevus cells in axillary lymph nodes. A prospective incidence and immunohistochemical study with literature review. Am. J. Clin. Pathol. *102*, 102–108.

Böhm, J., Buck, A., Borozdin, W., Mannan, A.U., Matysiak-Scholze, U., Adham, I., Schulz-Schaeffer, W., Floss, T., Wurst, W., Kohlhase, J., et al. (2008). Sall1, Sall2, and Sall4 Are Required for Neural Tube Closure in Mice. Am J Pathol *173*, 1455–1463.

Borozdin, W., Graham, J.M., Böhm, D., Bamshad, M.J., Spranger, S., Burke, L., Leipoldt, M., and Kohlhase, J. (2007). Multigene deletions on chromosome 20q13.13-q13.2 including SALL4 result in an expanded phenotype of Okihiro syndrome plus developmental delay. Human Mutation *28*, 830–830.

Bosenberg, M., Muthusamy, V., Curley, D.P., Wang, Z., Hobbs, C., Nelson, B., Nogueira, C., Horner, J.W., DePinho, R., and Chin, L. (2006). Characterization of melanocyte-specific inducible Cre recombinase transgenic mice. Genesis *44*, 262–267.

Brandl, C., Florian, C., Driemel, O., Weber, B.H.F., and Morsczeck, C. (2009). Identification of neural crest-derived stem cell-like cells from the corneal limbus of juvenile mice. Experimental Eye Research *89*, 209–217.

Bronner, M. (2015). Confetti Clarifies Controversy: Neural Crest Stem Cells Are Multipotent. Cell Stem Cell *16*, 217–218.

Bronner-Fraser, M., and Fraser, S. (1989). Developmental potential of avian trunk neural crest cells in situ. Neuron *3*, 755–766.

Bronner-Fraser, M., and Fraser, S.E. (1988). Cell lineage analysis reveals multipotency of some avian neural crest cells. Nature *335*, 161–164.

Cao, D., Humphrey, P.A., and Allan, R.W. (2009a). SALL4 is a novel sensitive and specific marker for metastatic germ cell tumors, with particular utility in detection of metastatic yolk sac tumors. Cancer *115*, 2640–2651.

Cao, D., Li, J., Guo, C.C., Allan, R.W., and Humphrey, P.A. (2009b). SALL4 is a novel diagnostic marker for testicular germ cell tumors. Am. J. Surg. Pathol. *33*, 1065–1077.

Caramel, J., Papadogeorgakis, E., Hill, L., Browne, G.J., Richard, G., Wierinckx, A., Saldanha, G., Osborne, J., Hutchinson, P., Tse, G., et al. (2013). A Switch in the Expression of Embryonic EMT-Inducers Drives the Development of Malignant Melanoma. Cancer Cell *24*, 466–480.

Carson, K.F., Wen, D.R., Li, P.X., Lana, A.M., Bailly, C., Morton, D.L., and Cochran, A.J. (1996). Nodal nevi and cutaneous melanomas. Am. J. Surg. Pathol. *20*, 834–840.

De Celis, J.F., and Barrio, R. (2009). Regulation and function of Spalt proteins during animal development. Int. J. Dev. Biol. *53*, 1385–1398.

Centanin, L., Hoeckendorf, B., and Wittbrodt, J. (2011). Fate restriction and multipotency in retinal stem cells. Cell Stem Cell *9*, 553–562.

Chen, X., Vega, V.B., and Ng, H.-H. (2008). Transcriptional Regulatory Networks in Embryonic Stem Cells. Cold Spring Harb Symp Quant Biol *73*, 203–209.

Clark, W.H., Elder, D.E., Guerry, D., Epstein, M.N., Greene, M.H., and Van

Horn, M. (1984). A study of tumor progression: the precursor lesions of superficial spreading and nodular melanoma. Hum. Pathol. *15*, 1147–1165.

Cordero, D.R., Brugmann, S., Chu, Y., Bajpai, R., Jame, M., and Helms, J.A. (2011). CRANIAL NEURAL CREST CELLS ON THE MOVE: THEIR ROLES IN CRANIOFACIAL DEVELOPMENT. Am J Med Genet A *155*, 270–279.

Couly, G.F., and Le Douarin, N.M. (1985). Mapping of the early neural primordium in quail-chick chimeras. Developmental Biology *110*, 422–439.

Crane, J.F., and Trainor, P.A. (2006). Neural Crest Stem and Progenitor Cells. Annual Review of Cell and Developmental Biology *22*, 267–286.

Cristofano, A.D., Pesce, B., Cordon-Cardo, C., and Pandolfi, P.P. (1998). Pten is essential for embryonic development and tumour suppression. Nat Genet *19*, 348–355.

Damsky, W.E., Theodosakis, N., and Bosenberg, M. (2014). Melanoma metastasis: new concepts and evolving paradigms. Oncogene *33*, 2413–2422.

Delaunay, D., Heydon, K., Cumano, A., Schwab, M.H., Thomas, J.-L., Suter, U., Nave, K.-A., Zalc, B., and Spassky, N. (2008). Early neuronal and glial fate restriction of embryonic neural stem cells. J. Neurosci. *28*, 2551–2562.

Douarin, N.M.L., Creuzet, S., Couly, G., and Dupin, E. (2004). Neural crest cell plasticity and its limits. Development *131*, 4637–4650.

Douarin, N.M.L., Calloni, G.W., and Dupin, E. (2008). The stem cells of the neural crest. Cell Cycle *7*, 1013–1019.

Dupin, E., and Le Douarin, N.M. (2014). The neural crest, A multifaceted structure of the vertebrates. Birth Defect Res C *102*, 187–209.

Dupin, E., and Sommer, L. (2012). Neural crest progenitors and stem cells: From early development to adulthood. Developmental Biology *366*, 83–95.

Dupin, E., Creuzet, S., and Le Douarin, N.M. (2006). The contribution of the neural crest to the vertebrate body. Adv. Exp. Med. Biol. *589*, 96–119.

Dupin, E., Calloni, G.W., and Le Douarin, N.M. (2010). The cephalic neural crest of amniote vertebrates is composed of a large majority of precursors endowed with neural, melanocytic, chondrogenic and osteogenic potentialities. Cell Cycle *9*, 238–249.

Eggermont, A.M., Spatz, A., and Robert, C. (2014). Cutaneous melanoma. The Lancet *383*, 816–827.

El-Helou, V., Beguin, P.C., Assimakopoulos, J., Clement, R., Gosselin, H., Brugada, R., Aumont, A., Biernaskie, J., Villeneuve, L., Leung, T.K., et al. (2008). The rat heart contains a neural stem cell population; Role in sympathetic sprouting and angiogenesis. Journal of Molecular and Cellular Cardiology *45*, 694–702.

Elling, U., Klasen, C., Eisenberger, T., Anlag, K., and Treier, M. (2006). Murine inner cell mass-derived lineages depend on Sall4 function. Proc Natl Acad Sci U S A *103*, 16319–16324.

Erickson, C.A., Duong, T.D., and Tosney, K.W. (1992). Descriptive and experimental analysis of the dispersion of neural crest cells along the dorsolateral path and their entry into ectoderm in the chick embryo. Developmental Biology *151*, 251–272.

Etchevers, H.C., Amiel, J., and Lyonnet, S. (2006). Molecular bases of human neurocristopathies. Adv. Exp. Med. Biol. *589*, 213–234.

Fisher, C.J., Hill, S., and Millis, R.R. (1994). Benign lymph node inclusions mimicking metastatic carcinoma. J Clin Pathol *47*, 245–247.

FitzGerald, M.G., Harkin, D.P., Silva-Arrieta, S., MacDonald, D.J., Lucchina, L.C., Unsal, H., O'Neill, E., Koh, J., Finkelstein, D.M., Isselbacher, K.J., et al. (1996). Prevalence of germ-line mutations in p16, p19ARF, and CDK4 in familial melanoma: analysis of a clinic-based population. Proc Natl Acad Sci U

S A *93*, 8541–8545.

Forghanifard, M.M., Moghbeli, M., Raeisossadati, R., Tavassoli, A., Mallak, A.J., Boroumand-Noughabi, S., and Abbaszadegan, M.R. (2013). Role of SALL4 in the progression and metastasis of colorectal cancer. J Biomed Sci *20*, 6.

Fujimoto, M., Sumiyoshi, S., Yoshizawa, A., Sonobe, M., Kobayashi, M., Moriyoshi, K., Kido, A., Tanaka, C., Koyanagi, I., Date, H., et al. (2014). SALL4 immunohistochemistry in non-small-cell lung carcinomas. Histopathology *64*, 309–311.

Gans, C., and Northcutt, R.G. (1983). Neural crest and the origin of vertebrates: a new head. Science *220*, 268–273.

Gao, C., Kong, N.R., and Chai, L. (2011). The role of stem cell factor SALL4 in leukemogenesis. Crit Rev Oncog *16*, 117–127.

Gao, C., Dimitrov, T., Yong, K.J., Tatetsu, H., Jeong, H., Luo, H.R., Bradner, J.E., Tenen, D.G., and Chai, L. (2013). Targeting transcription factor SALL4 in acute myeloid leukemia by interrupting its interaction with an epigenetic complex. Blood *121*, 1413–1421.

Giuliano, A.E., Moseley, H.S., and Morton, D.L. (1980). Clinical Aspects of Unknown Primary Melanoma. Ann Surg *191*, 98–104.

Gonsalvez, D.G., Cane, K.N., Landman, K.A., Enomoto, H., Young, H.M., and Anderson, C.R. (2013). Proliferation and Cell Cycle Dynamics in the Developing Stellate Ganglion. J. Neurosci. *33*, 5969–5979.

Green, S.A., Simoes-Costa, M., and Bronner, M.E. (2015). Evolution of vertebrates as viewed from the crest. Nature *520*, 474–482.

Hackl, M.J., Burford, J.L., Villanueva, K., Lam, L., Suszták, K., Schermer, B., Benzing, T., and Peti-Peterdi, J. (2013). Tracking the fate of glomerular epithelial cells in vivo using serial multiphoton imaging in new mouse models

with fluorescent lineage tags. Nat Med *19*, 1661–1666.

Hari, L., Miescher, I., Shakhova, O., Suter, U., Chin, L., Taketo, M., Richardson, W.D., Kessaris, N., and Sommer, L. (2012). Temporal control of neural crest lineage generation by Wnt/β-catenin signaling. Development *139*, 2107–2117.

Heanue, T.A., and Pachnis, V. (2007). Enteric nervous system development and Hirschsprung's disease: advances in genetic and stem cell studies. Nat Rev Neurosci *8*, 466–479.

Henion, P.D., and Weston, J.A. (1997). Timing and pattern of cell fate restrictions in the neural crest lineage. Development *124*, 4351–4359.

Hodis, E., Watson, I.R., Kryukov, G.V., Arold, S.T., Imielinski, M., Theurillat, J.-P., Nickerson, E., Auclair, D., Li, L., Place, C., et al. (2012). A Landscape of Driver Mutations in Melanoma. Cell *150*, 251–263.

Hupfeld, T., Chapuy, B., Schrader, V., Beutler, M., Veltkamp, C., Koch, R., Cameron, S., Aung, T., Haase, D., LaRosee, P., et al. (2013). Tyrosinekinase inhibition facilitates cooperation of transcription factor SALL4 and ABC transporter A3 towards intrinsic CML cell drug resistance. Br J Haematol *161*, 204–213.

Itou, J., Matsumoto, Y., Yoshikawa, K., and Toi, M. (2013). Sal-like 4 (SALL4) suppresses CDH1 expression and maintains cell dispersion in basal-like breast cancer. FEBS Letters *587*, 3115–3121.

Jiang, X., Rowitch, D.H., Soriano, P., McMahon, A.P., and Sucov, H.M. (2000). Fate of the mammalian cardiac neural crest. Development *127*, 1607–1616.

John, N., Cinelli, P., Wegner, M., and Sommer, L. (2011). Transforming growth factor β-mediated Sox10 suppression controls mesenchymal progenitor generation in neural crest stem cells. Stem Cells *29*, 689–699.

Jones, B. (2013). Liver cancer: SALL4—a cancer marker and target. Nat Rev Clin Oncol *10*, 426–426.

Jürgens, G. (1988). Head and tail development of the Drosophila embryo involves spalt, a novel homeotic gene. EMBO J *7*, 189–196.

Ke, M.-T., Fujimoto, S., and Imai, T. (2013). SeeDB: a simple and morphology-preserving optical clearing agent for neuronal circuit reconstruction. Nat Neurosci *16*, 1154–1161.

Kobayashi, D., Kuribayashi, K., Tanaka, M., and Watanabe, N. (2011a). Overexpression of SALL4 in lung cancer and its importance in cell proliferation. Oncol. Rep. *26*, 965–970.

Kobayashi, D., Kuribayshi, K., Tanaka, M., and Watanabe, N. (2011b). SALL4 is essential for cancer cell proliferation and is overexpressed at early clinical stages in breast cancer. Int. J. Oncol. *38*, 933–939.

Kohlhase, J., Heinrich, M., Schubert, L., Liebers, M., Kispert, A., Laccone, F., Turnpenny, P., Winter, R.M., and Reardon, W. (2002). Okihiro syndrome is caused by SALL4 mutations. Hum. Mol. Genet. *11*, 2979–2987.

Kohlhase, J., Schubert, L., Liebers, M., Rauch, A., Becker, K., Mohammed, S., Newbury-Ecob, R., and Reardon, W. (2003). Mutations at the SALL4 locus on chromosome 20 result in a range of clinically overlapping phenotypes, including Okihiro syndrome, Holt-Oram syndrome, acro-renal-ocular syndrome, and patients previously reported to represent thalidomide embryopathy. J Med Genet *40*, 473–478.

Kretzschmar, K., and Watt, F.M. (2012). Lineage Tracing. Cell *148*, 33–45.

Krispin, S., Nitzan, E., and Kalcheim, C. (2010a). The dorsal neural tube: A dynamic setting for cell fate decisions. Developmental Neurobiology *70*, 796–812.

Krispin, S., Nitzan, E., Kassem, Y., and Kalcheim, C. (2010b). Evidence for a

Dynamic Spatiotemporal Fate Map and Early Fate Restrictions of Premigratory Avian Neural Crest. Development *137*, 585–595.

Kruger, G.M., Mosher, J.T., Bixby, S., Joseph, N., Iwashita, T., and Morrison, S.J. (2002). Neural Crest Stem Cells Persist in the Adult Gut but Undergo Changes in Self-Renewal, Neuronal Subtype Potential, and Factor Responsiveness. Neuron *35*, 657–669.

Kulesa, P.M., Kasemeier-Kulesa, J.C., Teddy, J.M., Margaryan, N.V., Seftor, E.A., Seftor, R.E.B., and Hendrix, M.J.C. (2006). Reprogramming metastatic melanoma cells to assume a neural crest cell-like phenotype in an embryonic microenvironment. PNAS *103*, 3752–3757.

Lee, G., Kim, H., Elkabetz, Y., Al Shamy, G., Panagiotakos, G., Barberi, T., Tabar, V., and Studer, L. (2007). Isolation and directed differentiation of neural crest stem cells derived from human embryonic stem cells. Nat. Biotechnol. *25*, 1468–1475.

Lee, G., Papapetrou, E.P., Kim, H., Chambers, S.M., Tomishima, M.J., Fasano, C.A., Ganat, Y.M., Menon, J., Shimizu, F., Viale, A., et al. (2009). Modeling Pathogenesis and Treatment of Familial Dysautonomia using Patient Specific iPSCs. Nature *461*, 402–406.

Lee, G., Ramirez, C.N., Kim, H., Zeltner, N., Liu, B., Radu, C., Bhinder, B., Kim, Y.J., Choi, I.Y., Mukherjee-Clavin, B., et al. (2012). Large-scale screening using familial dysautonomia induced pluripotent stem cells identifies compounds that rescue IKBKAP expression. Nat. Biotechnol. *30*, 1244–1248.

Lehoczky, J.A., Robert, B., and Tabin, C.J. (2011). Mouse digit tip regeneration is mediated by fate-restricted progenitor cells. Proc Natl Acad Sci U S A *108*, 20609–20614.

Lescroart, F., Kelly, R.G., Garrec, J.-F.L., Nicolas, J.-F., Meilhac, S.M., and Buckingham, M. (2010). Clonal analysis reveals common lineage relationships between head muscles and second heart field derivatives in the

mouse embryo. Development *137*, 3269–3279.

Leslie, M. (2015). Sall4 won't give stem cells a break. J Cell Biol *208*, 494–494.

Leushacke, M., Ng, A., Galle, J., Loeffler, M., and Barker, N. Lgr5+ Gastric Stem Cells Divide Symmetrically to Effect Epithelial Homeostasis in the Pylorus. Cell Reports.

Li, Y.-Q. (2010). Master Stem Cell Transcription Factors and Signaling Regulation. Cellular Reprogramming *12*, 3–13.

Li, A., Jiao, Y., Yong, K.J., Wang, F., Gao, C., Yan, B., Srivastava, S., Lim, G.S.D., Tang, P., Yang, H., et al. (2015). SALL4 is a new target in endometrial cancer. Oncogene *34*, 63–72.

Li, H.-Y., Say, E.H.M., and Zhou, X.-F. (2007). Isolation and Characterization of Neural Crest Progenitors from Adult Dorsal Root Ganglia. STEM CELLS *25*, 2053–2065.

Li, M., He, Y., Dubois, W., Wu, X., Shi, J., and Huang, J. (2012). Distinct Regulatory Mechanisms and Functions for p53-Activated and p53-Repressed DNA Damage Response Genes in Embryonic Stem Cells. Molecular Cell *46*, 30–42.

Liu, L., Souto, J., Liao, W., Jiang, Y., Li, Y., Nishinakamura, R., Huang, S., Rosengart, T., Yang, V.W., Schuster, M., et al. (2013). Histone Lysine-specific Demethylase 1 (LSD1) Protein Is Involved in Sal-like Protein 4 (SALL4)-mediated Transcriptional Repression in Hematopoietic Stem Cells. J Biol Chem *288*, 34719–34728.

Liu, L., Zhang, J., Yang, X., Fang, C., Xu, H., and Xi, X. (2015). SALL4 as an Epithelial-Mesenchymal Transition and Drug Resistance Inducer through the Regulation of c-Myc in Endometrial Cancer. PLoS One *10*.

Lomuto, M., Calabrese, P., and Giuliani, A. (2004). Prognostic signs in

melanoma: state of the art. Journal of the European Academy of Dermatology and Venereology *18*, 291–300.

Loulier, K., Barry, R., Mahou, P., Yann Le Franc, Supatto, W., Matho, K.S., Ieng, S., Fouquet, S., Dupin, E., Benosman, R., et al. (2014). Multiplex Cell and Lineage Tracking with Combinatorial Labels. Neuron *81*, 505–520.

Lu, J., Jeong, H., Kong, N., Yang, Y., Carroll, J., Luo, H.R., Silberstein, L.E., YupoMa, and Chai, L. (2009). Stem Cell Factor SALL4 Represses the Transcriptions of PTEN and SALL1 through an Epigenetic Repressor Complex. PLoS ONE *4*.

Lu, J., Ma, Y., Kong, N., Alipio, Z., Gao, C., Krause, D.S., Silberstein, L.E., and Chai, L. (2011). Dissecting the role of SALL4, a newly identified stem cell factor, in chronic myelogenous leukemia. Leukemia *25*, 1211–1213.

Lyon, V.B. (2010). Congenital Melanocytic Nevi. Pediatric Clinics of North America *57*, 1155–1176.

Ma, Y., Cui, W., Yang, J., Qu, J., Di, C., Amin, H.M., Lai, R., Ritz, J., Krause, D.S., and Chai, L. (2006). SALL4, a novel oncogene, is constitutively expressed in human acute myeloid leukemia (AML) and induces AML in transgenic mice. Blood *108*, 2726–2735.

Maguire, L.H., Thomas, A.R., and Goldstein, A.M. (2015). Tumors of the neural crest: Common themes in development and cancer. Dev. Dyn. *244*, 311–322.

Mathis, L., Bonnerot, C., Puelles, L., and Nicolas, J.F. (1997). Retrospective clonal analysis of the cerebellum using genetic laacZ/lacZ mouse mosaics. Development *124*, 4089–4104.

McKinney, M.C., Fukatsu, K., Morrison, J., McLennan, R., Bronner, M.E., and Kulesa, P.M. (2013). Evidence for dynamic rearrangements but lack of fate or position restrictions in premigratory avian trunk neural crest. Development *140*, 820–830.

Miettinen, M., Wang, Z., McCue, P.A., Sarlomo-Rikala, M., Rys, J., Biernat, W., Lasota, J., and Lee, Y.-S. (2014). SALL4 expression in germ cell and non-germ cell tumors: a systematic immunohistochemical study of 3215 cases. Am. J. Surg. Pathol. *38*, 410–420.

Morrison, S.J., White, P.M., Zock, C., and Anderson, D.J. (1999). Prospective Identification, Isolation by Flow Cytometry, and In Vivo Self-Renewal of Multipotent Mammalian Neural Crest Stem Cells. Cell *96*, 737–749.

Nagoshi, N., Shibata, S., Kubota, Y., Nakamura, M., Nagai, Y., Satoh, E., Morikawa, S., Okada, Y., Mabuchi, Y., Katoh, H., et al. (2008). Ontogeny and Multipotency of Neural Crest-Derived Stem Cells in Mouse Bone Marrow, Dorsal Root Ganglia, and Whisker Pad. Cell Stem Cell *2*, 392–403.

Nitzan, E., and Kalcheim, C. (2013). Neural crest and somitic mesoderm as paradigms to investigate cell fate decisions during development. Dev. Growth Differ. *55*, 60–78.

Norman, J., Cruse, C.W., Wells, K.E., Saba, H.I., and Reintgen, D.S. (1992). Metastatic melanoma with an unknown primary. Ann Plast Surg *28*, 81–84.

Oikawa, T., Kamiya, A., Zeniya, M., Chikada, H., Hyuck, A.D., Yamazaki, Y., Wauthier, E., Tajiri, H., Miller, L.D., Wang, X.W., et al. (2013). Sal-like protein 4 (SALL4), a stem cell biomarker in liver cancers. Hepatology *57*, 1469–1483.

Park, D., Spencer, J.A., Koh, B.I., Kobayashi, T., Fujisaki, J., Clemens, T.L., Lin, C.P., Kronenberg, H.M., and Scadden, D.T. (2012). Endogenous Bone Marrow MSCs Are Dynamic, Fate-Restricted Participants in Bone Maintenance and Regeneration. Cell Stem Cell *10*, 259–272.

Podsypanina, K., Ellenson, L.H., Nemes, A., Gu, J., Tamura, M., Yamada, K.M., Cordon-Cardo, C., Catoretti, G., Fisher, P.E., and Parsons, R. (1999). Mutation of Pten/Mmac1 in mice causes neoplasia in multiple organ systems. Proc Natl Acad Sci U S A *96*, 1563–1568.

Rao, S., Zhen, S., Roumiantsev, S., McDonald, L.T., Yuan, G.-C., and Orkin,

S.H. (2010). Differential Roles of Sall4 Isoforms in Embryonic Stem Cell Pluripotency. Mol. Cell. Biol. *30*, 5364–5380.

Reintgen, D.S., McCarty, K.S., Woodard, B., Cox, E., and Seigler, H.F. (1983). Metastatic malignant melanoma with an unknown primary. Surg Gynecol Obstet *156*, 335–340.

Ritsma, L., Ellenbroek, S.I.J., Zomer, A., Snippert, H.J., de Sauvage, F.J., Simons, B.D., Clevers, H., and van Rheenen, J. (2014). Intestinal crypt homeostasis revealed at single-stem-cell level by in vivo live imaging. Nature *507*, 362–365.

Saadai, P., Wang, A., Nout, Y.S., Downing, T.L., Lofberg, K., Beattie, M.S., Bresnahan, J.C., Li, S., and Farmer, D.L. (2013). Human induced pluripotent stem cell-derived neural crest stem cells integrate into the injured spinal cord in the fetal lamb model of myelomeningocele. Journal of Pediatric Surgery *48*, 158–163.

Sakaki-Yumoto, M., Kobayashi, C., Sato, A., Fujimura, S., Matsumoto, Y., Takasato, M., Kodama, T., Aburatani, H., Asashima, M., Yoshida, N., et al. (2006). The murine homolog of SALL4, a causative gene in Okihiro syndrome, is essential for embryonic stem cell proliferation, and cooperates with Sall1 in anorectal, heart, brain and kidney development. Development *133*, 3005–3013.

Sauka-Spengler, T., and Bronner-Fraser, M. (2008). A gene regulatory network orchestrates neural crest formation. Nature Reviews Molecular Cell Biology *9*, 557–568.

Schadendorf, D., and Hauschild, A. (2014). Melanoma in 2013: Melanoma—the run of success continues. Nat Rev Clin Oncol *11*, 75–76.

Schadendorf, D., Fisher, D.E., Garbe, C., Gershenwald, J.E., Grob, J.-J., Halpern, A., Herlyn, M., Marchetti, M.A., McArthur, G., Ribas, A., et al. (2015). Melanoma. Nature Reviews Disease Primers 15003.

Schepers, A.G., Snippert, H.J., Stange, D.E., Born, M. van den, Es, J.H. van, Wetering, M. van de, and Clevers, H. (2012). Lineage Tracing Reveals Lgr5+ Stem Cell Activity in Mouse Intestinal Adenomas. Science *337*, 730–735.

Serbedzija, G.N., Fraser, S.E., and Bronner-Fraser, M. (1990). Pathways of Trunk Neural Crest Cell Migration in the Mouse Embryo as Revealed by Vital Dye Labelling. Development *108*, 605–612.

Serrano, M., Lee, H.-W., Chin, L., Cordon-Cardo, C., Beach, D., and DePinho, R.A. (1996). Role of the INK4a Locus in Tumor Suppression and Cell Mortality. Cell *85*, 27–37.

Shakhova, O., and Sommer, L. (2008). Neural crest-derived stem cells. In StemBook, (Cambridge (MA): Harvard Stem Cell Institute),.

Shakhova, O., Zingg, D., Schaefer, S.M., Hari, L., Civenni, G., Blunschi, J., Claudinot, S., Okoniewski, M., Beermann, F., Mihic-Probst, D., et al. (2012). Sox10 promotes the formation and maintenance of giant congenital naevi and melanoma. Nat Cell Biol *14*, 882–890.

Shirley, S.H., Greene, V.R., Duncan, L.M., Torres Cabala, C.A., Grimm, E.A., and Kusewitt, D.F. (2012). Slug Expression during Melanoma Progression. Am J Pathol *180*, 2479–2489.

Sieber-Blum, M. (2004). Cardiac neural crest stem cells. Anat. Rec. *276A*, 34–42.

Simon, C., Lickert, H., Götz, M., and Dimou, L. (2012). Sox10-iCreERT2: A mouse line to inducibly trace the neural crest and oligodendrocyte lineage. Genesis *50*, 506–515.

Smith, A. (2006). A glossary for stem-cell biology. Nature *441*, 1060–1060.

Snippert, H.J., van der Flier, L.G., Sato, T., van Es, J.H., van den Born, M., Kroon-Veenboer, C., Barker, N., Klein, A.M., van Rheenen, J., Simons, B.D., et al. (2010). Intestinal Crypt Homeostasis Results from Neutral Competition

between Symmetrically Dividing Lgr5 Stem Cells. Cell *143*, 134–144.

Soriano, P. (1999). Generalized lacZ expression with the ROSA26 Cre reporter strain. Nat. Genet. *21*, 70–71.

Stemple, D.L., and Anderson, D.J. (1992). Isolation of a stem cell for neurons and glia from the mammalian neural crest. Cell *71*, 973–985.

Stemple, D.L., and Anderson, D.J. (1993). Lineage Diversification of the Neural Crest: In Vitro Investigations. Developmental Biology *159*, 12–23.

Sweetman, D., and Münsterberg, A. (2006). The vertebrate spalt genes in development and disease. Developmental Biology *293*, 285–293.

Tabansky, I., Lenarcic, A., Draft, R.W., Loulier, K., Keskin, D.B., Rosains, J., Rivera-Feliciano, J., Lichtman, J.W., Livet, J., Stern, J.N.H., et al. (2013). Developmental Bias in Cleavage-Stage Mouse Blastomeres. Current Biology *23*, 21–31.

Taneyhill, L.A. (2008). To adhere or not to adhere: the role of Cadherins in neural crest development. Cell Adh Migr *2*, 223–230.

Tanimura, N., Saito, M., Ebisuya, M., Nishida, E., and Ishikawa, F. (2013). Stemness-related Factor Sall4 Interacts with Transcription Factors Oct-3/4 and Sox2 and Occupies Oct-Sox Elements in Mouse Embryonic Stem Cells. J. Biol. Chem. *288*, 5027–5038.

Taran, J.M., and Heenan, P.J. (2001). Clinical and histologic features of level 2 cutaneous malignant melanoma associated with metastasis. Cancer *91*, 1822–1825.

Toma, J.G., McKenzie, I.A., Bagli, D., and Miller, F.D. (2005). Isolation and Characterization of Multipotent Skin-Derived Precursors from Human Skin. STEM CELLS *23*, 727–737.

Tomita, Y., Matsumura, K., Wakamatsu, Y., Matsuzaki, Y., Shibuya, I., Kawaguchi, H., Ieda, M., Kanakubo, S., Shimazaki, T., Ogawa, S., et al.

(2005). Cardiac neural crest cells contribute to the dormant multipotent stem cell in the mammalian heart. J Cell Biol *170*, 1135–1146.

Tzouanacou, E., Wegener, A., Wymeersch, F.J., Wilson, V., and Nicolas, J.-F. (2009). Redefining the Progression of Lineage Segregations during Mammalian Embryogenesis by Clonal Analysis. Developmental Cell *17*, 365–376.

Ueno, S., Lu, J., He, J., Li, A., Zhang, X., Ritz, J., Silberstein, L.E., and Chai, L. (2014). Aberrant expression of SALL4 in acute B cell lymphoblastic leukemia: Mechanism, function, and implication for a potential novel therapeutic target. Exp Hematol *42*, 307–316.e8.

Venneti, S., Le, P., Martinez, D., Xie, S.X., Sullivan, L.M., Rorke-Adams, L.B., Pawel, B., and Judkins, A.R. (2011). Malignant rhabdoid tumors express stem cell factors, which relate to the expression of EZH2 and Id proteins. Am. J. Surg. Pathol. *35*, 1463–1472.

Wang, B., Li, L., Xie, X., Wang, J., Yan, J., Mu, Y., and Ma, X. (2010). Genetic variation of SAL-Like 4 (SALL4) in ventricular septal defect. International Journal of Cardiology *145*, 224–226.

Weiss, M.B., Abel, E.V., Mayberry, M.M., Basile, K.J., Berger, A.C., and Aplin, A.E. (2012). TWIST1 is an ERK1/2 effector that promotes invasion and regulates MMP-1 expression in human melanoma cells. Cancer Res *72*, 6382–6392.

Wong, C.E., Paratore, C., Dours-Zimmermann, M.T., Rochat, A., Pietri, T., Suter, U., Zimmermann, D.R., Dufour, S., Thiery, J.P., Meijer, D., et al. (2006). Neural crest–derived cells with stem cell features can be traced back to multiple lineages in the adult skin. J Cell Biol *175*, 1005–1015.

Wu, Q., Chen, X., Zhang, J., Loh, Y.-H., Low, T.-Y., Zhang, W., Zhang, W., Sze, S.-K., Lim, B., and Ng, H.-H. (2006). Sall4 Interacts with Nanog and Co-occupies Nanog Genomic Sites in Embryonic Stem Cells. J. Biol. Chem. *281*,

24090–24094.

Xiong, J., Todorova, D., Su, N.-Y., Kim, J., Lee, P.-J., Shen, Z., Briggs, S.P., and Xu, Y. (2015). Stemness factor Sall4 is required for DNA damage response in embryonic stem cells. J Cell Biol *208*, 513–520.

Xu, W., Wang, Y., Liu, E., Sun, Y., Luo, Z., Xu, Z., Liu, W., Zhong, L., Lv, Y., Wang, A., et al. (2013). Human iPSC-Derived Neural Crest Stem Cells Promote Tendon Repair in a Rat Patellar Tendon Window Defect Model. Tissue Engineering Part A *19*, 2439–2451.

Yamaguchi, Y.L., Tanaka, S.S., Kumagai, M., Fujimoto, Y., Terabayashi, T., Matsui, Y., and Nishinakamura, R. (2015). Sall4 Is Essential for Mouse Primordial Germ Cell Specification by Suppressing Somatic Cell Program Genes. Stem Cells *33*, 289–300.

Yang, J., Chai, L., Liu, F., Fink, L.M., Lin, P., Silberstein, L.E., Amin, H.M., Ward, D.C., and Ma, Y. (2007). Bmi-1 is a target gene for SALL4 in hematopoietic and leukemic cells. Proc Natl Acad Sci U S A *104*, 10494–10499.

Yang, J., Chai, L., Fowles, T.C., Alipio, Z., Xu, D., Fink, L.M., Ward, D.C., and Ma, Y. (2008). Genome-wide analysis reveals Sall4 to be a major regulator of pluripotency in murine-embryonic stem cells. Proc Natl Acad Sci U S A *105*, 19756–19761.

Yang, J., Corsello, T.R., and Ma, Y. (2012). Stem Cell Gene SALL4 Suppresses Transcription through Recruitment of DNA Methyltransferases. J. Biol. Chem. *287*, 1996–2005.

Yong, K.J., Gao, C., Lim, J.S.J., Yan, B., Yang, H., Dimitrov, T., Kawasaki, A., Ong, C.W., Wong, K.-F., Lee, S., et al. (2013). Oncofetal Gene SALL4 in Aggressive Hepatocellular Carcinoma. N Engl J Med *368*, 2266–2276.

Yoshida, S., Shimmura, S., Nagoshi, N., Fukuda, K., Matsuzaki, Y., Okano, H., and Tsubota, K. (2006). Isolation of Multipotent Neural Crest-Derived Stem

8 Publications

8.1 Scientific publications

Locatelli, G., Baggiolini, A., Schreiner, B., Palle, P., Waisman, A., Becher, B., and Buch, T. (2015). Mature oligodendrocytes actively increase in vivo cytoskeletal plasticity following CNS damage. Journal of Neuroinflammation *12*, 62.

Baggiolini, A., Varum, S., Mateos, J.M., Bettosini, D., John, N., Bonalli, M., Ziegler, U., Dimou, L., Clevers, H., Furrer, R., Sommer, L. (2015). Premigratory and Migratory Neural Crest Cells Are Multipotent In Vivo. Cell Stem Cell *16*, 314–322.

- Preview by Marianne Bronner in Cell Stem Cell *16*, 217-8.

Jacob, C., Lötscher, P., Engler, S., Baggiolini, A., Tavares, S.V., Brügger, V., John, N., Büchmann-Møller, S., Snider, P.L., Conway, S.J., Yamaguchi, T., Matthias, P., Sommer, L., Mantei, N., Suter, U. (2014). HDAC1 and HDAC2 Control the Specification of Neural Crest Cells into Peripheral Glia. J. Neurosci. *34*, 6112–6122.

Schwarz, D., Varum, S., Zemke, M., Schöler, A., Baggiolini, A., Draganova, K., Koseki, H., Schübeler, D., and Sommer, L. (2014). Ezh2 is required for neural crest-derived cartilage and bone formation. Development *141*, 867–877.

Jacob, C., Christen, C.N., Pereira, J.A., Somandin, C., Baggiolini, A., Lötscher, P., Özçelik, M., Tricaud, N., Meijer, D., Yamaguchi, T., Matthias, P., Suter, U. (2011). HDAC1 and HDAC2 control the transcriptional program of myelination and the survival of Schwann cells. Nat Neurosci *14*, 429–436.

Mario Bonalli, Leda Dimou, Urs Ziegler, Hans Clevers, Reinhard Furrer, Lukas Sommer.

February 2013 Lineage tracing demonstrates multipotency of premigratory and migratory neural crest cells in vivo. **9th Swiss Stem Cells Network (SSCN) in Bern.** Arianna Baggiolini, Sandra Tavares Varum, José María Mateos, Damiano Bettosini, Nessy John, Mario Bonalli, Leda Dimou, Urs Ziegler, Hans Clevers, Reinhard Furrer, Lukas Sommer.

12 Acknowledgments

I would like to give my most sincere gratitude to the following persons:

Prof. Dr. Lukas Sommer,
for all these exiting years in his laboratory. Not only you have been a great boss, but also a tremendous mentor. Thank you for caring about my future scientific career and for always being ready to give good advice. And thank you for being an example that one can be a great scientist and at the same time a great person.

Prof. Dr. Sebastian Jessberger, Prof. Dr. Konrad Basler and Prof. Dr. Reinhard Dummer,
for co-reviewing my PhD thesis and for the important scientific inputs during my PhD study.

Sandra,
for being a fantastic supervisor and for being a really great friend.

Simon, Martina, Gaia, Kalina and Eylül,
for the philosophical discussions, for patiently handling me as a office colleague, for your positivity and joy of life, for your tenacity and for your sweetness, respectively.

Jessica and Annika,
for you great support in the lab.

The whole Sommer's lab,
for rendering these years a lot of fun. Without all of you the years of my PhD study would have not been even half as fun as they have been. Thank you to all of you.

Nicole, Jenny, Edda,
for allowing the Sommer's laboratory to work as it does.

Sara, Fabiano and Tina
for being amazing friends and for always supporting me.

The whole Ticino crew Irina, Lorenzo, Mauro, Brigitt, Ceppi, Stefania,
for rendering Zurich a really great place where to live.

My dad, Danilo,
for teaching me to be responsible and that we are making our own destiny.

Amanda, my sister,
for being the best sister on earth and at the same time also my best friend. For always being with me as much in the great and as in the dark moments and for always believing in me, whatever I was doing.

Antonella,
not only for being a great mum, but also for being a great friend. Thank you for believing in me, for teaching me in believing in myself and for always giving me strength.

Lorenzo,
for being my life partner. For sharing troubles and fun and for always supporting me. Whatever I managed was also thanks to you.